EPISTEMIC UNCERTAINTIES IN PROBABILISTIC EARTHQUAKE HAZARD MODELS AND THEIR EFFECTS ON THE RESULTS: THE CASE OF MARMARA REGION

by

Hülya Yüksel Perdıbuka

B.S., Civil Engineering, Kocaeli University, 2013

Submitted to the Kandilli Observatory and Earthquake Research Institute
in partial fulfillment of the requirements for the degree of
Master of Science

Graduate Program in Earthquake Engineering

Boğaziçi University

2021

EPISTEMIC UNCERTAINTIES IN PROBABILISTIC EARTHQUAKE HAZARD MODELS AND THEIR EFFECTS ON THE RESULTS: THE CASE OF MARMARA REGION

DATE OF APPROVAL: 15/11/2021

ACKNOWLEDGEMENTS

I would like to express my deepest gratitude to my supervisor Dr. Karin Şeşetyan for her continuous support, patience, and guidance. Being my pillar of support in any circumstances, I could gather my strength to keep studying. If I am writing these sentences today, it is thanks to her endless assistance. Also, I would like to express my special thanks to my dissertation defence committee members, Prof. Dr. Eser Çaktı and Dr. Özden Saygılı, for their valuable comments.

I would like to thank Şafak Söylemez, who never spared his help with his experience and knowledge, for all his support and guidance.

I owe all Earthquake Engineering Department faculty members a debt of gratitude for broadening my horizons by sharing their valuable knowledge and experience and for their very delicate attitude all the time. And I would like to thank my co-workers for supporting me throughout my graduate studies.

I also wish thank to my dearest friends, Yasemin Özaydın, Medine Akkuş and Ümmü Gülsüm Bilgin, for standing by me, sharing their sincere friendship with me and cheering me up in all circumstances.

Finally, and most importantly, I would like to express my gratitude to my parents, Emine Yüksel and Yılmaz Yüksel for their constant support, for everything that makes me who I am and their endless love. Also, I would like to thank my spouse Dardan Perdibuka, who has always been with me in all circumstances, for his love, support and insightfulness all the time.

ABSTRACT

EPISTEMIC UNCERTAINTIES IN PROBABILISTIC EARTHQUAKE HAZARD MODELS AND THEIR EFFECTS ON THE RESULTS: THE CASE OF MARMARA REGION

Throughout the history and also in the not too distant past, Marmara region has been a center that hosted several of the most destructive earthquakes around the World. Considering the density of population and building stock and the concentration of economic activities, the performance of comprehensive earthquake hazard assessment studies is one of the essential steps towards the mitigation of the seismic risk in the Marmara region. The seismicity and the earthquake characteristics of this region have been studied extensively in the last decades, and various hazard maps have been created.

In the light of the increasing amount and quality of data and new studies on seismotectonic and the developments in the earthquake hazard calculation methods, the need for a regular updating of the earthquake hazard estimates for regions with high seismic activity arises. Therefore, new earthquake hazard maps for specific regions or regions covering many countries are being generated continually. In today's practice, the use of the probabilistic earthquake hazard assessment method has become a common implementation in the preparation of earthquake hazard maps. However, as opposed to site-specific assessments, large scale regional studies usually investigate the effects of epistemic uncertainties only in a limited way, and in most cases, only the mean hazard outputs are reported. Nonetheless, analysis of epistemic uncertainties in the hazard assessment and reporting of the uncertainty ranges associated with the ground motion estimations can provide valuable insights towards a better understanding of the seismic hazard and consequently of the seismic risk. Starting from this point of view, developing an earthquake hazard assessment model specific to the Marmara region, dealing specifically with the uncertainties associated with the modelling approaches, is quite meaningful when the earthquake history of the region is also considered.

In this thesis, in order to examine the effects of uncertainties on probabilistic earthquake hazard analysis results specific to the Marmara region, the Turkish Seismic Hazard Map developed within the scope of the “Update of seismic hazard maps of Turkey (UDAP-Ç-13-06)” project was evaluated. Alternative models were included in the earthquake hazard calculations by obtaining uncertainties related to the data and modelling parameters and combining them in a logic tree structure. Accordingly, hazard maps are obtained for PGA and 5 % damped Spectral Accelerations at T = 0.2 s and 1.0 s for 475 and 2475 years return periods, and uncertainty ranges for the computed ground motion parameters are presented. The sensitivity of the results to the uncertainties associated with different modelling parameters is investigated. The results indicate that, even for the Marmara region, which is one of the best-studied regions in terms of seismic activity and geological structure, the seismic hazard models can be associated with large uncertainties.

ÖZET

OLASILIKSAL DEPREM TEHLİKE MODELLERİNDE EPİSTEMİK BELİRSİZLİKLER VE SONUÇLARA ETKİLERİ: MARMARA BÖLGESİ ÖRNEĞİ

Tarih boyunca ve çok uzak olmayan bir geçmişte de Marmara bölgesi, dünyanın en yıkıcı depremlerinden birkaçına ev sahipliği yapan bir merkez olmuştur. Türkiye genelindeki nüfus ve yapı stoku dağılımı yanında ekonomik aktivite yoğunluğu da göz önüne alındığında, Marmara bölgesinin sismik riskini azaltmak için atılacak önemli adımların başında deprem tehlike değerlendirmeleri gelmektedir. Bölgenin sismisitesi ve deprem karakteristikleri son yıllarda kapsamlı şekilde araştırılmış ve çeşitli tehlike haritaları oluşturulmuştur.

Artan veri sayısı ve niteliği ile sismotektoniğe ilişkin yeni çalışmalar ve deprem tehlike hesaplama yöntemlerindeki gelişmeler ışığında, sismik aktivitenin yüksek olduğu bölgeler için deprem tehlike tahminlerinin düzenli olarak güncellenmesi ihtiyacı ortaya çıkmaktadır. Bu nedenle, belirli bölgeler veya birçok ülkeyi kapsayan bölgeler için sürekli olarak yeni deprem tehlike haritaları oluşturulmaktadır. Günümüz teknolojisinde deprem tehlike haritalarının hazırlanmasında olasılıksal deprem tehlike değerlendirme yönteminin kullanılması yaygın bir uygulama haline gelmiştir. Ancak, sahaya özel değerlendirmelerin aksine, büyük ölçekli bölgesel çalışmalar genellikle epistemik belirsizliklerin etkilerini sadece sınırlı bir şekilde araştırılarak çoğu durumda sadece ortalama tehlike çıktıları rapor edilmektedir. Bununla birlikte, tehlike değerlendirmesindeki epistemik belirsizliklerin analizi ve yer hareketi tahminleriyle ilişkili belirsizlik aralıklarının işlenmesi, sismik tehlikenin ve dolayısıyla sismik riskin daha iyi anlaşılmasına yönelik kıymetli bilgiler sağlayabilir. Buradan yola çıkarak, Marmara bölgesi özelinde modelleme yaklaşımlarına ilişkin belirsizlikleri özel olarak ele alan bir deprem tehlike değerlendirmesi yapmak bölgenin deprem geçmişi de göz önünde bulundurulduğunda oldukça anlamlıdır.

Bu tez çalışmasında, deprem belirsizliklerinin Marmara bölgesine özgü olasılıksal deprem tehlike analizi sonuçlarına etkisini incelemek amacıyla, Türkiye'nin güncellenmiş sismik tehlike haritası çalışmaları projesi (UDAP-Ç-13-06) kapsamında hazırlanan Türkiye Sismik Tehlike Haritası 2018 değerlendirilmiştir. Verilere ve modelleme parametrelerine ilişkin belirsizlikler elde edilerek, mantık ağacı yöntemi kullanılarak deprem tehlike hesaplamalarına alternatif modeller dahil edilmiştir. Bu doğrultuda, 475 ve 2475 tekerrür yıllarına karşılık gelen PGA, %5 sönümlü SA (0.2 s) ve SA (1.0 s) için yer hareketi dağılım haritaları elde edilmiş, hesaplanan yer hareketi parametreleri için belirsizlik aralıkları sunulmuş ve sonuçların farklı modelleme parametreleriyle ilişkili belirsizliklere duyarlılığı incelenmiştir. Sonuçlar, sismik aktivite ve jeolojik yapı açısından en iyi çalışılan bölgelerden biri olan Marmara bölgesi için dahi sismik tehlike modellerinin geniş belirsizliklerle ilişkilendirilebileceğini göstermiştir.

TABLE OF CONTENTS

LIST OF FIGURES

LIST OF TABLES

LIST OF SYMBOLS / ABBREVIATIONS

a	The absolute seismicity level of the magnitude probability density function curve
b	The slope of the magnitude probability density function curve
A_f	Area of the fault
c	Exceedance of a specified ground motion level
C	The seismic hazard with the frequency of occurrence
Δ	The total variability in the GMPE model
j	Source
m^0	Arbitrary reference magnitude
m^u	Maximum magnitude of the fault source
M	Magnitude
Ms	Surface wave magnitude
Mw	Moment magnitude
N	The annual number of events
P	Probability
R_{epi}	Epicentral distance
R_{hyp}	Hypocentral distance
R_{JB}	Joyner-Boore distance
R_{RUP}	The closest distance to the rupture plane
R_X	The surface projection of the distance to the updip edge of the rupture
s	The source properties
S	The slip rate of the fault
t	Time interval
ν	Occurrence rate of the ground motion
Y	The observed ground motion
X_{es}	The ground motion model parameters in the GMPE model
γ	The exceedance of the ground motion value
λ_M	The annual rate of earthquakes
σ	Standard deviation
μ	The shear modulus
θ	The coefficients described the GMPE in model

AS	Area source
AFAD	Disaster and Emergency Management Authority of Turkey
DSHA	Deterministic seismic hazard assessment
EAFZ	The East Anatolian Fault Zone
FS	Fault Source
GIS	Geographic information system
MARsite	The New Directions in Seismic Hazard Assessment through Focused Earth Observation in the Marmara Supersite project
NAFZ	The North Anatolian Fault Zone
NGA	The Next Generation Attenuation Relationships
PGA	Peak ground acceleration (in g)
PGV	Peak ground velocity (in g)
PSHA	Probabilistic seismic hazard assessment
RP	Return period (in years)
SA	Pseudo spectral acceleration
SHA	Seismic hazard assessment
SRL	Surface rupture length
T	Time period (in seconds)
UDAP-Ç-13-06	The Revision of Turkish Seismic Hazard Map Project
Vs30	The shear wave velocity of the upper 30m of the subsurface profile
WGCEP	The Working Group on California Earthquake Probabilities

1. INTRODUCTION

As one of the natural events, earthquakes occur as a result of the constant movement of the earth's crust. They can be associated with random characteristics and have destructive consequences. The possible influences of the future earthquakes cannot yet be thoroughly evaluated; nonetheless, estimates can be made within the context of the probabilistic models through a method which is called seismic hazard analysis. By enabling us to obtain a numerical prediction of earthquake ground motion hazard at a location, seismic hazard analysis is one of the most efficient tools to understand the possible outcomes of earthquakes and is an important component of earthquake risk mitigation activities. At this stage, we can say that the seismic hazard analysis is a crucial step in earthquake-resistant design, in seismic risk analyses and even for insurance rate calculations. Site-specific assessments or seismic zoning maps can be developed with the use of this method.

The seismic hazard assessment method can be divided into two subheadings, which are deterministic (DSHA) and probabilistic (PSHA). The main element of the deterministic hazard analysis is to obtain the largest possible hazard that could occur at a site in terms of a ground motion intensity measure of interest (e.g. peak ground acceleration, PGA; peak ground velocity, PGV, or spectral accelerations at specific periods, SA), while the probabilistic hazard analysis tries to determine different scenarios of possibilities and defines an annual probability of the ground motion level being exceeded, again for the ground motion intensity measure of interest. By virtue of the fact that earthquakes have random properties as location, time, magnitude or uncertainties due to incomplete knowledge, the probabilistic seismic hazard assessment method might be called as a method that is more convenient than the deterministic hazard assessment for many cases (Bommer, 2002).

The first seismic zoning map studies for Turkey date back to the 1940s. The hazard maps generated from these studies were studied in line with the earthquake catalogs composed within the period information and the distribution of the observed damage as a result of these earthquakes (Akkar et al., 2018). Later on, first probabilistic earthquake hazard assessment studies have been conducted for Turkey since the 1970s (e.g. Erdik et al., 1985). In the light of these studies, the national seismic design codes published both in 1997

and 2007 used the response spectrum of the first officially published seismic zoning map, which was based on a probabilistic seismic hazard analysis (Gülkan et al., 1993). In recent years, with the development of new methods and accumulation of new data related to seismic hazard studies, the need for a comprehensive and an updated seismic hazard study covering the Turkish territory became apparent, and for this aim, the "Revision of Turkish Seismic Hazard Map Project (UDAP-Ç-13-06)" has been carried under the sponsorship of "AFAD (Disaster and Emergency Management Authority of Turkey)" (Şeşetyan et al., 2018; Demircioğlu et al., 2018).

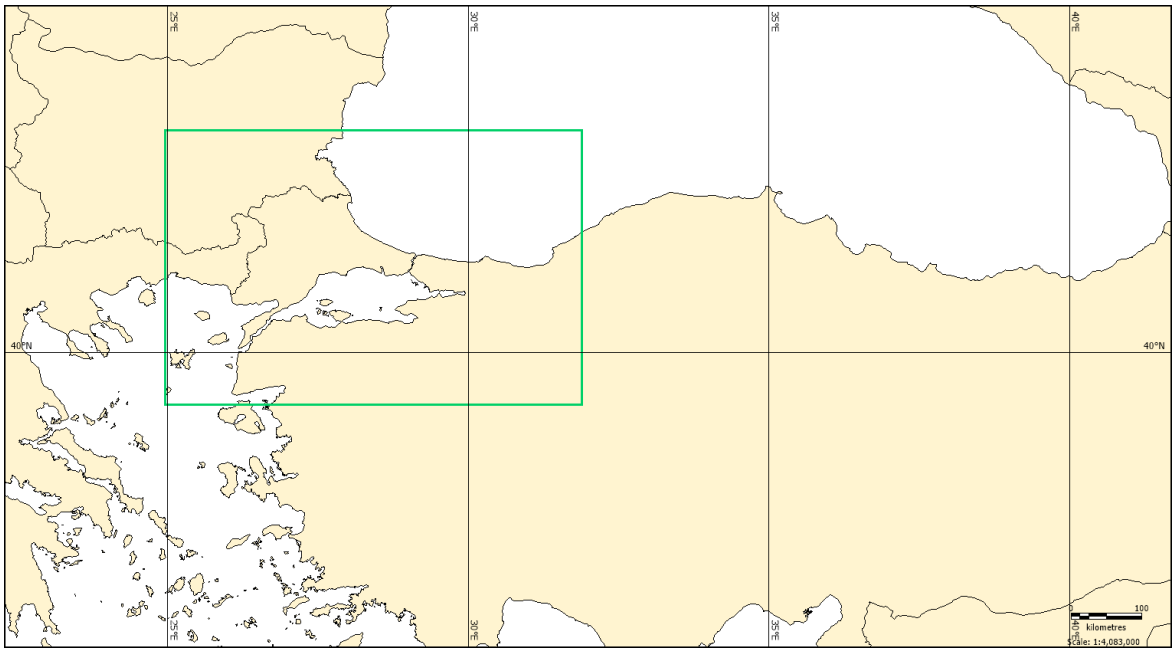

Figure 1.1. The Study Region

In this thesis, in order to see the effects of model uncertainties on probabilistic earthquake hazard analysis results specific to the Marmara region, the epistemic uncertainties considered in "UDAP-Ç-13-06" project are reevaluated, and by developing a more comprehensive uncertainty model, the contribution of uncertainties related to individual modelling parameters and their effects on the final mean hazard and associated uncertainty ranges are examined. The earthquake catalog from "UDAP-Ç-13-06" project is directly used for the analyses. The area source and the completeness model developed by Şeşetyan et al. (2018) and similarly the fault source model developed by Demircioğlu et al. (2018) reevaluated and uncertainties in several modelling parameters, not originally used in

the respective models due to computation limitations, are incorporated and the effects are evaluated in the present study.

The hazard model presented in this thesis considers a rectangular area (24.9550°-31.8980°E, 39.3260°-42.8160°N) that covers the Marmara region in Turkey (Figure 1.1) and the results for 475 and 2475 years return periods (RP) are mapped for PGA, and 5% damped spectral acceleration (SA) at T=0.2 s and 1.0 s for rock conditions (Vs30=760m/s). Comparisons are made with the "UDAP-Ç-13-06" project results in terms of mean hazard values, and uncertainties associated with each map are represented in terms of 16% and 84% quantiles. In addition to the mapped intensity distributions, hazard curves for selected city centers located in the study region are presented, and those results are examined with respect to epistemic uncertainties considered.

1.1. Objectives and Scope of the Study

The purpose of the present study is to investigate the sensitivity of seismic hazard results to the uncertainties which are or might be associated with parameters used in the development of probabilistic seismic hazard models. The region of Marmara is selected as a case study due to the high earthquake hazard; it is obvious that conducting various seismic hazard assessment studies considering different perspectives in the Marmara region can end up with serious benefits in terms of reducing the earthquake risk in the region. The scope of this thesis covers a re-evaluation of the results of the recent "Revision of Turkish Seismic Hazard Map Project (UDAP-Ç-13-06)", which is resulted in Turkey's new earthquake hazard map as a step of an update of "the Earthquake Resistant Design Code" in 2018, with specific emphasis on the examination of epistemic uncertainties of the modelling parameters in the Marmara Region.

The study focuses on the influence of different assumptions, such as the epistemic uncertainties related to completeness of the earthquake catalog, maximum magnitudes, earthquake recurrence parameters, fault characteristics and finally, ground motion prediction equations. With the application of logic tree methodology, sensitivities to different uncertainties are evaluated in terms of mean hazard curves. Here it should be noted that the databases (i.e., earthquake catalog and active fault database) developed within the scope of

the project “UDAP-Ç-13-06” are used as they are, and uncertainties related to database development are presently not considered.

This thesis begins with the literature review of Turkey hazard map evaluation (Chapter 2), gives a brief information on seismotectonic of Marmara region (Chapter 3) and basics of seismic hazard analysis methods and uncertainty concept (Chapter 4). In further chapters, the method followed for the analysis and the uncertainties evaluated are examined (Chapter 5). The last two chapters present the obtained results in terms of hazard maps for PGA, 5% damped spectral accelerations of T= 0.2 s and T= 1.0 s corresponding to 475 and 2475 years, hazard curves for selected sites, comparison maps with the “UDAP-Ç-13-06” project results, the sensitivity of the hazard to the selected parameters and associated discussions.

2. LITERATURE SURVEY: PSHA HISTORY AND HAZARD MAPS IN TURKEY

The seismic hazard analysis method has evolved from deterministic approaches to complex probabilistic approaches today. In early studies, a single value was assigned to each independent variable, and a model predicted a specific value for the dependent variable (McGuire and Arabasz, 1990). Today, we are able to conduct analyses with complex models, but we need to understand the evolution of the seismic hazard studies and analyze the recent studies to produce a study that can respond to today's needs.

The history of probabilistic earthquake hazard studies has not yet reached a century. The model published by C. Allin Cornell in 1968 was the first model based on a probabilistic approach to estimate the seismic hazard giving the selected seismic hazard parameter versus the exceedance probabilities (Cornell, 1968). The first published seismic zone map and the first national seismic hazard map was developed for Mexico by Luis Esteva in 1970, that included the first PGA and PGV distribution for 50, 100, and 500 years return periods (McGuire, 2008).

In Turkey, the first studies of seismic hazard assessment began in the 1940s, which relied on the spatial distribution of earthquake catalogs and the structural damage caused by ground motion (Akkar et al., 2018). An earlier attempt of an unofficial seismic zoning map was published by Sieberg in 1932. To list all officially published earthquake hazard maps until today, these are: in 1945 and in 1947, with the name of "Yersarsıntısı Bölgeleri Haritası (the Earthquake Zones Map)"; in 1963, 1972 and 1996, with the name of "Türkiye Deprem Bölgeleri Haritası (the Turkey Earthquake Zones Map)" and in 2018 "the Turkish Seismic Hazard Map" respectively. All these seismic maps have been prepared on the basis of different principles, with the developments and the new understandings in the field of seismic hazard analysis.

After the Great Erzincan Earthquake in 1939 and the following earthquakes that happened throughout the North Anatolian Fault, the first official seismic zoning map, also used for the seismic design code of buildings entered into force in 1949 which was published in 1945. This map considered three types of zones in Turkey, which can be summarized as

“regions of serious danger”, “dangerous earthquake regions”, and “regions without danger” (Özmen, 2012). The first two seismic maps of Turkey are prepared on the basis of the structural damage distribution of the previous earthquakes. The first application of the design spectrum for seismic hazard maps in Turkey was carried out with the seismic design code published in 1968. The code used the seismic zonation map published in 1963 that considered the first, second and third-degree of earthquake zones and the non-hazardous zones as the fourth zone for Turkey. (Akkar et al., 2018). With the introduction of deterministic seismic hazard analysis to the literature, the following two seismic maps, which were published in 1963 and 1972, are entered into force, respectively (Özmen 2012).

The study of (Erdik et al., 1985) was the first seismic hazard model that used the probabilistic seismic hazard analysis approach and PGA and intensity distributions with 475 years return period were proposed for the Turkish territory. Area sources were the only seismic source type used to conduct the hazard analysis, and the Poisson earthquake occurrence model was adopted.

The Turkish Earthquake Zoning Map published in 1996 was based on the study conducted by Gülkan et al. (1993) and was the first seismic zoning map based on the probabilistic approach. Similar to the study of Erdik et al. (1985), the area source modelling approach was adopted. Rupture location was the only aleatory uncertainty in the study, and to calculate the resulting ground motions, the attenuation relationship (i.e., the ground motion prediction model in today’s terminology) of Boore and Joyner (1982) was used in the study (Gülkan et al., 1993). Finally, “the Turkish Seismic Hazard Map”, which is in force today, was published in 2018 and entered into force on January 1, 2019, and inspired this study. The probabilistic hazard analysis method is used for this map. The map, which is prepared within the “UDAP-Ç-13-06” project, used “the active fault database of Turkey” by Emre et al. (2016) and the renewed instrumental earthquake catalog of Turkey by Kadirioğlu et al. (2018). In addition to the area sources, fault sources with background seismicity are developed to conduct a two-stage analysis for these seismic sources. The analyses are conducted for engineering bedrock site conditions (Vs30=760m/s). PGA, PGV, 5% damped spectral accelerations (SA) at T=1.0 s and T=0.2 s for 43, 72, 475, and 2475 years return periods are provided (Şeşetyan et al., 2018; Demircioğlu et al., 2018).

Besides the countrywide seismic zoning map studies, until the 2000s, a number of probabilistic seismic hazard assessment studies had been conducted for a part or whole region of Marmara. From the triggering events in 1999 (17 August Mw 7.6 İzmit and 12 November Mw 7.1 Düzce), the studies on regional and countrywide earthquake hazard maps have increased, and various scenarios with different hazard assessment approaches have been studied since then.

To mention some of the recent noteworthy seismic hazard studies conducted for the Marmara region, Atakan et al. (2002) performed a probabilistic hazard assessment for İstanbul, İzmit and the Marmara Sea territory. They conducted their analyses with 12 scenarios, consisting of four ground motion prediction equations and three different earthquake source models, which are Poissonian (time-independent) (Cornell, 1968) and two different renewal (time-dependent) models (McGuire, 1993). With the assessment of these twelve scenarios separately, depending on the analyses they conducted, they inferred that although associated with uncertainties, the response spectra levels of "the Turkish Earthquake Zoning Map (1996)", which was in force at that date, were satisfactory compared to the results they observed.

Erdik et al. (2004) conducted an analysis with the use of a fault source model with smoothed seismicity for the Marmara region that covers a window centering the Sea of Marmara. They used both Poissonian and renewal models to estimate earthquake recurrence of the sources they defined and conducted their analyses with the use of three different ground motion prediction equations. They considered both single-segment and multi-segment rupturing scenarios and used two models for multi-segmentation. For the case of the analyses conducted here, the multi-segment renewal model ruptures provided slightly higher hazard results than single segment ruptures, which in their turn provided higher hazard values when compared to Poisson model ruptures, in regions close to the recently un-ruptured fault segments.

As a further performance of Atakan et al. (2002) and Erdik et al. (2004) studies, Kalkan et al. (2009) conducted a reassessment of seismic hazard in the Marmara region. They compiled an updated and homogenized earthquake catalog and used an extended fault source modelling with elaborated submarine faults besides the smoothed seismicity model. "The

Next Generation Attenuation Relationships (NGA)" and a regional attenuation relationship, Kalkan and Gülkan (2004) are preferred and observed PGA levels for 475 years are 0.8 g for the Marmara Sea and 0.4 g for İstanbul as a result of this assessment.

Gülerce and Ocak (2013) evaluated the seismic hazard of the Eastern Marmara region by generating alternative multi-segment rupture models and using the basis proposed by WGCEP (2003). They also implemented "The Next Generation Attenuation Relationships (NGA)" to their model for the fault source model they compiled. As a result of the analysis they conducted, they observed 1,05 g PGA for 475 years return period as the highest ground motion level, which is significantly higher than corresponding earthquake activity assigned, 0.4 g, in "the Turkish Earthquake Zoning Map (1996)" for the region they studied.

Spagnuolo et al. (2016) introduced the directivity effect to make an assessment of the near-field effects on the hazard level within the scope of the project "New Directions in Seismic Hazard Assessment through Focused Earth Observation in the Marmara Supersite (MARsite)". They observed an increase of up to 25% with the inclusion of the directivity effect for near-field regions.

Şeşetyan et al. (2019) conducted a probabilistic hazard assessment for the Marmara region with the use of recently updated data which include the earthquake catalogue, the updated fault source model and fault characteristics. They also used recently developed regional ground motion prediction equations using both Poissonian and renewal models to estimate the ground motion level at the region. At the end of the analyses they conducted, they obtained higher hazard levels with the renewal model analysis at sites closer to the fault segments, which did not produce large magnitude events in the recent periods.

3. SEISMOTECTONICS OF MARMARA REGION

Experiencing many devastating earthquakes, Anatolia hosts one of the most active tectonic regions in Eurasia. The Anatolian micro-plate, located at the junction of Arabian, African and Eurasian tectonic plates, has a continuous counterclockwise movement as documented by studies based on the GPS measurements (e.g., Reilinger et al., 2006). The governing structures of the neotectonics of Turkey can be counted as three major different fault zones, which are “North Anatolian Fault Zone (NAFZ)”, “East Anatolian Fault Zone (EAFZ)” and “Hellenic–Cyprian Arc”. Between the NAFZ and EAFZ (Figure 3.1). Located within the Alpine-Himalayan orogenic belt, the Central Anatolian micro-plate drags away from the Eastern Anatolia with a westward movement under the influence of the continent-to-continent collision of the Arabian and the Eurasian plates. The rate of this westward motion is in the order of ∼20 mm per year (Bozkurt, 2001). and is accommodated through the right-lateral North Anatolian Fault (NAF) and left-lateral East Anatolian Fault (EAF), forming the boundaries with the Eurasian Plate and the East Anatolian contraction province, respectively (Şengör et al., 1985).

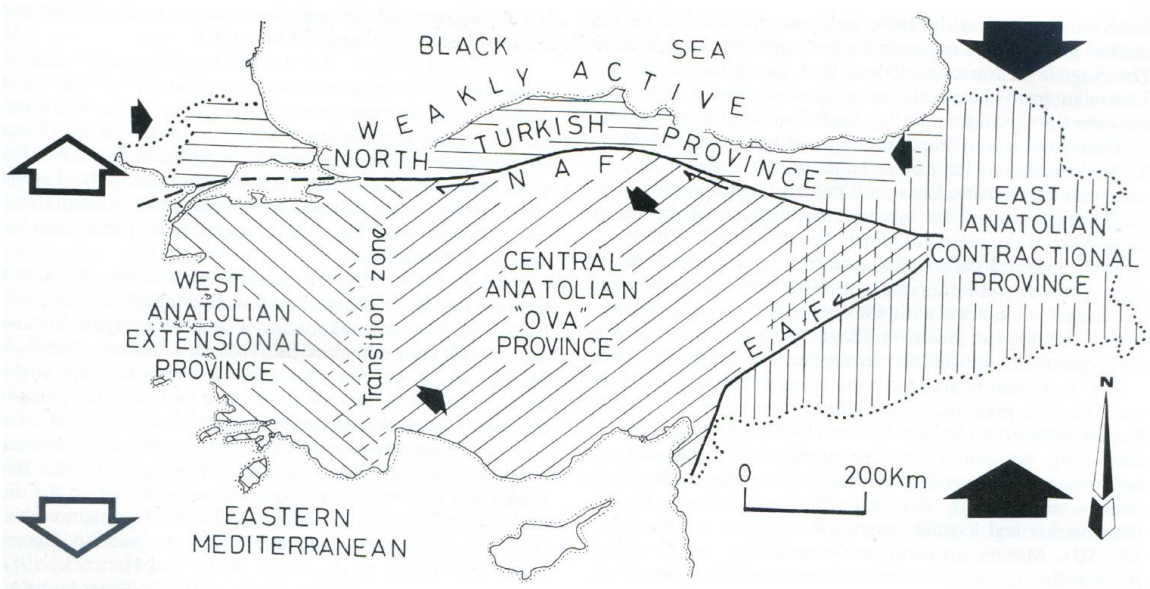

Figure 3.1. "Neotectonic provinces of Turkey" (Şengör et al., 1985)

The Central Anatolian part of the Anatolian micro-plate is relatively stable (Bozkurt, 2001) with limited internal deformation, while the tectonic structure of the western part, also termed as West Anatolian Extensional Province (Figure 3.1), becomes extensional as a result

of the subduction of African Plate under Eurasia through the Hellenic Arc. NAF forming the northern boundary of the Anatolian micro-plate is a simple, through-going fault zone at the central part (ref e.g., Şengör et al., 2005) while it assumes a more complex structure in the Marmara region, where the transition to the extensional regime also becomes important.

In 1999, after the two violent earthquakes, which are 17 August Mw 7.6 İzmit (Barka et al., 2002) and 12 November Mw 7.1 Düzce (Duman et al., 2005), the Marmara region became a center of interest for scientists from all branches of science that may be related to earthquakes aiming to mitigate any kind of earthquake risk at the region which hosts a very high population and is also one of the main centers of the economic activities in Turkey. In this direction, for any study to be carried out in this region, especially for the assessment of earthquake hazard, understanding the seismotectonics of the Marmara region can be counted as a fundamental step.

Being the dominating fault system in the Marmara region, the NAF is a strike-slip intracontinental transform fault system, with a 1200 km length extending from Karlıova (east of Erzincan) in the east to the Aegean Sea in the west. In its eastern and central parts, the NAF zone can be described as a narrow zone with a single through-going trace, intercepted by a few releasing or restraining bends (Barka, 1998). However, the fault zone reaches its maximum width of about 100km in its western part, i.e., in the Sea of Marmara (Şengör et al., 2014). To clarify, transform fault is a form of crustal boundary that connect two plates. Although having relatively higher return periods of large magnitude events, compared to the eastern segments of NAF, and other fault systems in Turkey (e.g. the extensional faults systems of the Aegean region), the capacity of generating destructive earthquakes (Tan et al., 2008), also documented by historical seismicity studies (e.g. Ambraseys and Jackson, 2000), necessitates comprehensive assessments to be conducted to understand the characteristics and to model future earthquake effects in the region.

The faulting mechanism studies have shown that the North Anatolian Fault (NAF) has a clean right-lateral strike-slip character. However, in the Marmara region, the fault is divided into two main branches, the northern one running through the Marmara Sea and reaching the Aegean Sea at the Saros Bay, and the southern one running mostly on-land in the southern Marmara region. As mentioned earlier, the fault zone in this region has a width

of 100 km in the NS direction and faulting characteristics also change, as earthquakes with normal faulting mechanisms are also observed with the dominant direction of the maximum stress axis changing to N-S (Kalafat, 2011).

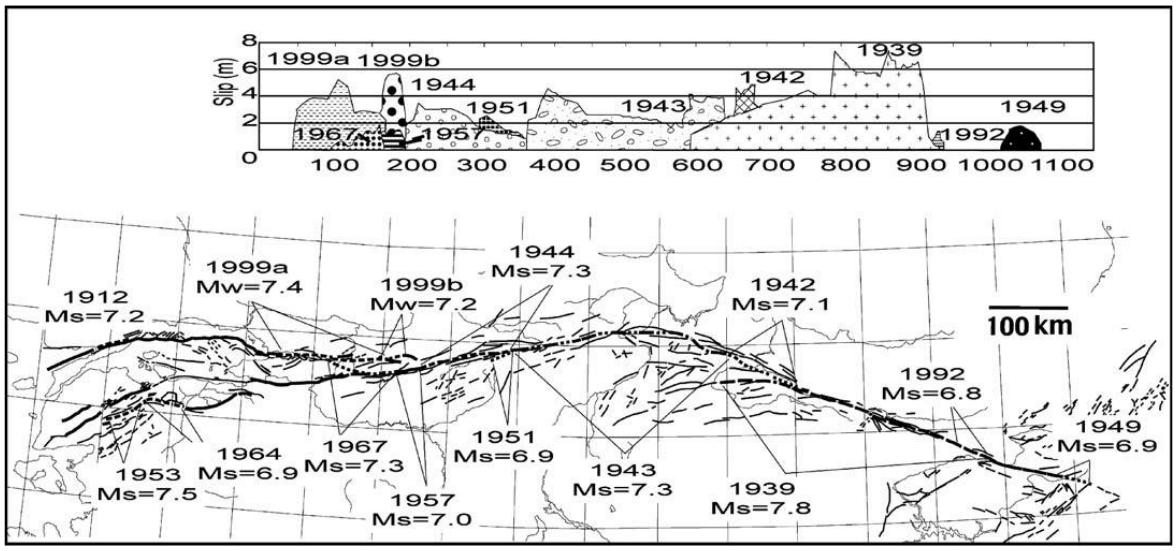

Figure 3.2. From the Figure 3 of study by Şengör et al. (2005) "Earthquakes and related fault displacements along the NAF since the December 26/27, 1939, Erzincan earthquake."

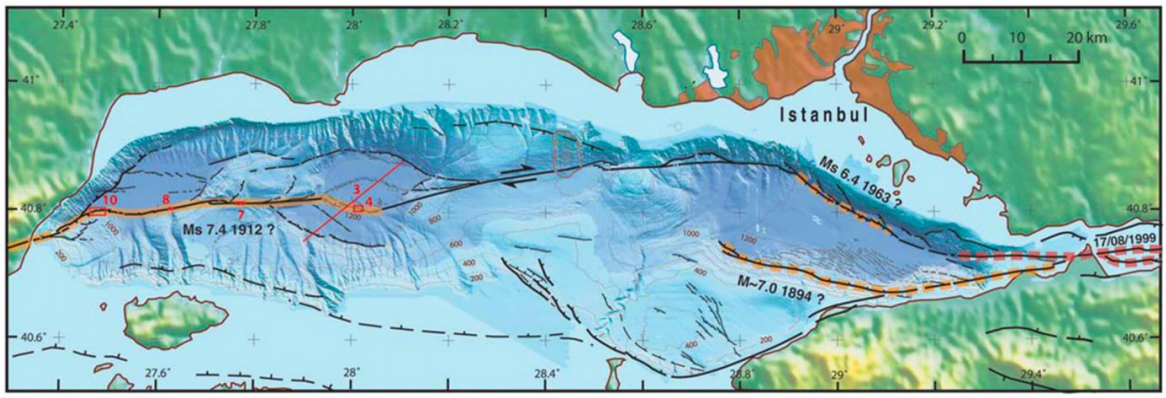

Figure 3.3. Tectonic model of Marmara Sea region and most recently ruptured segments (Figure from the study by Armijo et al. (2005))

Since the beginning of the 20th century on the NAF, a very destructive earthquake sequence; of which the significant ones can be referred respectively as 1939 Erzincan (Mw 7.8), 1942 Niksar-Erbaa (Mw 7.0), 1943 Tosya-Ladik (Mw 7.2), 1944 Bolu-Gerede (Mw 7.2), 1951 Kurşunlu (Mw 6.9), 1957 Abant (Mw 7.1), 1967 Mudurnu Valley (Mw 7.1); progressed from the eastern end of the fault to the west towards the Marmara region and

finally the 1999 Kocaeli and Düzce earthquakes occurred leaving (Figure 3.2) an approximately 160 km long “seismic gap” through the Marmara Sea (Hubert-Ferrari et al., 2000), extending from west of Hersek peninsula in the east to the Central basin in the west (Figure 4 and Figure 3.4). The western end of NAF in the Marmara Sea region, between the Central basin and Saros Bay, had already ruptured in the 1912 Şarköy-Mürefte (Mw 7.2) earthquake. 1935 Marmara Island (Ms 6.4) and 1963 Çınarcık (Ms 6.3) earthquakes are examples of few medium scale events that occurred in the Marmara Sea during the 20th century. A very recent event in the region is the Mw 5.8 Silivri earthquake that occurred on 26 September 2019 (Karabulut et al., 2021), which caused some damage and considerable concern throughout the Marmara region. Due to the lack of medium to large magnitude events in the Marmara Sea region (concerning mainly the northern branch of NAF) during the recent periods, both earthquake occurrence and ground motion modelling become challenging, resulting in large uncertainties be associated with the estimated ground motion levels.

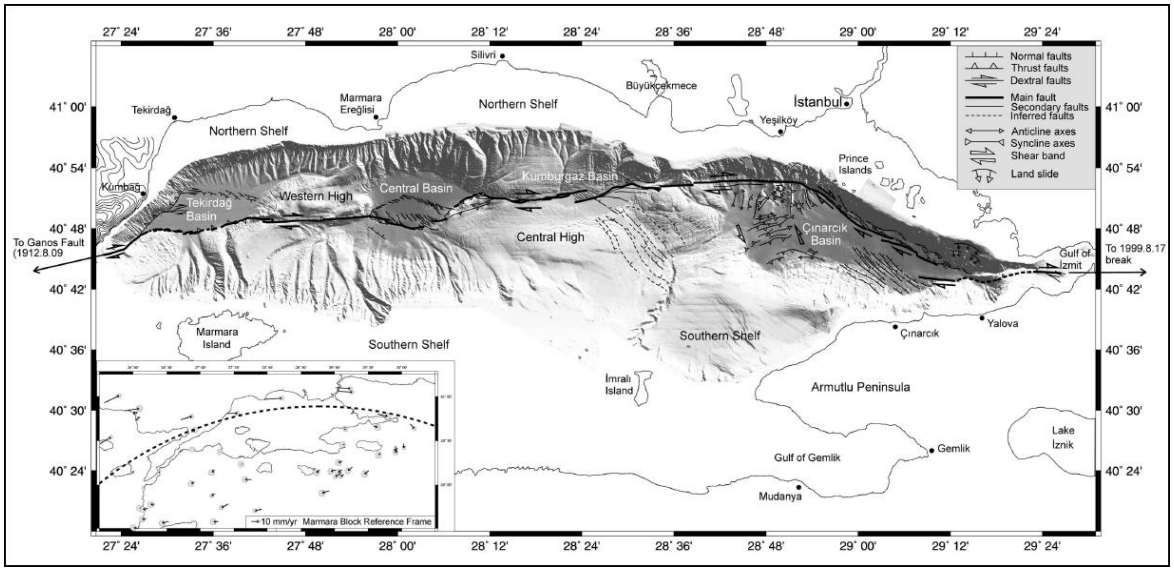

Figure 3.4. “Bathymetric map of the Marmara Sea” (Figure from the study by Le Pichon et al., 2001)

Although less active, the southern branch of NAF where hosts the Bursa, Ulubat, Manyas Yenice-Gönen and Edremit fault segments, has also experienced some large magnitude earthquakes during the 20th century (Kürçer et al., 2008). Among these, the 1953

Yenice-Gönen (Mw7.0) and 1964 Manyas (Mw 6.9) can be cited as the largest earthquakes experienced at the eastern vicinity of the Biga Peninsula (Figure 3.5).

As presented in Figure 3.4, as the northern branch of the NAF goes through the Marmara Sea, it forms the boundaries of sub-marine basins and highs. Three of these basins with depths more than 1 km are called Çınarcık, Central Marmara and Tekirdağ basins from east to west, also evidencing the extensional "pull-apart" character of the Marmara Sea (Armijo et al., 2002).

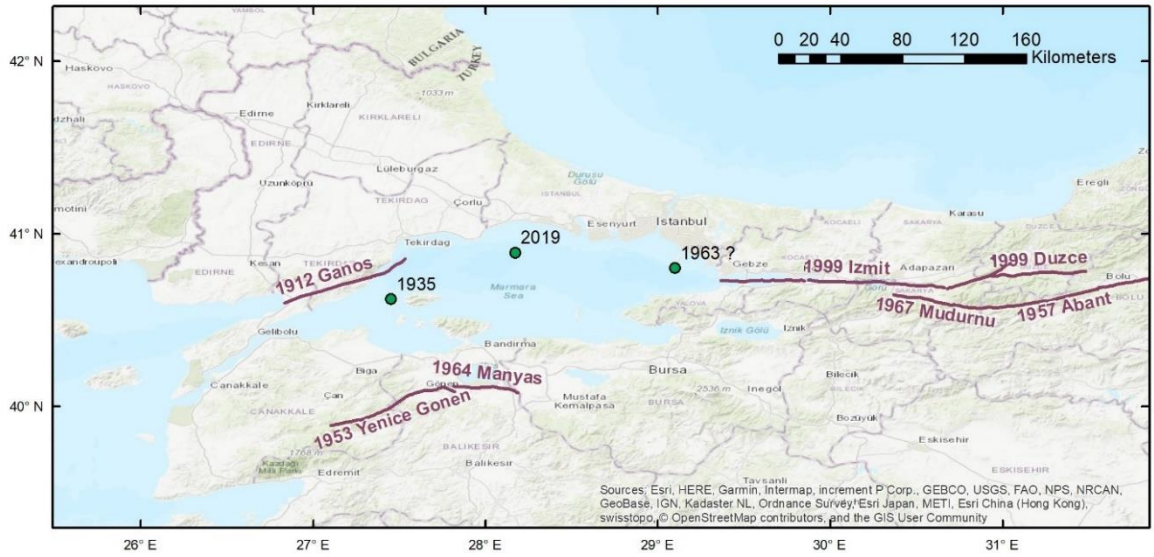

Figure 3.5. Major earthquakes of the 20th century in the Marmara region (Şeşetyan et al., 2019)

To touch the route of the NAF through the Marmara Sea, the fault traverses the Gulf of İzmit where hosts the fault segments, which are Karadere, Sapanca-Akyazı, İzmit-Sapanca Lake, Karamürsel-Gölcük and Hersek from east to west, that are ruptured with the 17th of August 1999 Kocaeli (Mw7.6) earthquake (Barka et al., 2002). Mostly following a single branch until the bay mouth of the Gulf of İzmit, the NAF splays into branches through to the west where we meet the Çınarcık Basin. A complicated fault segment filled with the 10km width, the Çınarcık Basin harbored the aftershocks of the 1999 Kocaeli earthquake (Le Pichon et al., 2001). Travelling from east to center of the Marmara Sea, we meet the Kumburgaz Basin, the Central Basin and finally the Tekirdağ Basin, a deep strike-slip basin underwater (1150m) that reaches the Ganos fault (Okay et al., 1999; Le Pichon et al., 2001).

A threshold before the Gulf of Saros and by this means the Aegean Sea, the Ganos fault hosted 30th of July, 2013 Gökçeada (Mw 5.3) and the 1912 Mürefte (Mw7.2) earthquake which is the largest earthquake of the 20th century observed in the Marmara region until the 1999 Kocaeli (Mw7.6) earthquake (Ambraseys and Finkel, 1987).

Figure 3.6 presents the regional active fault characterization as proposed by Emre et al. (2013) and Emre et al. (2016), where we observe that entering in the Marmara region, NAF becomes a wider zone and branches into two main strands. The northern branch of NAF passing through the Marmara Sea from Izmit Bay in the east to Ganos in the most active one and accommodates a mainly right-lateral slip rate varying between 14 and 24 mm/yr, with some normal component (Reilinger et al., 2006; Emre et al., 2016). The southern branch of NAF, which splays from the main strand at the vicinity of Mudurnu, includes a number of parallel faults running on-land in the southern Marmara region, with slip rates in the order of 2 to 6 mm/yr, with both strike-slip and normal components (Meade et al., 2002; Selim et al., 2013).

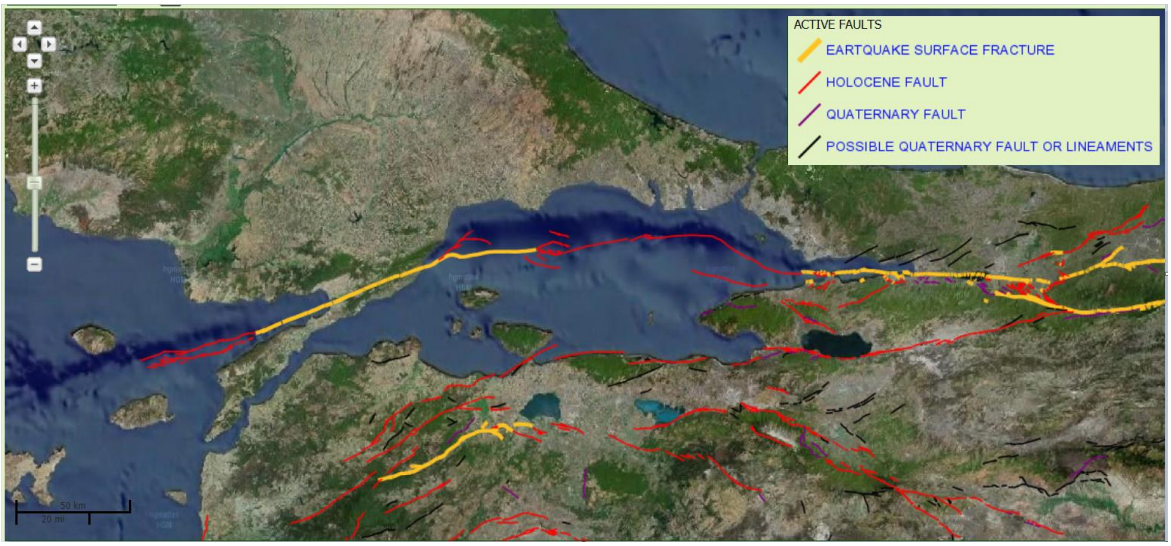

Figure 3.6. Regional active fault characterization by Emre et al. (2013), (Figure from Sesetyan et al., 2019)

The active fault database presented in Figure 3.6 forms the basis of the fault source model developed in the “UDAP-Ç-13-06” project (Demircioğlu et al., 2018), which is also used in this study (Section 5.2.2).

4. SEISMIC HAZARD ANALYSIS: PRINCIPLES AND METHODOLOGY

Being one of the most damaging natural hazards, the phenomenon of ground shaking is the most widespread earthquake related hazard. The characterization and estimation of the hazard caused by an earthquake at a site for a specific period of time has a vital role on reducing the earthquake risk, which also ensures the fundamental information for earthquake resistant design of structures.

Seismic hazard can be defined as any physical feature as ground shaking or failure which is caused by an earthquake that can end up with any effect on human activities (McGuire and Arabasz, 1990). Starting from this point of view, a quantitative projection of the hazard level of an earthquake at a site can be called as seismic hazard analysis. Basically, assessment for any earthquake hazard is a composition of the description of the site, examination of the ground motion amplitude and the probability of exceedance at a period of time, and this requires the size, spatial distribution, and time information of the earthquakes (McGuire and Arabasz, 1990).

The estimation of future earthquake hazard, namely seismic hazard assessment methodology, is divided into two basic types, which are deterministic and probabilistic.

Being a very popular seismic hazard analysis method in the early years of these efforts (Kramer, 1996), the deterministic seismic hazard analysis (DSHA) adopts the method of choosing the scenario that might produce the largest ground motion at the study region among one or more possible earthquake rupture scenarios. Since a single ground motion amplitude is obtained as a result of a single magnitude, distance, ground motion prediction equation combination, regardless of being how unlikely, the DSHA approach tries to find out the worst earthquake scenario. However, obtaining a ground motion amplitude value requires an inevitable thrust on subjective decisions made through the analysis with limited and uncertain data and information in this approach (Bommer, 2002).

Although both deterministic (DSHA) and probabilistic seismic hazard analysis (PSHA) methodologies have many common properties, there is a specific difference that is

the most important feature that distinguishes the two methodologies from each other: while probabilistic seismic hazard assessment has units of time, deterministic seismic hazard assessment does not have (Bommer, 2002). Compared to PSHA, lacking the time variable, DSHA does not have the ability to estimate the exceedance of a ground motion level for a time interval (Hanks and Cornell, 2001). Although neither deterministic nor probabilistic seismic hazard analysis can be called as an ideal method and each of them has specific benefits for different objectives, having no information of the most likely ground motion level in a particular period of time, the likelihood of specific magnitudes or other combinations of scenarios and their effect on the hazard level as an outcome of this method and even having multiple controlling events; deterministic SHA might be called as unsatisfactory for many cases, i.e. construction of a seismic hazard map of a region (McGuire and Arabasz, 1990; Bommer, 2002).

The main property which comes forward with the PSHA is handling all earthquake scenarios that are possible at a site considering various combinations of ground motion characteristics, attenuation relationships or distances with the ability of different weights assigned for each (Bommer, 2002). This property makes PSHA the first choice to obtain the design ground motion parameters for earthquake resistant design for many types of structures. To list the advantages of PSHA, these can be defined as; the ability of specifying all possible assumptions, using skills and the data of the combination of particular scientific fields, having the option of defining the uncertainty level for earthquake risk calculations, opportunity to analyze and comment on the effect of the estimations and the information separately field by field (McGuire and Arabasz, 1990). PSHA uses the probability theory to create probability distributions of the uncertainties of these estimations made and results in the probabilities of different ground motion levels.

4.1. Probabilistic Seismic Hazard Analysis

For seismic hazard analysis methodology, with the inclusion of the uncertainty concept, probabilistic seismic hazard analysis began being used until the late 1960s (Cornell, 1968). The common examples of the uncertainties taken into consideration in PSHA can be listed as size, distance, time and ground motion characteristics. With the help of the PSHA method, all these uncertainties can be combined and analyzed levelly (Kramer, 1996).

There are two assumptions adopted, which are mostly adopted to conduct PSHA, Poissonian (time-independent) (Cornell, 1968) and renewal (time-dependent) models (McGuire, 1993). While the Poissonian model is interested in the return period and thus produces a uniform probability of exceedance for a ground motion level, the renewal model considers the stress accumulation and takes into account the time from the last earthquake to the date of assessment (McGuire, 1993). We can understand better the discrepancy between the two models by examining a comparative study. Şeşetyan et al. (2019) applied both Poissonian and renewal models for their study and evaluated the results separately for the same fault segments. When the results of their study are examined, it is seen that the most striking differences between the two models. While the annual exceedance rates for the segments, where the 1999 Kocaeli and Düzce earthquakes are experienced, are quite low with the renewal model compared to the Poisson model, completely adverse results are observed for the basins in the Marmara Sea, where have not hosted earthquakes for a comparatively long time (Şeşetyan et al., 2019).In this thesis, the standard Poissonian model is preferred to be used as it is also adopted by the "UDAP-Ç-13-06" project studies (Demircioğlu et al., 2018; Şeşetyan et al., 2018).

Basically, the main methodology of PSHA can be defined in four steps which are; delineation and characterization of seismic sources, quantification of the recurrence level of ground motion will be exceeded for each seismic source, obtaining the ground motion level at the target coordinates with the use of chosen ground motion attenuation relationships, combining the ground motion parameters while considering the uncertainties with a computation of the arrangement of ground motion from different seismic sources and obtaining the probability of exceedance of the ground motion level in a particular time interval (Reiter, 1990). In Figure 4.1, the illustrated steps are presented.

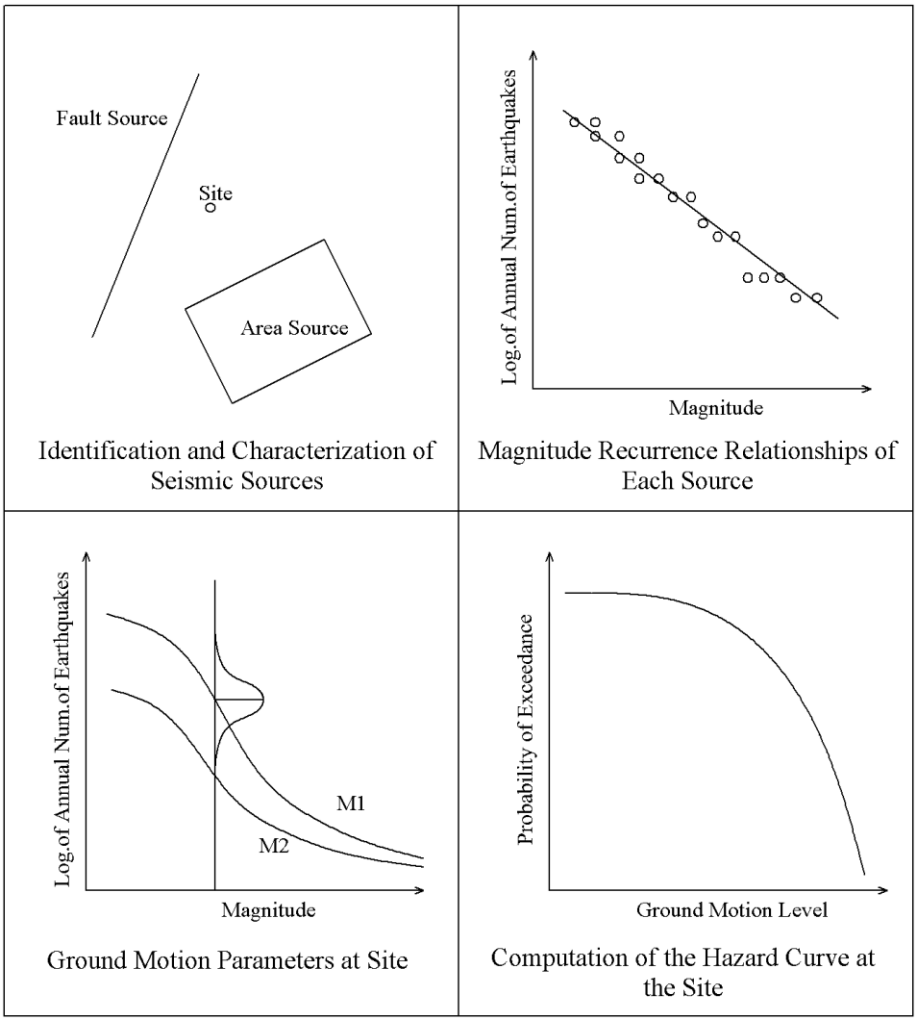

Figure 4.1. Basic method principles of probabilistic seismic hazard analysis (Kramer, 1996)

The hazard model definition by McGuire (2004) is presented in equation (1).

$$\gamma(\mathrm{C} > \mathrm{c}) = \sum_{j} \nu_j \int \int P_j(C > c | \, \bar{s} \; at \; I) P(\, \bar{s} \; at \; I) d\bar{s} \; dl \tag{1}$$

Here," C" refers to the seismic hazard with the frequency of occurrence "γ" of the exceedance of the value "c" in a time interval "t" for the source "j". P is the abbreviation of the probability and while "$\bar{s}$"means the source properties, "ν_j" corresponds to the occurrence rate of the ground motion.

4.2. Treatment of Uncertainties

The assessment of uncertainties is an indivisible part of seismic hazard analysis. With PSHA, the uncertainties, which may affect the observed seismic hazard level, can be efficiently evaluated.

There are two main types of uncertainty that the PSHA method deals with:

(i) Aleatory variability,

(ii) Epistemic uncertainty.

The "aleatory variability" represents the randomness in earthquake occurrences and is modelled with a probability density distribution for each parameter of interest.

The "epistemic uncertainty" on the other hand, deals with the level of information, in other words, with the absence of knowledge related to the parameters under consideration. The development of alternative models is the approach generally adopted for the solution of this problem.

Examining the effects on the quantitative results of the seismic hazard analysis, the main difference between the two sources of uncertainties can be expressed in the following way: Aleatory variabilities are the ones that affect the shape of the hazard curve. On the other hand, as the epistemic uncertainties considered in the study increase, the number of hazard curves increase accordingly (Abrahamson and Bommer, 2005). While there are so many variables that can affect the seismic hazard, a hazard curve calculated by ignoring standard deviations cannot be considered an adequate hazard curve (Abrahamson and Bommer, 2005).

The construction of a logic tree structure that includes all the plausible alternative models is the basic solution to incorporate the epistemic uncertainties in the hazard model. Each branch of the logic tree presents a complete hazard model with specific modelling choices. Uncertainties associated with each modelling parameter form a node of the logic

tree structure, the ramification becoming more and more complex as new nodes are added. The model or parameter uncertainties are usually investigated separately for the two main components of the hazard model i.e., the seismic source characterization and the ground motion characterization, which are, at the end, combined to form the master logic tree structure. The weights assigned to the alternative branches (summing up to 1.0) reflect the confidence level of the model developer to each alternative.

The formation of a logic tree structure with weights assigned to each branch allows for the calculation of the weighted mean hazard, as well as for the statistical treatment of the outputs yielding median and quantile hazard values. When plotted together, the results obtained from individual branches show the full range of the resulting uncertainty while the range between quantiles such as 16 and 84 percentiles may represent the body.

4.3. The PSHA Model Developed in the "UDAP-Ç-13-06" Project

The hazard model developed with the framework of the project "Update of the Seismic Hazard Maps in Turkey (UDAP-Ç-13-06)" is used as the base model for this study. The seismic source characterization model developed in the project consists of an area source model (Şeşetyan et al., 2018) and a fault source model with background seismicity (Demircioğlu et al., 2018). The databases and source models developed therein are used as the base models for the assessment of uncertainty ranges of the hazard results. In the base model being developed for the entire Turkish territory, the parameter uncertainties are treated in a more limited way and only mean hazard results are provided. The development of two independent source models (i.e., the area source model and the fault source complemented with smoothed seismicity is the main node of the seismic source characterization part of the logic tree (Figure 4.2). The second node of the area source model branch is the treatment of maximum magnitude, while the fault source model has no other node. The ground motion characterization part of the logic tree consists of a single node, with a set of GMPE models for each tectonic region, i.e., active shallow, subduction interface and subduction in-slab (Akkar et al., 2018b). The seismic hazard analyses are conducted with the use simple Poissonian model for V_{S30} of 760m/s. As the result of the analyses, the mean PGA and 5% damped spectral accelerations at T=0.2 and T=1.0 s are provided for return periods of 43, 72, 475 and 2475 years (Demircioğlu et al., 2018; Şeşetyan et al., 2018).

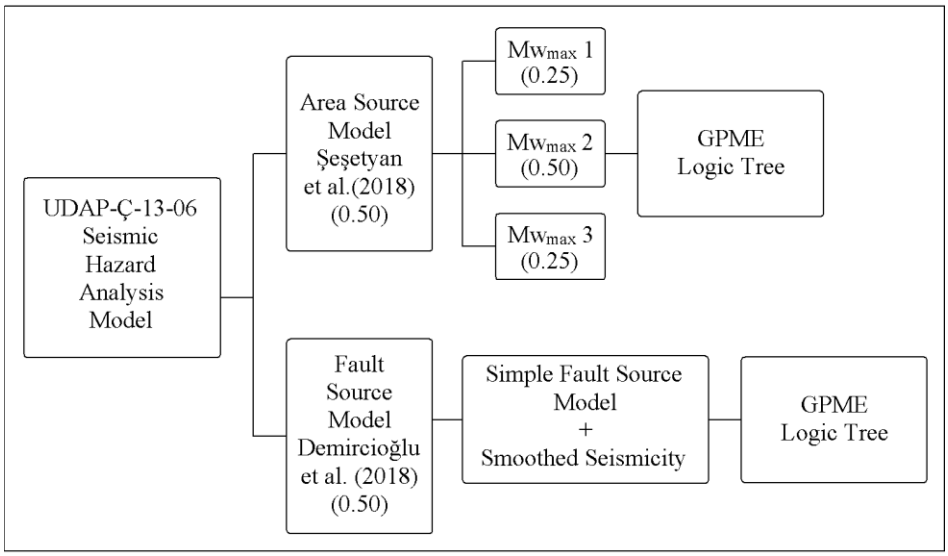

Figure 4.2. Logic tree structure of the PSHA model of the "UDAP-Ç-12-06 Project "

5. DEVELOPMENT OF A MORE COMPREHENSIVE UNCERTAINTY MODEL FOR THE MARMARA REGION

The main aim of the present study is to provide insights with respect to the uncertainty ranges associated with the hazard estimates, the logic tree of the "UDAP-Ç-13-06" Project provided in Figure 4.2 has been expanded to incorporate the uncertainties associated with the different parameters used in seismic source characterization.

The following four stages define the steps and also the limitations of this work:

(i) The databases developed for the project (the earthquake catalog and the active fault database) are used in their original versions, i.e., uncertainties associated with database development are not incorporated in the present model.

(ii) Completeness analysis being one of the most important contributors to the earthquake recurrence modelling, especially for the area source model, alternative completeness models are developed.

(iii) Uncertainties associated with earthquake recurrence modelling for both the area source model and the fault source and smoothed seismicity model (i.e., parameters defining the magnitude probability density functions for both source types) are analyzed.

(iv) The active shallow crustal region GMPE logic tree of the "UDAP-Ç-13-06" Project is directly adopted; however, the resulting uncertainties are also investigated.

The following sections elaborate on the different items listed above and finally presents the logic tree structure proposed in this study.

5.1. The Earthquake Catalog and Completeness Analysis

Before defining and examining the seismic source zones, a comprehensive list of earthquakes that occurred at the site of interest needs to be compiled. Being a quite important step for seismic hazard analysis, uncertainties or errors in magnitude, location, or date may result in unrealistic conclusions (Kadirioğlu et al., 2018).

5.1.1. The Homogenized and Declustered Earthquake Catalog

Since the early 1900s, the instrumental earthquake records have been recorded, however until 1960s, the records observed were not precise enough, and only large earthquakes could be recorded (Kramer, 1996). Although there is more opportunity to record comparatively satisfactory records after the second half of the twentieth century, considering the recurrence period of the earthquakes, the need of more data to compile a processable earthquake catalogue requires more and wider observation.

Having the instrumental catalog only for a century, historical (pre-instrumental) records are needed to be identified. Examining the historical sources, records may date back to about 2000 years from now in the Middle East (Kramer, 1996). The locations with the highest intensity are generally chosen to define the epicenter of these events and the geographic pattern, and also the earthquake recurrence rate can be examined to specify a more accurate pre-instrumental seismicity (Kramer, 1996).

There are several earthquake catalogues compiled both for Turkish territory and specific to the Marmara region. To mention some examples of these catalogs, one of the first earthquake catalogues compiled by Pınar and Lahn (1952) however, this study is descriptive and does not contain coordinate and magnitude information (Tan et al., 2008). Alsan et al. (1976) conducted a homogeneity analysis for the earthquakes recorded between 1913 and 1970 with the use of a computer program for a recalculation of catalog parameters as magnitude, epicenter location or depth. Ambraseys and Jackson (2000) generated a catalog for the Marmara region that contains earthquakes for $Ms \geq 6.0$ and homogenized the intensity measurements for pre1900 recordings.

The earthquake catalog used in this thesis is taken from the "UDAP-Ç-13-06" project (Şeşetyan et al., 2018; Demircioğlu et al., 2018). The catalog is generated from the combination of two parts which are the post-1900 and pre-1900 period. While the post-1900 part of the catalog is taken from the study by Kadirioğlu et al. (2018), the pre-1900 part is compiled from multiple studies by Şeşetyan et al. (2018). For the post-1900 catalog, the spatial distributions of the earthquakes compiled are assessed with the correlation of the fault lines from the Emre et al. (2016) study and re-located by Kadirioğlu et al. (2018).

The final post-1900 catalog by Kadirioğlu et al. (2018) covering the period 1900 to 2012 is homogenized in Mw scale (Hanks and Kanamori, 1979) by the catalog compilers and declustered with the windowing method of Gardner and Knopoff (1974) by Eroğlu Azak et al. (2018). The declustering process can simply be defined as filtering the earthquake catalog from the triggered and background events. Although the declustering method chosen does not have a dramatic effect on the probability of exceedance of large events, it can affect the completeness periods of the small magnitude events and this can play a role on the recurrence parameters of the seismic source in interest (Eroğlu Azak et al., 2018). For this reason, declustering is a primary need for the estimation of the recurrence parameters of a seismic source. To conduct a proper PSHA, Poisson distribution is necessary, and for a convenient Poisson model, independent events, which means the mainshocks, are required (Eroğlu Azak et al., 2018).

To understand the declustering method, the definitions of a mainshock, aftershock and a foreshock are essential. The largest magnitude event observed in an earthquake series in a time window, and a confined space is called the mainshock, and the events of the sequence that occur before and after the mainshock are named as foreshocks and aftershocks, respectively (Utsu, 1969). Although the definition of a mainshock seems to be easy, there are different methods to distinguish a mainshock from other events. Various declustering methods are studied by Eroğlu Azak et al. (2018), and they decided to focus on the techniques by Gardner and Knopoff (1974), Reasenberg (1985) and Zaliapin et al. (2008) for the earthquake catalogue compiled (Eroğlu Azak et al., 2018). The methods basically depend on the application of fixed distance and time windows to detect and comb out the aftershocks and foreshocks. As a result, the method by Gardner and Knopoff (1974) was

chosen for the earthquake catalog of Kadirioğlu et al. (2018) covering the Turkish territory. The same catalog, as presented in Figure 5.4, is used in this study.

The final catalog is evaluated separately for the area source and fault source models obtained according to different limits determined for each model (see sections 5.2.1.1 and 5.2.2.1). The spatial boundaries of the catalog for each source model type will be mentioned in the relevant sections.

5.1.2. Completeness Analysis

The completeness analysis of the earthquake catalog in different magnitude ranges is another aspect of catalog treatment. Earthquake recurrence modelling based on statistical treatment of seismicity data necessitates the complete reporting of events in a certain magnitude range over a certain period. However, different completeness periods can be adopted for different magnitude ranges. For instance, longer periods, including historical events, may be used for large magnitude events, and more recent periods with larger number of recorded data may be used for small magnitude events. This choice is also in line with the observation that large magnitude events repeat themselves in much longer periods, while smaller magnitude events are more frequent (Gutenberg and Richter, 1954). In the scope of the "UDAP-Ç-13-06" project, Şeşetyan et al. (2018) conducted a catalog completeness regionalization study for the Turkish territory. They delineated 11 completeness regions (Figure 5.1), including one in-slab (deep) region for the Eastern Mediterranean Sea, and conducted completeness analysis for each region using the Stepp (1972) method (Şeşetyan et al., 2018). The completeness regions with shallow seismicity are listed in Table 5.1 and Figure 5.2.

As it will be mentioned again in the relevant source model sections, the completeness regions prepared by Şeşetyan et al. (2018) are re-evaluated, and alternative completeness models are proposed for the Marmara region. The earthquake recurrence parameters of the sources are calculated accordingly.

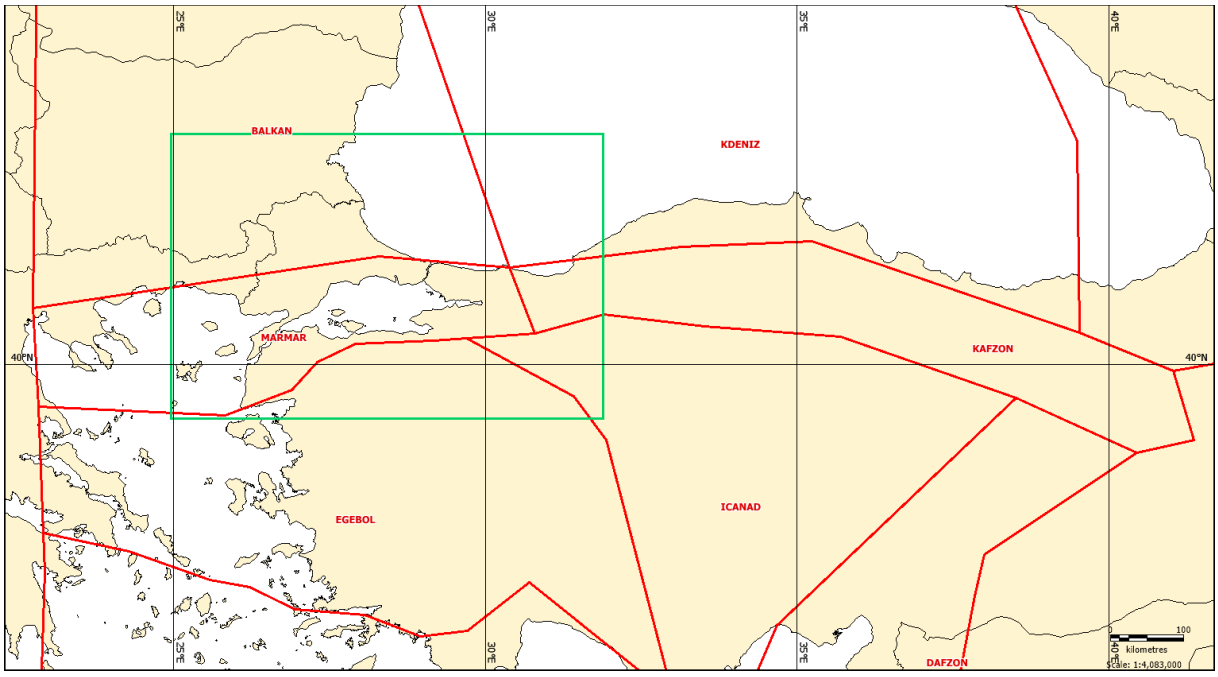

Figure 5.1. Completeness regions by Şeşetyan et al. (2018)

Table 5.1. Completeness periods for magnitude bins for each completeness zone (Şeşetyan et al., 2018)

Completeness Zone ID	Magnitude Bins (Mw)							
	4.3–4.7	4.8–5.2	5.3–5.7	5.8–6.2	6.3–6.7	6.8–7.2	7.3–7.7	7.8–8.2
Balkan	1977	1902	1902	1850	1850	1850	1850	1850
Black Sea	1997	1922	1900	1900	1900	1900	1900	1900
Caucasus	1962	1962	1897	1887	1887	1887	1887	1887
Marmara	1962	1952	1900	1850	1750	1700	1700	1700
Naf Zone	1987	1947	1897	1850	1850	1850	1650	1650
Eastern Anatolia	1987	1967	1897	1857	1857	1857	1840	1840
Aegean	1967	1967	1897	1862	1842	1842	1842	1842
Central Anatolia	1967	1967	1907	1907	1907	1907	1907	1907
Eaf Zone	1962	1900	1900	1867	1750	1750	1750	1750
Mediterranean Shallow	1982	1962	1917	1907	1902	1902	1902	1902
Mediterranean Deep	1982	1962	1917	1907	1902	1902	1902	1902

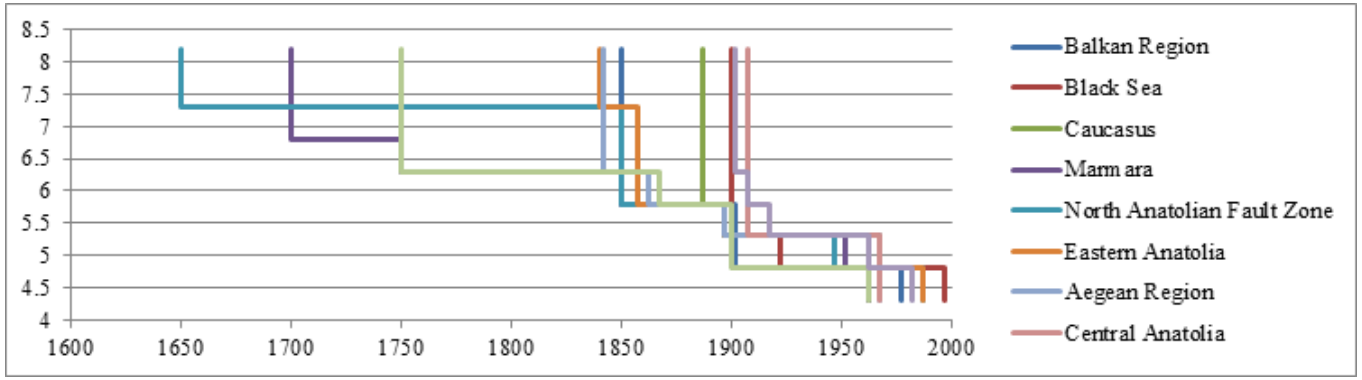

Figure 5.2. Completeness period representation for different completeness regions (Şeşetyan et al., 2018)

5.2. Identification of Seismic Sources

According to the theory of plate tectonics, the generation of the earthquakes depends on the relative movements of the tectonic plates. Identification of the seismic sources, i.e., zones of the crust that are prone to earthquakes, such as plate boundaries, faults within the tectonic deformation zones, or regions where high seismic activity is observed, can be called as the first step of a seismic hazard analysis procedure (Reiter, 1990). Following the identification of these sources, delineation of the boundaries or definition of different segments helps the hazard analyst to define and study the earthquake characteristics of those regions (faults or areas) separately. The main assumption with the separation is that those sources act independently (McGuire, 2004). To make the segmentation, the earthquake characteristics of the source and the annual earthquake occurrence rate, which means the potential for generating future earthquakes, need to be evaluated. Besides the annual occurrence rate, the possible maximum earthquake magnitude, the characteristics of the fault mechanism and attenuation characteristics (i.e., tectonic regionalization) need to be defined for each seismic source (Figure 5.3).

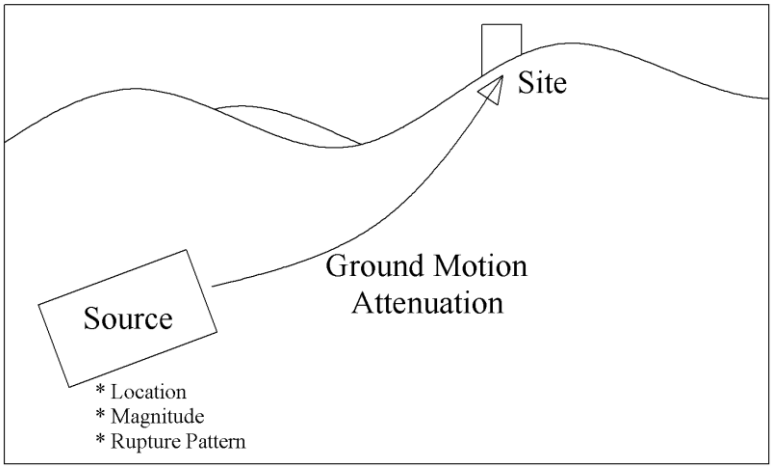

Figure 5.3. Ground motion propagation

The geometry of the seismic sources can be modelled under three basic categories, which are point sources (usually developed as a grid of points), linear sources (fault model) and area sources (areal zonation model). In general, area sources are used to define the seismicity for the earthquakes which cannot be associated with a well-defined fault source, and these types of zones are assumed that they have homogeneous seismic activity whereas,

the linear sources are used to model seismicity of well-defined faults, such as the boundary lines of tectonic plates (Baker, 2008).

In early seismic hazard assessment studies, due to the lack of comprehensive active faulting data, seismic sources were generally defined as area sources (Erdik et al., 1985). Today, with advancements in geophysical engineering, GPS and geographic information system (GIS) technology, we know more about active faults in terms of their geometry and kinematic properties (mechanism and slip rate) and thus have the ability to define those fault lines as separate fault sources besides area sources (Emre et al., 2016). This opportunity allows us to estimate more realistic scenarios closer to possible earthquake foci in our analyses.

The seismic source models to conduct the PSHA of this thesis are adopted from the source models developed for "the Revision of Turkish Seismic Hazard Map Project (UDAP-Ç-13-06)" (Şeşetyan et al., 2018; Demircioğlu et al., 2018).

5.2.1. The Area Source Model

Primarily, to define the area source model for the analysis of this thesis, the source models delineated by Şeşetyan et al. (2018) are evaluated. Şeşetyan et al. (2018) used "the Seismotectonic Database of Turkey" delineated by Duman et al. (2016) and the active fault database of Turkey compiled by Emre et al. (2016) to delineate the area sources (Şeşetyan et al., 2018). Being the first seismotectonic database compiled for Turkey, Duman et al. (2016) defined seismotectonic regions, in which there are 18 major regions, for the territory of Turkey and delineated those regions using the Geographic Information System (GIS) (Duman et al., 2016). "The Active Fault Database of Turkey (Emre et al., 2016)" used in this study includes the combination of 1964 active fault base maps and the basic parameters of the faults like length, activity or buffer zones and the fault source models which are transferred into the electronic environment including all these identifications of those by using the GIS technology (Emre et al., 2016).

The study region is defined with the green border and the area sources, which are compiled from the Şeşetyan et al. (2018) study that intersect with this area and the location

of the catalog earthquakes are presented in Figure 5.4. While there are also subduction interface and subduction in-slab (deep) tectonic regions, in Turkish territory, the Marmara region lies on the active shallow crustal part and all the area sources evaluated in this study are active shallow crustal sources which are within the upper 0-25km part of the earth's crust (Şeşetyan et al., 2018). The hypocentral depth distributions are studied for the area sources, and three levels of depths with associated percentages of earthquake occurrences are assigned to each source (Şeşetyan et al., 2018).

Considering the study region, a need for editing the original sources has arisen. The area sources, which are partially within the study region are clipped by the study region except for the sources, which have relatively fewer earthquake records to obtain satisfactory annual earthquake occurrence statistics. The sources that thus remained unchanged are BGRAS043, BGRAS048, BGRAS078 and GEOAS019 (Figure 5.5). Moreover, after the clipping process, the area sources named TURAS093, TURAS094 and TURAS104 are considered as a combined single area source with the name of NEWTURAS. Being located in the middle of the NEWTURAS source and being the largest contributor to its area, the distribution of nodal planes (strike, dip and rake) and the depth distribution of this new source are taken from the source TURAS093.

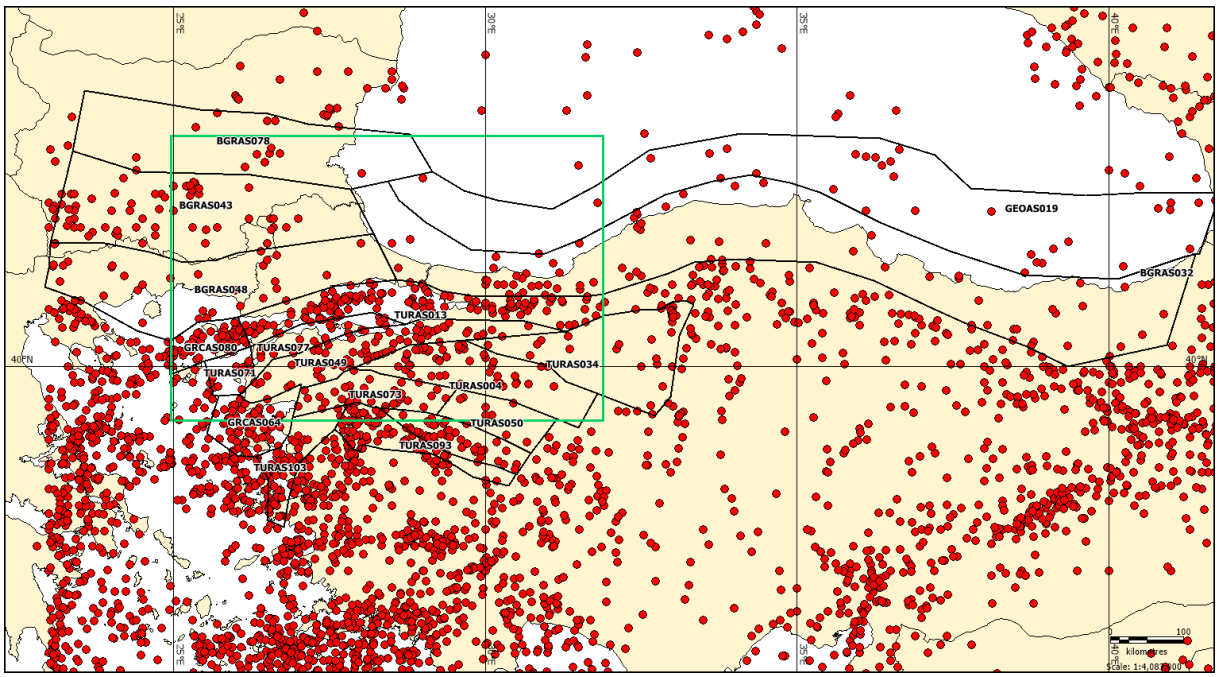

Figure 5.4. The study region, earthquake catalog and the area sources by Şeşetyan et al. (2018)

As a result of the assessment made, the area source model was revised in the GIS environment, and the final area source boundaries and their placement on the map are presented in Figure 5.5. All geometric and kinematic properties (e.g., depth and mechanical distributions) of the area source zones are adopted from the model proposed by Şesetyan et al. (2018). 666 earthquake records are obtained from the homogenized and declustered final catalog mentioned in Section 5.1 after evaluating it within the boundaries of these final area sources.

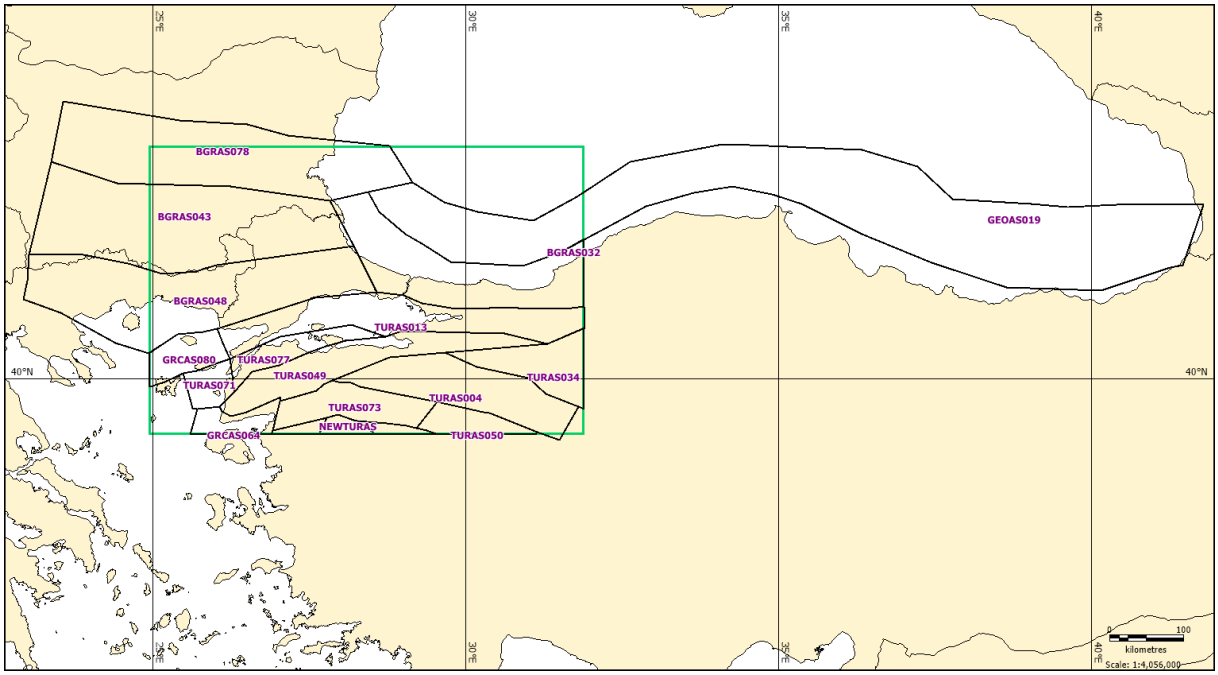

Figure 5.5. Revised area sources (in black) and the study region (in green)

Following the identification of the area sources and the corresponding earthquake catalog, the maximum magnitude potential is evaluated for each area source. The maximum magnitude (Mwmax), that could take place within a source zone within the range of possibility is a fundamental parameter considering the effect on the source characterization and hence, on the hazard level that will be calculated as the result of a SHA (Demircioğlu et al., 2018; Şeşetyan et al., 2018). The Mwmax designated for a source should capture all observed events and also correspond to the dimensions of known faults in the source zone.

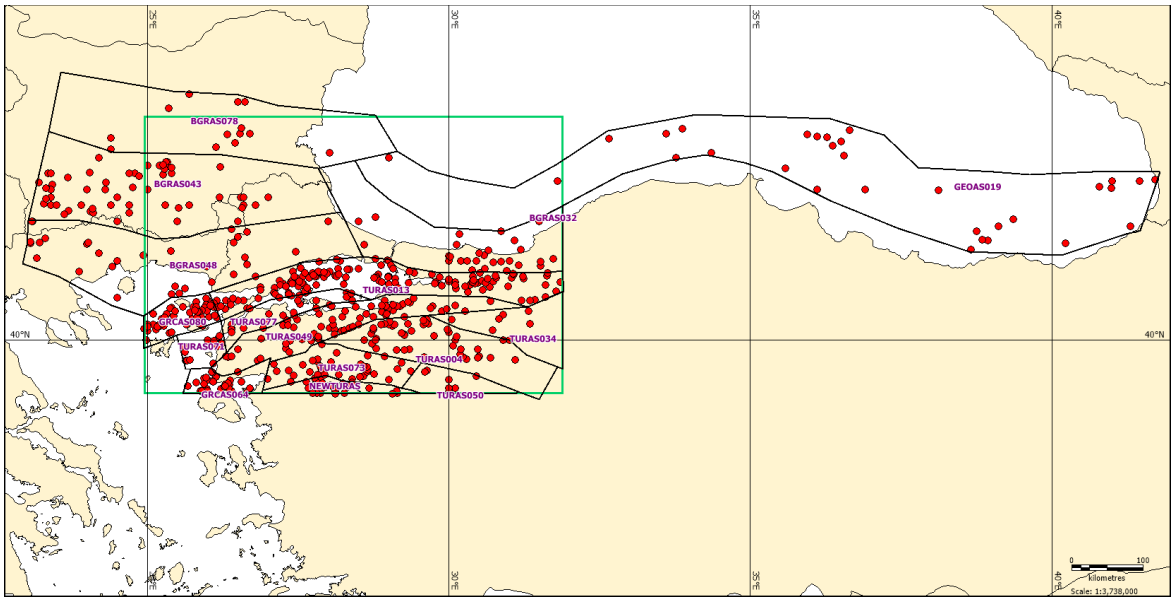

Figure 5.6. The final earthquake catalog to be used for area source recurrence analysis

The earthquake records are examined considering the seismicity of the sources, and as a result, two historical earthquake records are decided to be revised in terms of the area sources they are in. These are the 1692 Mw 7.2 earthquake, whose assumed epicenter was within the TURAS071 area source was moved to GRCAS066 source, and the 1737 Mw 7.4 earthquake with assumed epicenter in TURAS077 was moved to the source TURAS049. As it will be explained in the magnitude frequency distribution section, four area source pairs are decided to be handled together to determine the recurrence frequency distributions of them. With the evaluation of the four area source pairs together, the larger maximum magnitudes of the source pairs are taken to estimate the recurrence parameters of the sources to capture all records in the source pairs. As a result, the maximum magnitudes are examined according to the observed events, fault lengths and the maximum magnitude levels determined by Şeşetyan et al. (2018) and three levels of maximum magnitudes with 0.3 unit increments are decided to be evaluated as an epistemic uncertainty for the PSHA. The resulting maximum magnitudes are presented in Table 5.2.

The minimum completeness magnitude of the catalog to be used in earthquake recurrence parameters is determined as 4.3 Mw, similar to the study by Şeşetyan et al. (2018). In the further stages of the study, when the earthquakes within the BGRAS043 area source were examined, due to the inadequacy of the small magnitude earthquake records and its misleading effects on the Guttenberg-Richter recurrence parameters obtained when

compared with the annual earthquake numbers at the source, the corner magnitude for this source was revised as 4.5 Mw.

Table 5.2. The resulting maximum magnitudes with the maximum magnitudes evaluated for each area sources

Area Source ID	Şeşetyan, et al. (2018)			Mwmax Observed Within the Study Region	Mwmax Obtained From the Fault Length	Mwmax Observed Within the Area Sources Delineated by Şeşetyan, et al. (2018)	The Final Maximum Magnitude		
	Mwmax Level 1	Mwmax Level 2	Mwmax Level 3				Mwmax Level 1	Mwmax Level 2	Mwmax Level 3
BGRAS032	*6.0*	*6.3*	*6.6*	*5.6*	*7.0*	*6.5*	7.0	7.3	7.6
BGRAS043	*7.0*	*7.3*	*7.6*	*7.0*	*7.3*	*7.0*	7.3	7.6	7.9
BGRAS048	*7.0*	*7.3*	*7.6*	*7.1*	*7.6*	*7.1*	7.6	7.9	8.2
BGRAS078	*7.0*	*7.3*	*7.6*	*6.1*	*7.3*	*6.9*	7.3	7.6	7.9
GEOAS019	*7.0*	*7.3*	*7.6*	*5.6*	*8.0*	*5.6*	7.3	7.6	7.9
GRCAS064	*7.0*	*7.3*	*7.6*	*6.7*	*7.1*	*7.0*	7.5	7.8	8.1
GRCAS080	*7.0*	*7.3*	*7.6*	*6.8*	*7.5*	*6.8*	7.5	7.8	8.1
TURAS004	*7.0*	*7.3*	*7.6*	*7.1*	*7.1*	*7.1*	7.3	7.6	7.9
TURAS013	*7.4*	*7.7*	*8.0*	*7.6*	*7.6*	*7.6*	7.8	8.1	8.4
TURAS034	*6.0*	*6.3*	*6.6*	*5.8*	*6.8*	*6.0*	7.1	7.4	7.7
TURAS049	*7.0*	*7.3*	*7.6*	*7.4*	*7.2*	*7.0*	7.5	7.8	8.1
TURAS050	*7.0*	*7.3*	*7.6*	*5.7*	*7.1*	*6.6*	7.1	7.4	7.7
TURAS071	*7.0*	*7.3*	*7.6*	*7.2*	-	*7.2*	7.0	7.3	7.6
TURAS073	*7.0*	*7.3*	*7.6*	*6.6*	*6.9*	*6.6*	6.9	7.2	7.5
TURAS077	*7.0*	*7.3*	*7.6*	*7.4*	-	*7.4*	7.0	7.3	7.6
NEWTURAS	*7.0*	*7.3*	*7.6*	6.9	7.1	7.0	7.1	7.4	7.7
TURAS093	*7.0*	*7.3*	*7.6*	*6.9*	*7.1*	*6.9*			
TURAS094	*7.0*	*7.3*	*7.6*	*5.6*	*6.9*	*7.0*			
TURAS103	*7.0*	*7.3*	*7.6*	*4.6*	*7.0*	*6.8*			

The depth distribution of earthquakes within the area sources mentioned above, predominant strike and dip angles and the faulting mechanisms with the probability distributions are adopted from Şeşetyan et al. (2018), which were based on the data provided in “the Active Fault Database of Turkey” (Emre et al., 2016).

5.2.1.1. Magnitude Frequency Distribution and the Completeness Assessment of Area Sources.

Before calculating the magnitude frequency distribution, the completeness model taken from the study by Şeşetyan et al. (2018) is re-evaluated for each area source. As a result of the evaluation, considering that different completeness models could be adopted for certain sources, modified alternative completeness periods and alternative magnitude bins are evaluated for the sources BGRAS032, BGRAS043, TURAS004 and TURAS073 and alternative completeness models are developed (Figure 5.7 to Figure 5.10).

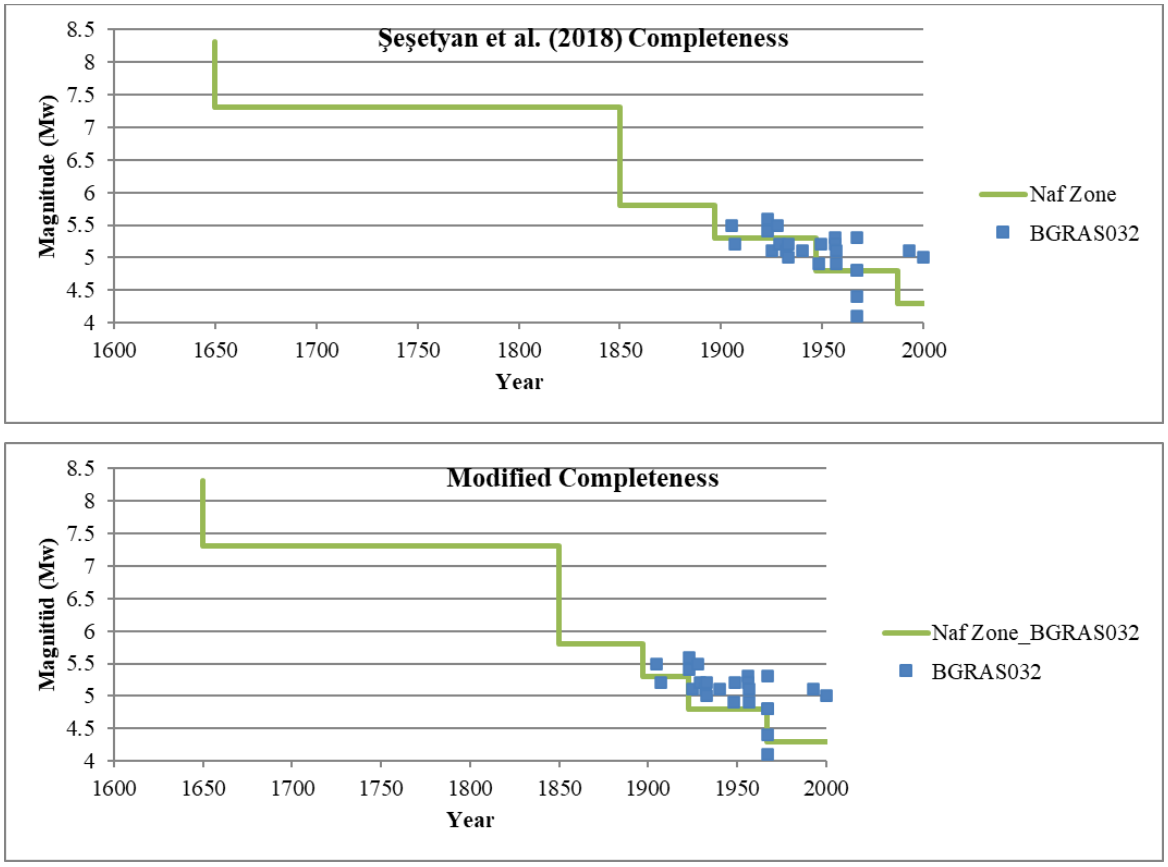

Figure 5.7. The completeness periods with the earthquake histories of BGRAS032; top chart: the completeness periods from the study by Şeşetyan et al. (2018), lower chart: the completeness periods from modified completeness

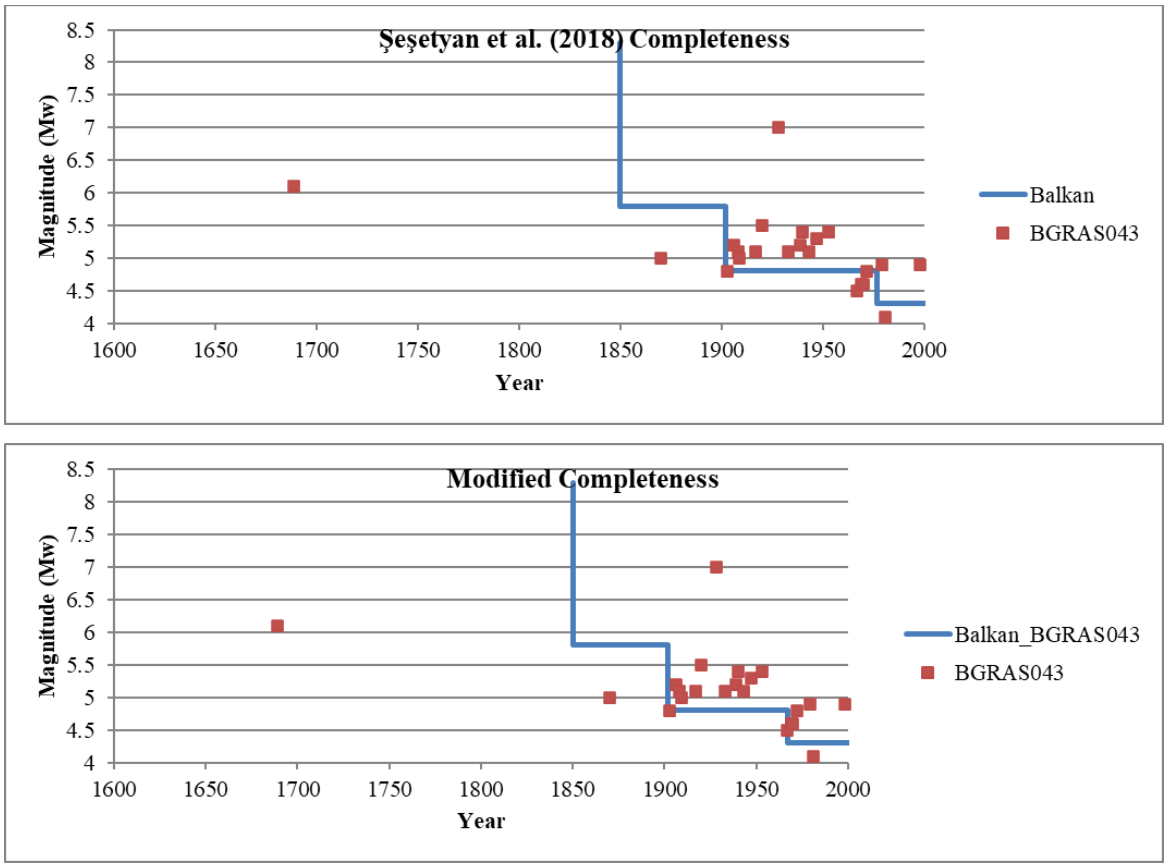

Figure 5.8. The completeness periods with the earthquake histories of BGRAS043; top chart: the completeness periods from the study by Şeşetyan et al. (2018), lower chart: the completeness periods from modified completeness

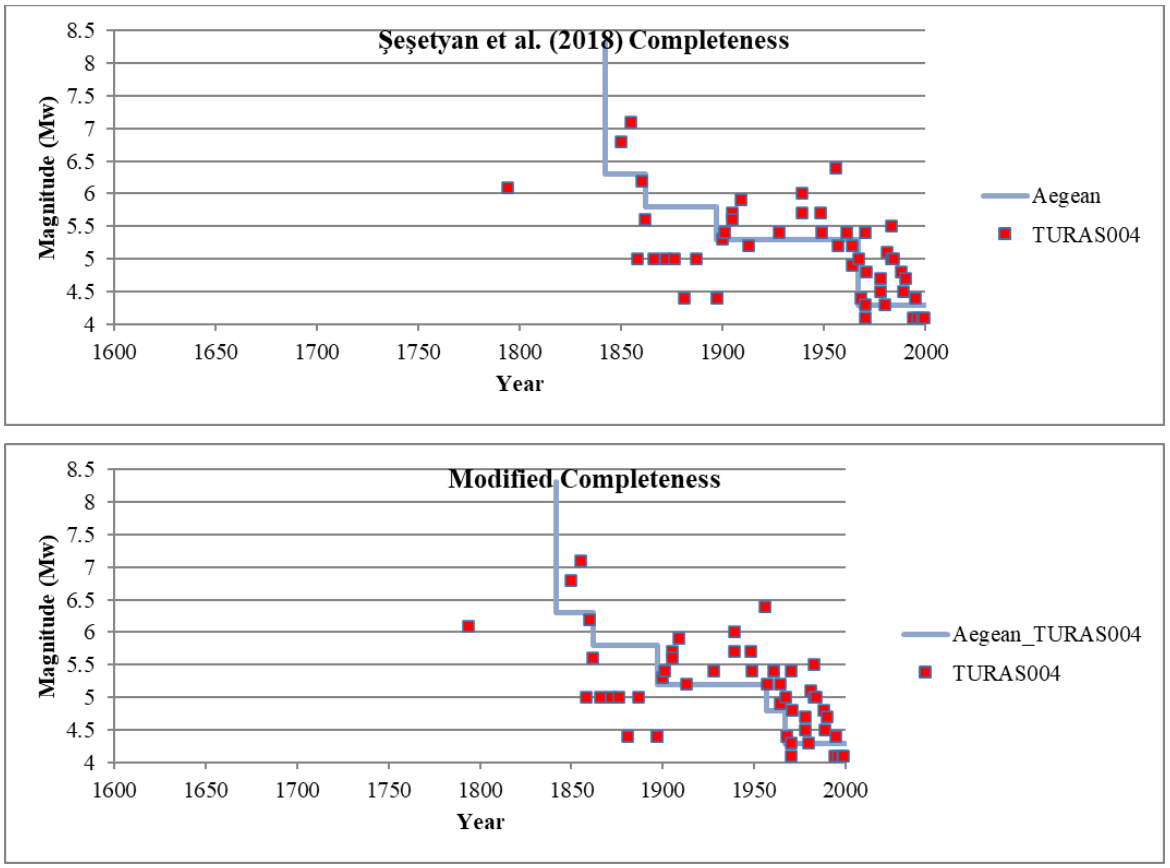

Figure 5.9. The completeness periods with the earthquake histories of BGRAS043; top chart: the completeness periods from the study by Şeşetyan et al. (2018), lower chart: the completeness periods from modified completeness

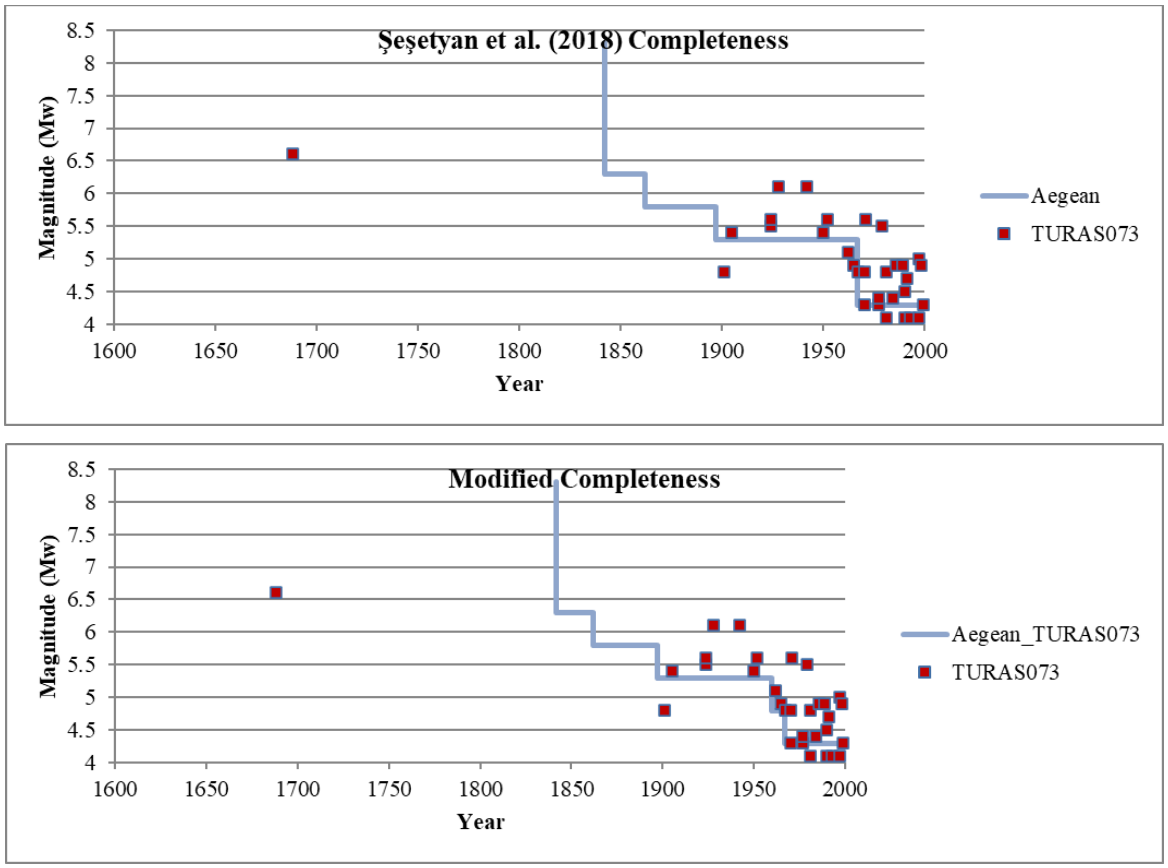

Figure 5.10. The completeness periods with the earthquake histories of TURAS073; top chart: the completeness periods from the study by Şeşetyan et al. (2018), lower chart: the completeness periods from modified completeness

In addition to the visual modification process for area sources, being the source, which has observed more earthquakes compared to the other area sources examined in this thesis, the Stepp (1972) procedure is conducted to re-examine completeness intervals for the source TURAS013. Moreover, the completeness periods determined by visually checked by a Stepp (1972) methodology is examined comparing the earthquake history with the completeness periods as done for the previous modifications, and a modified completeness is also came out from this process. The Stepp (1972) is method that is evaluated based on the exponential distribution of catalog earthquakes according to the magnitude versus time, based on the Guttenberg Richter (1954) relationship principles and represented for TURAS013 in Figure 5.11 and Figure 5.12.

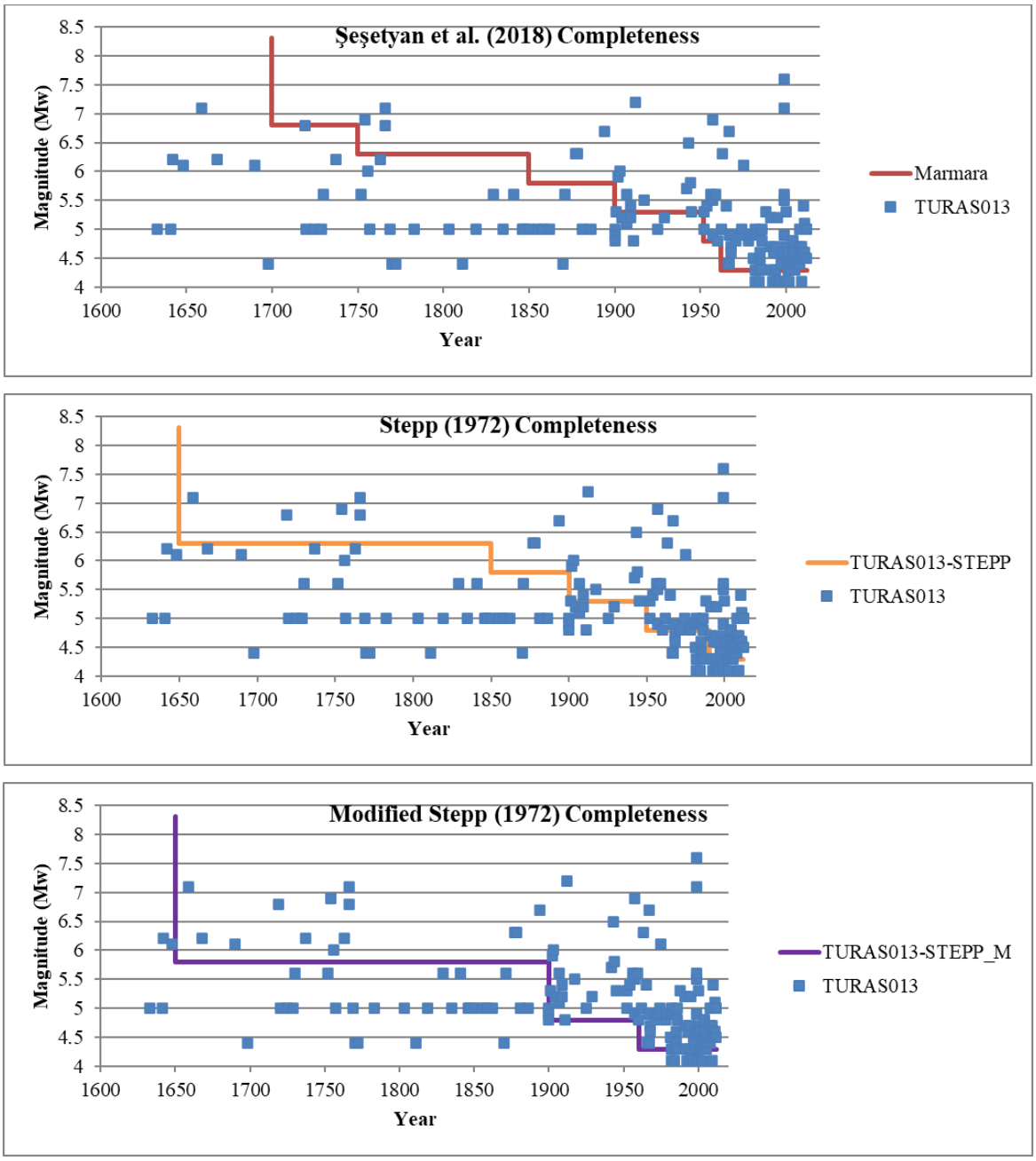

Figure 5.11. The Şeşetyan et al. (2018) completeness and the alternative models derived with the implementation of Stepp (1972) and modified Stepp (1972) analysis completeness periods with the earthquake histories of the modified sources

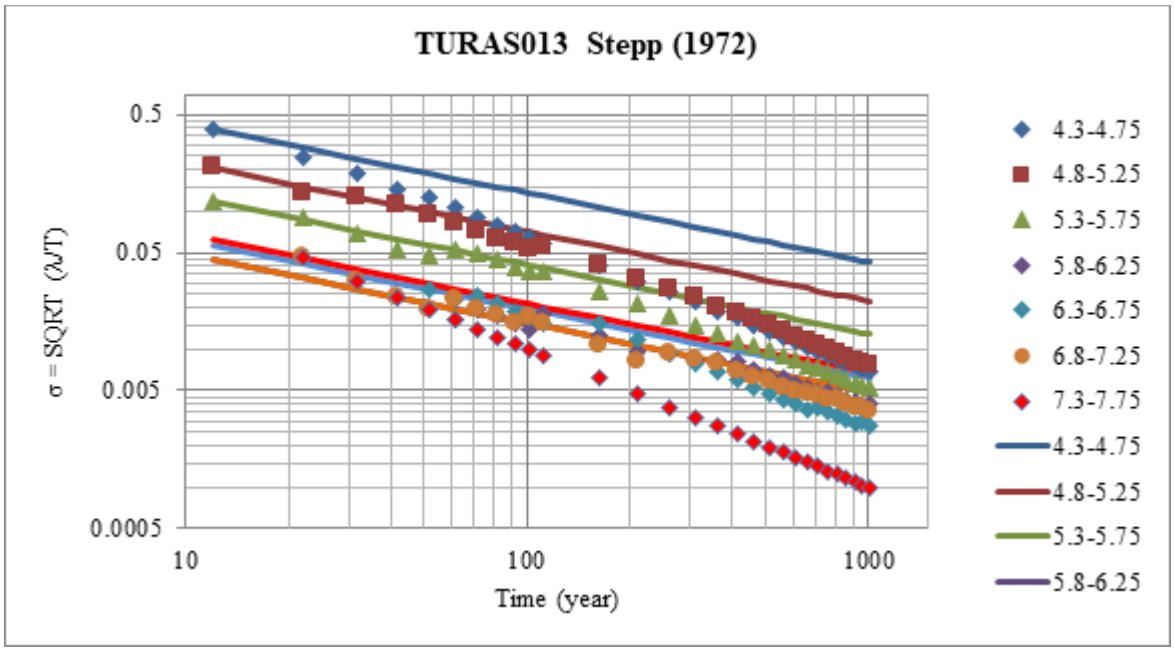

Figure 5.12. TURAS013 Stepp (1972) analysis

All the alternative completeness periods and the completeness modes conducted by Şeşetyan et al. (2018) are handled as epistemic uncertainties in the PSHA model.

Following the delineation of a seismic source, the magnitude frequency distribution (also can be called "the magnitude probability density function") of the source needs to be defined. As a seismic source can generate earthquakes with various magnitudes, with the evaluation of the magnitude recurrence relationship parameters of a source, the annual number of occurrences of any earthquake magnitude can be determined. The truncated exponential recurrence model by Gutenberg and Richter (1954) is used in this thesis to obtain the recurrence parameters of a source, i.e., to define "the magnitude frequency distribution" of the source. The Gutenberg-Richter (1954) relation is given in equation (2). Here, λ_M determines the annual rate of earthquakes, a means the absolute seismicity level, and b is the slope of the magnitude probability density function curve.

$$\log \lambda_M = a - bM \tag{2}$$

In this thesis, the method by Weichert (1980), which is one of the methods to obtain Gutenberg-Richter recurrence parameters, based on the maximum likelihood approach, is

chosen. The method Weichert (1980) allows for the use of different completeness periods for different magnitude ranges. With this method, besides the mean Gutenberg-Richter law mean recurrence parameters, the standard deviations of these parameters are also obtained. In the present study, the standard deviation of the b value is treated as an epistemic uncertainty parameter and mean, mean +1σ and mean -1σ b values are used in the logic tree. The earthquake recurrence parameters are obtained separately for the three levels of Mwmax assigned to each source.

The recurrence models of sources BGRAS032 and TURAS013 are presented in Figure 5.13 and Figure 5.14, respectively, for the alternative completeness models derived.

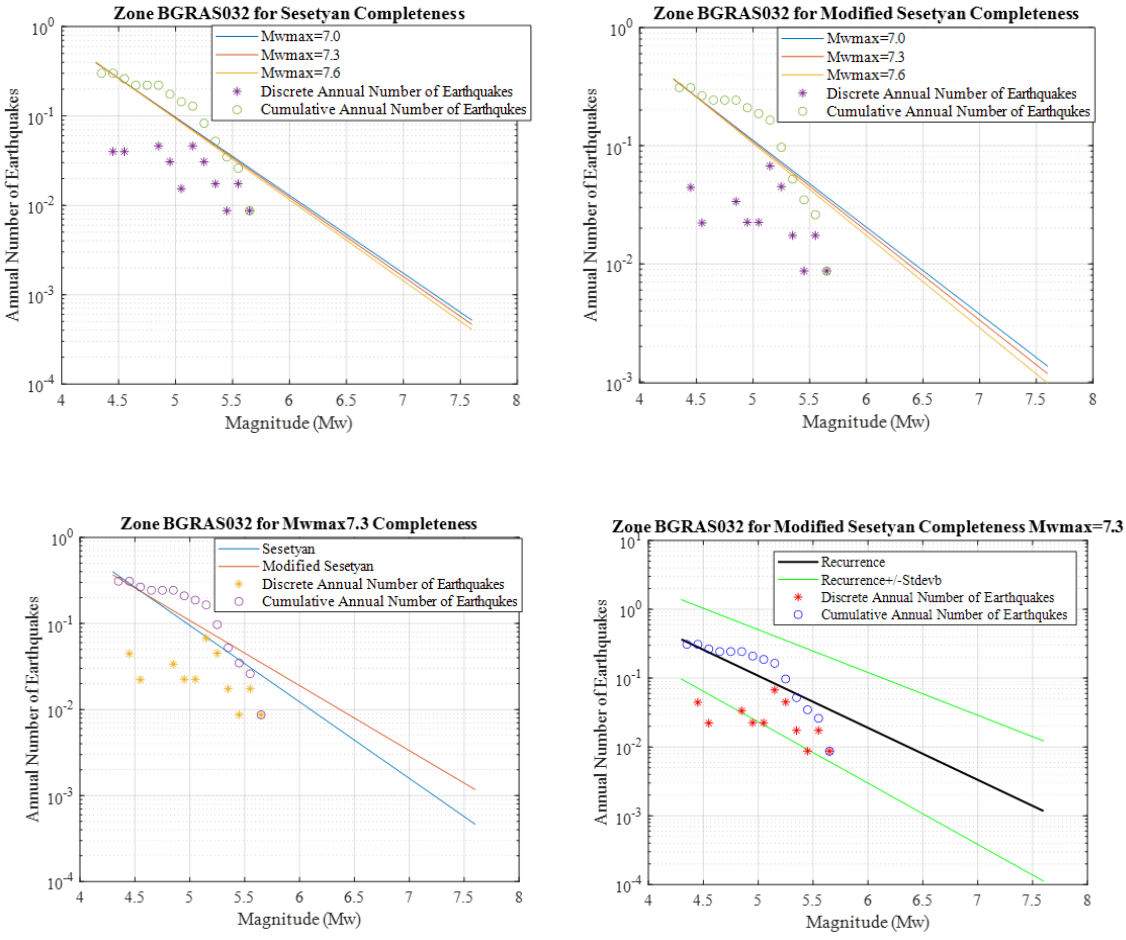

Figure 5.13. The earthquake recurrence data of BGRAS032 area source with completeness model and maximum magnitude alternatives

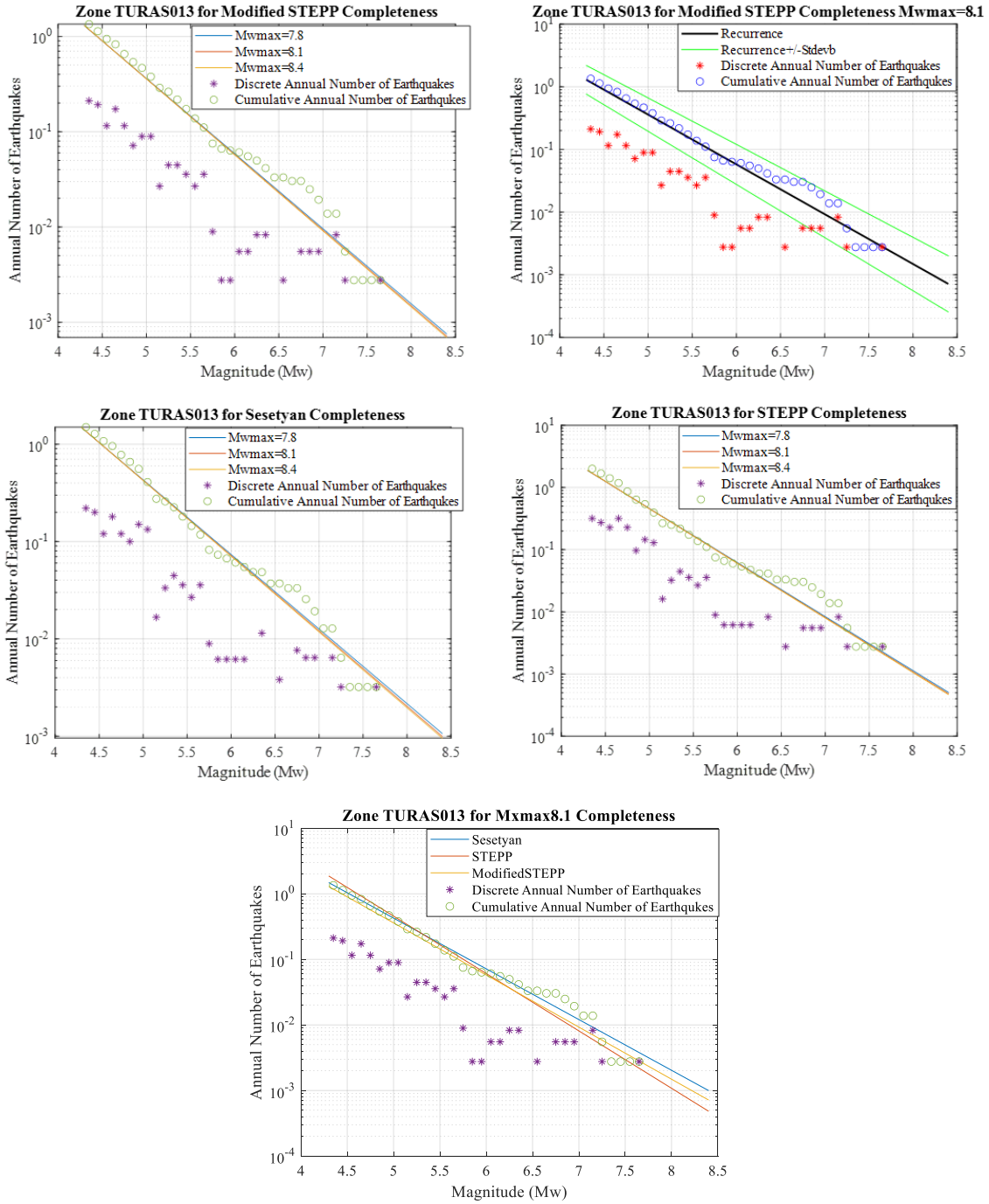

Figure 5.14. The earthquake recurrence data of TURAS013 area source with completeness model and maximum magnitude alternatives

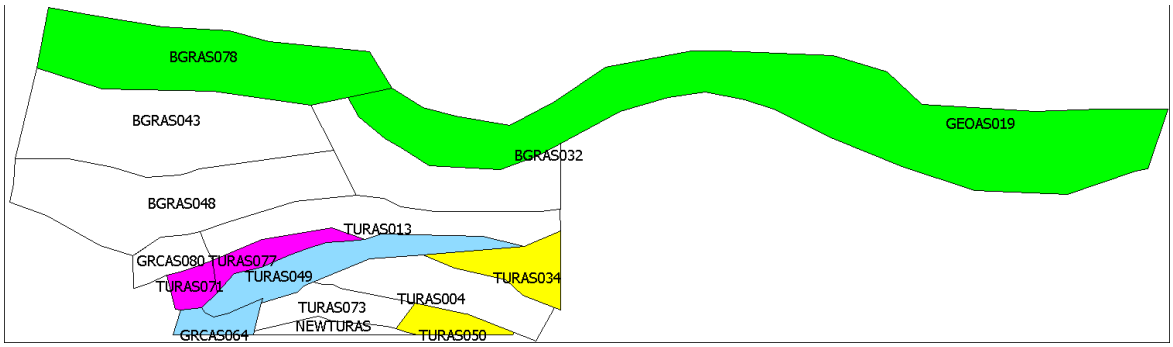

Figure 5.15. The linked area source couples for Guttenberg-Richter recurrence parameters calculation

In the light of the recurrence parameters obtained, the historical earthquakes that occurred at each area source are re-evaluated and four couples of sources with similar properties are decided to be considered as linked sources to build the magnitude probability density functions. The area source couples decided to be linked are BGRAS078-GEOAS019, GRCAS064-TURAS049, TURAS050-TURAS034 and TURAS071-TURAS077 as grouped and colored in Figure 5.15. For these sources, the b values and standard deviations are recalculated with the combined catalogs, and the seismicity rates (the 10^a value of the Guttenberg-Richter recurrence law) of those sources are redistributed in the light of the "b" parameters obtained and the total number of earthquakes in each of the source pairs. The completeness regions to which the area source pairs would be linked and maximum magnitudes of the combined sources were also evaluated, and the completeness periods and maximum magnitudes that could cover more earthquake numbers were selected among the alternatives. The results for these area sources obtained using Weichert (1980) method are listed in Table 5.3, and the redistributed "a" values are presented in Table 5.4.

Recurrence models for alternative maximum magnitudes and mean and ± 1standard deviation curves obtained for the four area source pairs thus treated are presented in Figure 5.16 to Figure 5.19.

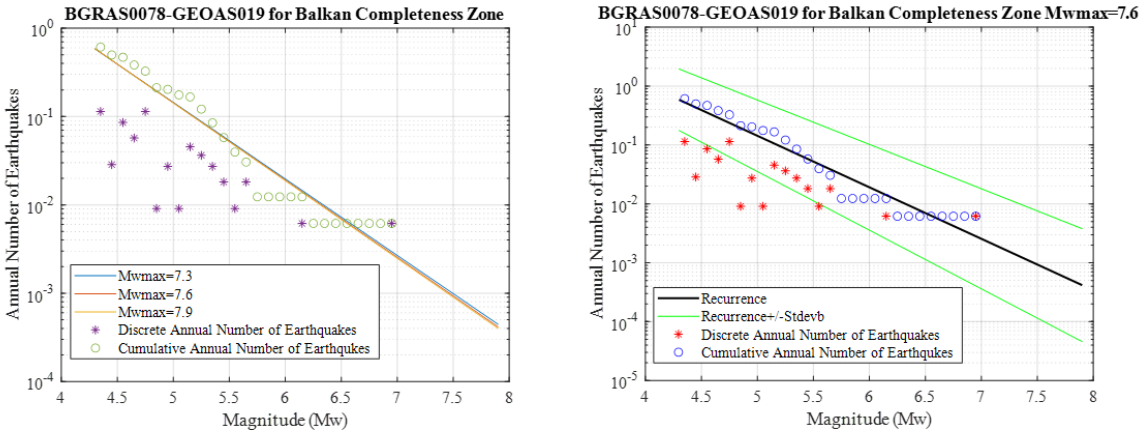

Figure 5.16. Recurrence models for linked area sources BGRAS078 and GRCAR019; left: for alternative maximum magnitudes, right: mean recurrence and ± 1standard deviation

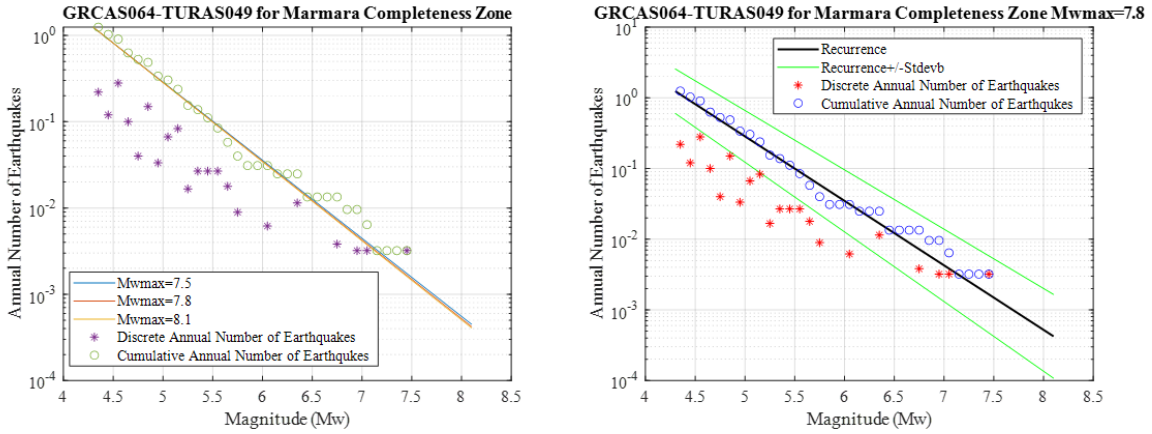

Figure 5.17. Recurrence models for linked area sources GRCAS064 and TURAS049; left: for alternative maximum magnitudes, right: mean recurrence and ± 1standard deviation

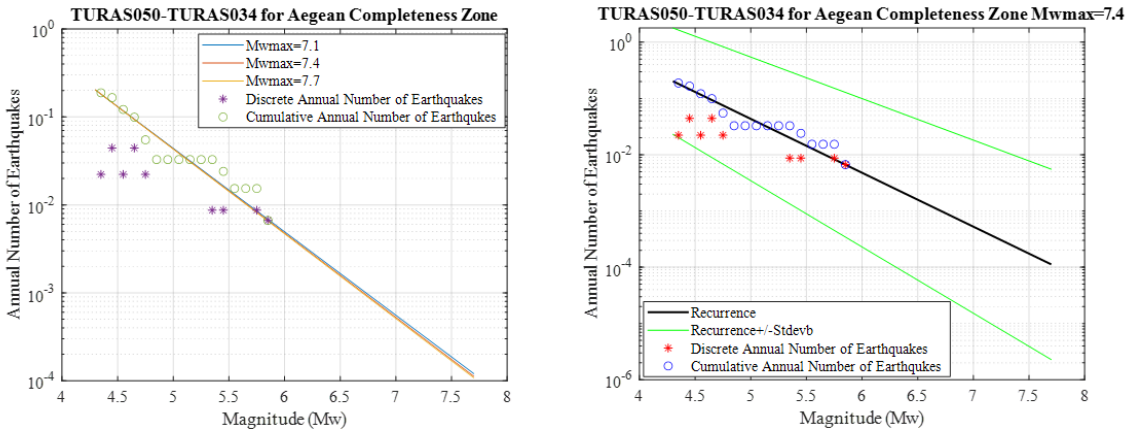

Figure 5.18. Recurrence models for linked area sources TURAS050 and TURAS034; left: for alternative maximum magnitudes, right: mean recurrence and ± 1standard deviation

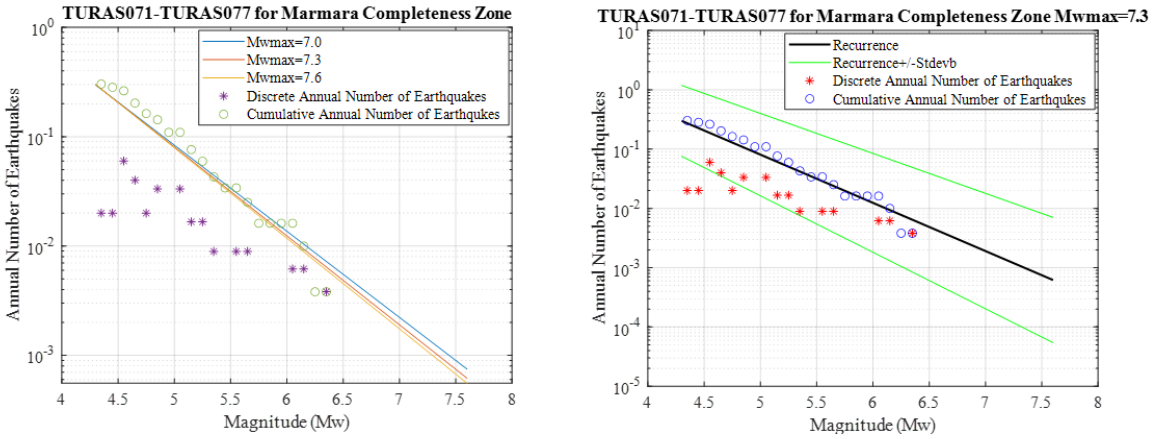

Figure 5.19. Recurrence models for linked area sources TURAS071 and TURAS077; left: for alternative maximum magnitudes, right: mean recurrence and ± 1standard deviation

The resulting recurrence parameters of area sources and maximum magnitudes for each completeness zone alternatives are presented in APPENDIX A: RECURRENCE PARAMETERS OF AREA SOURCES.

Table 5.3. Linked area source Weichert recurrence parameter outputs

BGRAS078-GEOAS019 Linked Catalog Weichert Recurrence Parameter Outputs						
Mw(Max)	Completeness	a	b	Stdev(b)	b+bStdev	b-bStdev
7.3	Balkan	3.4906	0.8660	0.1233	0.9893	0.7427
7.6	Balkan	3.5293	0.8747	0.1214	0.9961	0.7533
7.9	Balkan	3.5514	0.8796	0.1201	0.9997	0.7595
GRCAS064-TURAS049 Linked Catalog Weichert Recurrence Parameter Outputs						
Mw(Max)	Completeness	a	b	Stdev(b)	b+bStdev	b-bStdev
7.5	Marmara	3.9868	0.9054	0.0742	0.9796	0.8312
7.8	Marmara	4.0190	0.9127	0.0732	0.9859	0.8395
8.1	Marmara	4.0371	0.9168	0.0725	0.9893	0.8443
TURAS050-TURAS034 Linked Catalog Weichert Recurrence Parameter Outputs						
Mw(Max)	Completeness	a	b	Stdev(b)	b+bStdev	b-bStdev
7.1	Aegean	3.3871	0.9488	0.2232	1.1720	0.7256
7.4	Aegean	3.4278	0.9581	0.2198	1.1779	0.7383
7.7	Aegean	3.4500	0.9631	0.2176	1.1807	0.7455
TURAS071-TURAS077 Linked Catalog Weichert Recurrence Parameter Outputs						
Mw(Max)	Completeness	a	b	Stdev(b)	b+bStdev	b-bStdev
7.0	Marmara	2.8603	0.7876	0.1439	0.9315	0.6437
7.3	Marmara	2.9734	0.8134	0.1390	0.9524	0.6744
7.6	Marmara	3.0363	0.8277	0.1359	0.9636	0.6918

Table 5.4. Linked area source exponential redistribution of earthquake numbers for each Mwmax

Exponential Redistribution of Earthquake Numbers for Each Mwmax					
BGRAS078			GEOAS019		
Mw(Max)	Count	Resulting "a"	Mw(Max)	Count	Resulting "a"
7.3	12	2.9900	7.3	26	3.3258
7.6	12	3.0287	7.6	26	3.3645
7.9	12	3.0508	7.9	26	3.3866
GRCAS064			TURAS049		
Mw(Max)	Count	Resulting "a"	Mw(Max)	Count	Resulting "a"
7.5	24	3.4694	7.5	55	3.8295
7.8	24	3.5016	7.8	55	3.8617
8.1	24	3.5197	8.1	55	3.8798
TURAS050			TURAS034		
Mw(Max)	Count	Resulting "a"	Mw(Max)	Count	Resulting "a"
7.1	6	3.1239	7.1	5	3.0447
7.4	6	3.1646	7.4	5	3.0854
7.7	6	3.1868	7.7	5	3.1076
TURAS071			TURAS077		
Mw(Max)	Count	Resulting "a"	Mw(Max)	Count	Resulting "a"
7.0	7	2.4044	7.0	13	2.6732
7.3	7	2.5175	7.3	13	2.7863
7.6	7	2.5804	7.6	13	2.8492

5.2.2. The Fault Source Model

The fault source model of the "UDAP-Ç-13-06" project is developed by Demircioğlu et al. (2018) in the light of the studies, "the Seismotectonic Database of Turkey" by Duman et al. (2016) and "the Active Fault Database of Turkey" compiled by Emre et al. (2016). The fault source geometry as delineated by Demircioğlu et al. (2018) is evaluated within the boundaries of the study region, and the fault segments which are within or intersecting these boundaries are considered for the fault source analysis of this thesis. 95 fault sources were thus used in the fault source model (Figure 5.20).

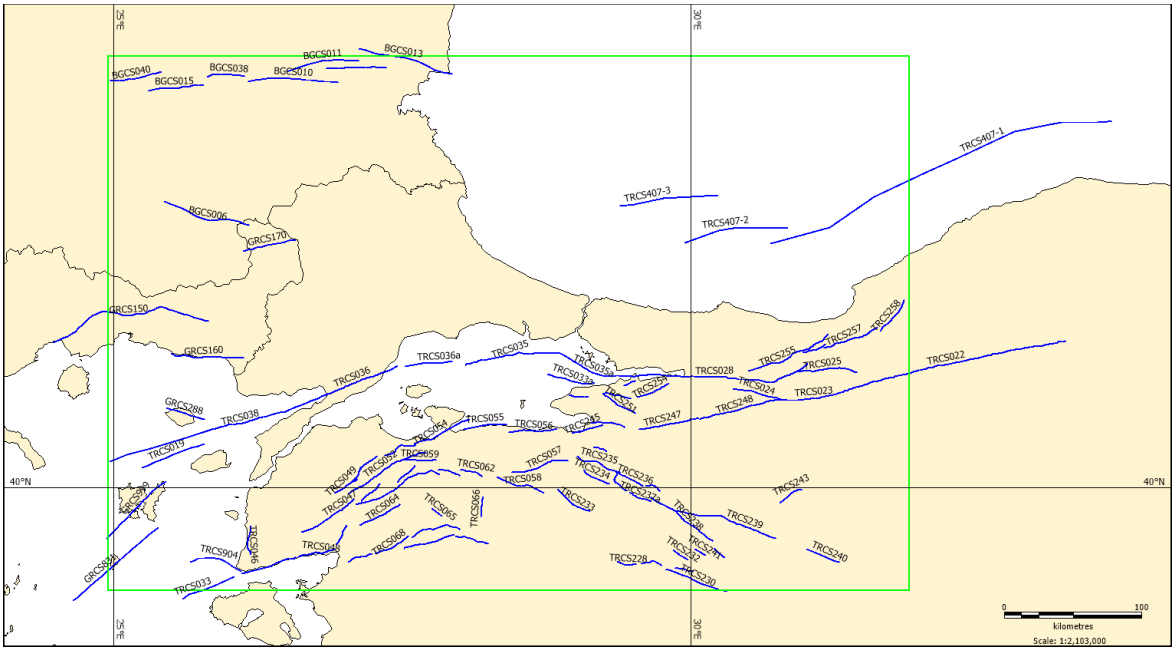

Figure 5.20. The fault sources to be evaluated and the study region settlement

In addition to the geometry, parameters related to each fault source, namely fault type, length, dip angle, mechanism, minimum and maximum GPS based slip rate were obtained from the studies mentioned above. The fault sources evaluated in this thesis are associated earthquakes in the active shallow crust with the depth distribution within 0 to 20 km. A buffer zone of 15km is generated around the surface projections of the fault sources (Figure 5.21), and earthquakes with Mw≥5.5 are associated with fault sources, while earthquakes with smaller magnitudes are modelled to occur in the buffer zones.

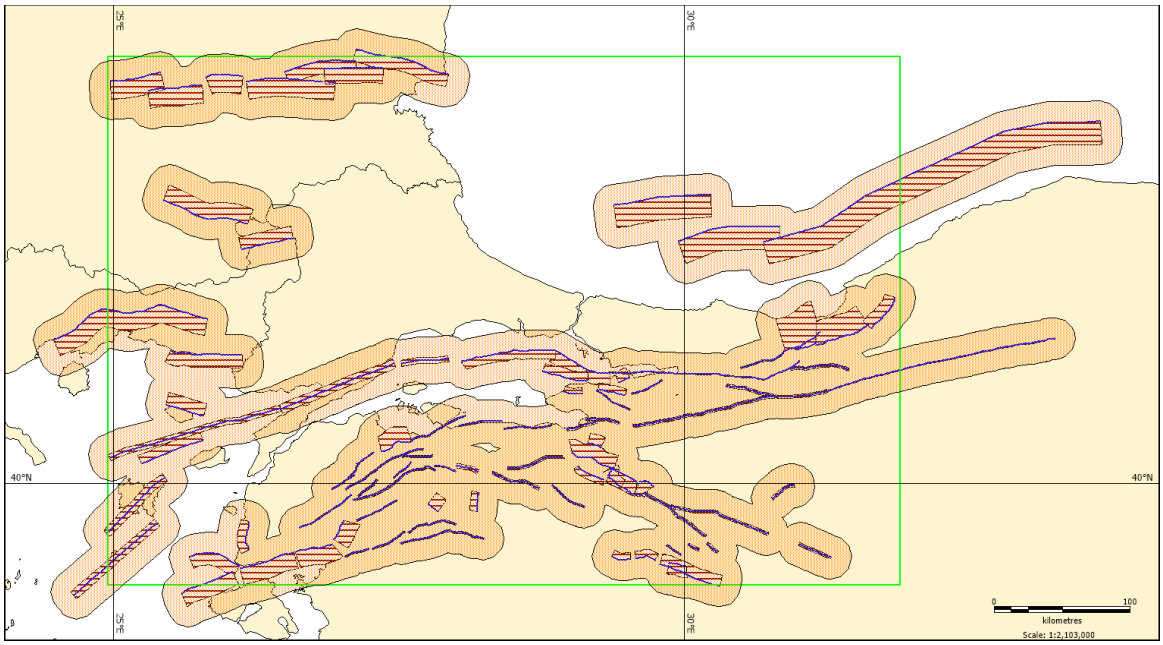

Figure 5.21. The representation of the fault sources with surface projection and 15km buffer zone

5.2.2.1. Magnitude Frequency Distribution of Fault Sources.

The earthquake catalog by Kadirioğlu et al. (2018) is used to examine the Guttenberg-Richter b value to be used in the earthquake recurrence modelling of the fault sources. Similar to the area sources, a reevaluation process is conducted for the completeness regions delineated in the "UDAP-Ç-13-06" project by Şeşetyan et al. (2018). Having a smaller number of observed seismicity within the study region, the completeness regions of Balkan Zone, Black Sea Zone, North Anatolian Fault Zone and Central Anatolia Zone are examined without any modification at the boundaries (no clipping), while the completeness regions of Marmara Zone and Aegean Region Zone are clipped at the study region boundaries. The resulting catalog obtained after the arrangements made consists of 1212 earthquakes (Figure 5.22).

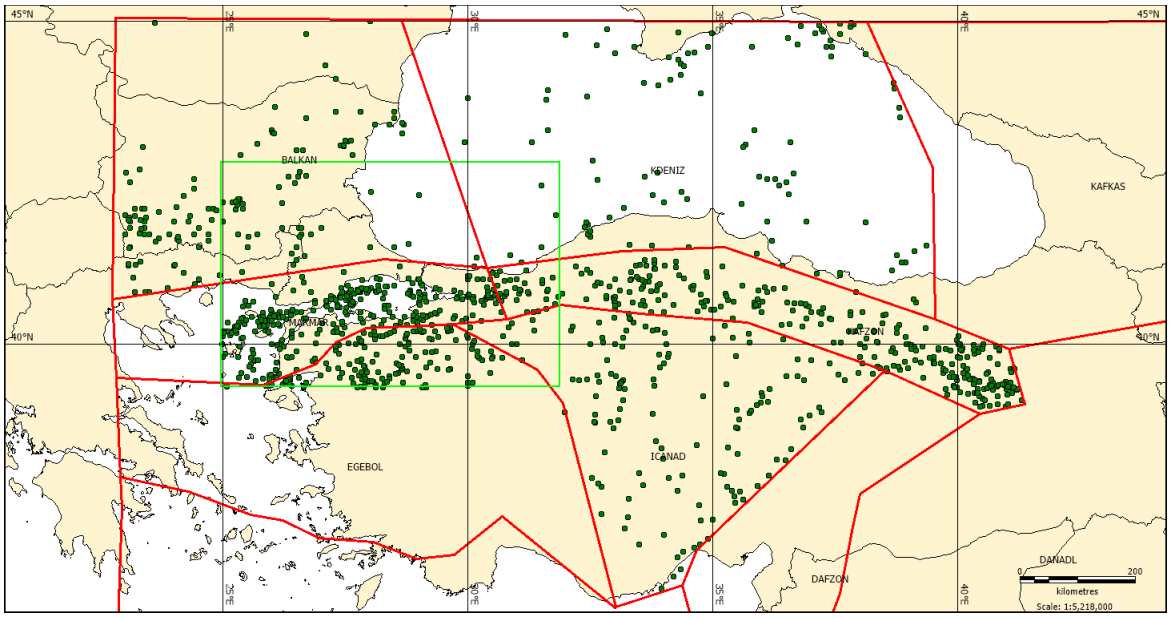

Figure 5.22. The earthquake catalog to be used to estimate b value of each completeness zone

The magnitude frequency distributions of the fault sources are obtained through the following steps:

First, the maximum magnitudes of the faults sources are calculated using “surface rupture length (SRL) versus magnitude” equations proposed by Wells and Coppersmith (1994). The parameters of these equations are represented in Table 5.5. Mean maximum magnitudes and their standard deviation are obtained with respect to the mechanism of each fault source.

Table 5.5. Wells and Coppersmith (1994) surface rupture length regressions

Equation	Slip Type	Num. Of Events	Coefficients and Standard Errors		Standard Deviation	Correlation Coefficient	Magnitude Range	Length/ Width Range(km)
			a(sa)	b(sb)	s	r		
M=a+b*log(SRL)	SS	43	5.16(0.13)	1.12(0.08)	0.28	0.91	5.6 to 8.1	1.3 to 432
	R	19	5.00(0.22)	1.22(0.16)	0.28	0.88	5.4 to 7.4	3.3 to 85
	N	15	4.86(0.34)	1.32(0.26)	0.34	0.81	5.2 to 7.3	2.5 to 41
	All	77	5.08(0.10)	1.16(0.07)	0.28	0.89	5.2 to 8.1	1.3 to 432

Second, Gutenberg-Richter b values are calculated for each completeness zone, using the Weichert (1980) method. To determine the maximum magnitude of a completeness zone (to be used for the b value computation), the highest mean maximum magnitude of the fault sources within each completeness zone is chosen. The completeness periods determined by Şeşetyan et al. (2018) are used with the earthquake catalog of each completeness zone, and the Gutenberg-Richter b values and their standard deviation are calculated. The maximum magnitudes assigned and the Guttenberg-Richter b values obtained for the completeness zones are shown in Table 5.6, while the resulting recurrence model and annual numbers of earthquakes for each completeness zone are presented in Figure 5.23.

Table 5.6. Guttenberg-Richter b recurrence parameters of the completeness zones

Fault Source Guttenberg-Richter Recurrence Parameters				
Completeness Zone	Mwmax	Mwmin	Stdev(b)	b
Balkan Region Zone	7.80	4.50	0.0707	0.8132
Black Sea Zone	8.00	4.50	0.126	0.9835
Marmara Zone	7.70	4.50	0.048	0.9116
North Anatolian Fault Zone	8.00	4.50	0.0471	0.7883
Aegean Region Zone	7.20	4.50	0.0759	0.8799
Central Anatolia Zone	6.60	4.50	0.101	0.9908

Finally, following the modelling choice in Demircioğlu et al. (2018), the magnitude frequency distributions of the fault sources are obtained using "the exponential magnitude distribution model" by Youngs and Coppersmith (1985). The fault activity rate calculation methodology, based on exponential magnitude distribution by Youngs and Coppersmith (1985), is given in the following equation (3).

$$N(\mathrm{m}^0) = \frac{\mu \mathrm{A_f} S(\mathrm{d}-\mathrm{b})[1-\mathrm{e}^{-\beta(\mathrm{m}^u-\mathrm{m}^0)}]}{\mathrm{b}\mathrm{M}_0^u \mathrm{e}^{-\beta(\mathrm{m}^u-\mathrm{m}^0)}} \quad (3)$$

The equation results in the annual number of events (N) for some arbitrary reference magnitude (m^0), which is taken as Mw 5.5, μ is the shear modulus, the fault area is $\mathrm{A_f} =$

LW, S is the slip rate of the fault, m^u refers to the maximum magnitude of the fault source, $\beta = b\ln(10)$, obtained for the corresponding completeness zone, and M_0 is the seismic moment corresponding to m^u.

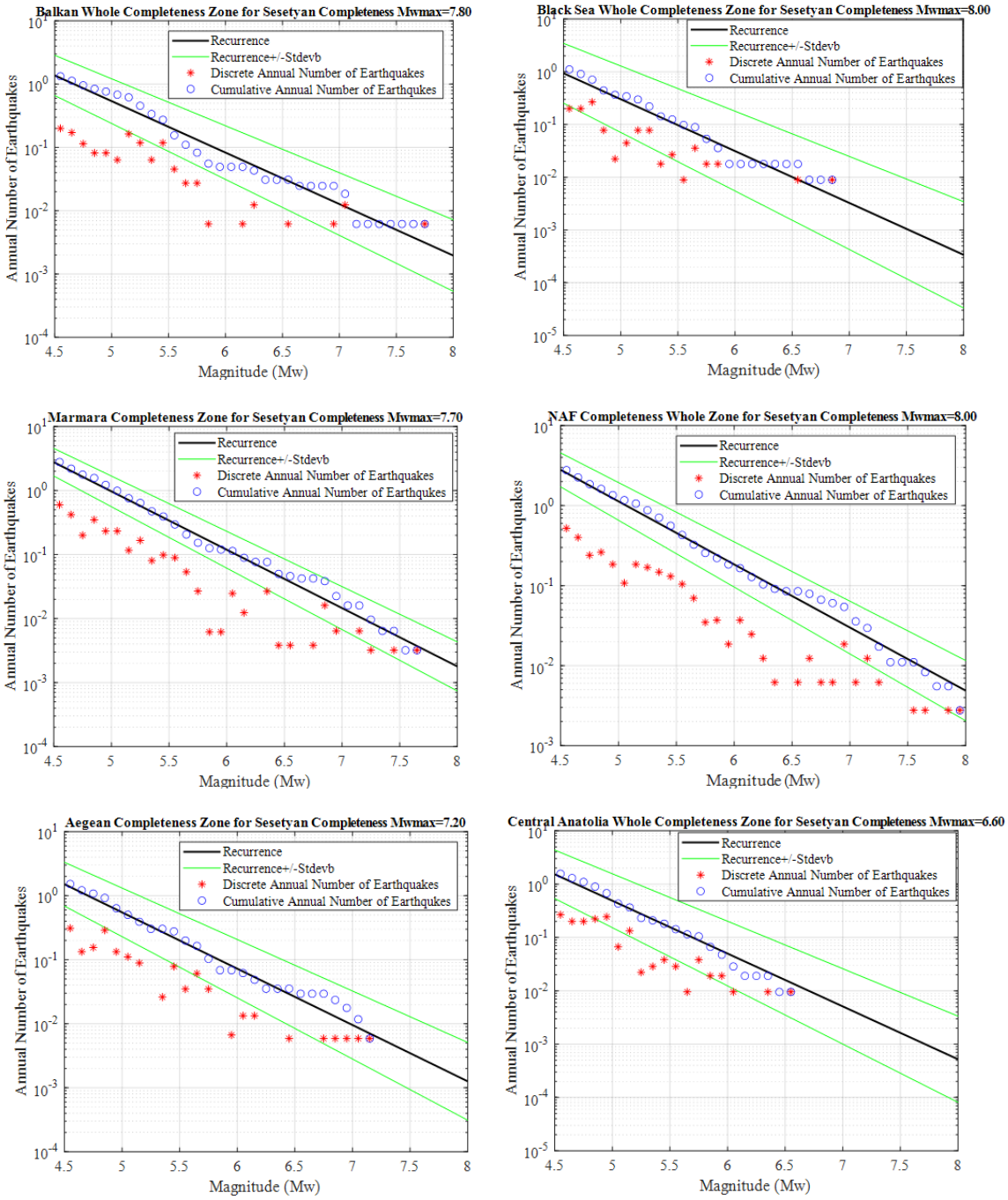

Figure 5.23. Earthquake recurrences with annual number of earthquakes for each completeness zone

As it can be seen in Eq. 3, the slip rate (S), the maximum magnitude (m^u) and the regional b value are the parameters controlling the earthquake recurrence modelling for the fault sources. Due to computation limitations, Demircioğlu et al. (2018) used only the mean values of these parameters, while in the present study, we investigate the effects of the uncertainties associated with each of these parameters.

For the slip rates, the minimum and maximum values compiled in the "UDAP-Ç-13-06" project are used. For the maximum magnitude, the mean and the ± 1 standard deviation values obtained from the "surface rupture length" based regression of Wells and Coppersmith (1984) are adopted. In the preliminary sensitivity studies, it was observed that, unlike the area sources, the standard deviations of the b value had only a minimal effect on the earthquake recurrence of the fault sources, as such the uncertainty of this parameter was not included in the final analysis.

The minimum magnitude assigned to the fault sources was Mw 6.0 in Demircioğlu et al. (2018). In the present study, Mw 5.5 was adopted as the minimum magnitude of the fault sources (m^0), as this value was more compatible with the smallest maximum magnitude (the mean – 1 standard deviation) of the fault source model.

To exemplify the epistemic uncertainty ranges introduced in the magnitude frequency distribution of the fault sources, through consideration of maximum magnitude and slip rate uncertainties, the activity rates of the sources closest to Istanbul city center (TRCS035 and TRCS035a) and two sources with high seismicity, which are passing through the Gulf of İzmit (TRCS028) and the Gallipoli peninsula (TRCS036) highlighted in Figure 5.24 are presented in Figure 5.25. The truncated exponential recurrence rates obtained from the combination of three maximum magnitude levels and two slip rates are introduced as alternative branches of the fault source model logic tree in the final analysis.

The resulting recurrence parameters of fault sources as obtained in the study are presented in APPENDIX B: RECURRENCE PARAMETERS OF FAULT SOURCES.

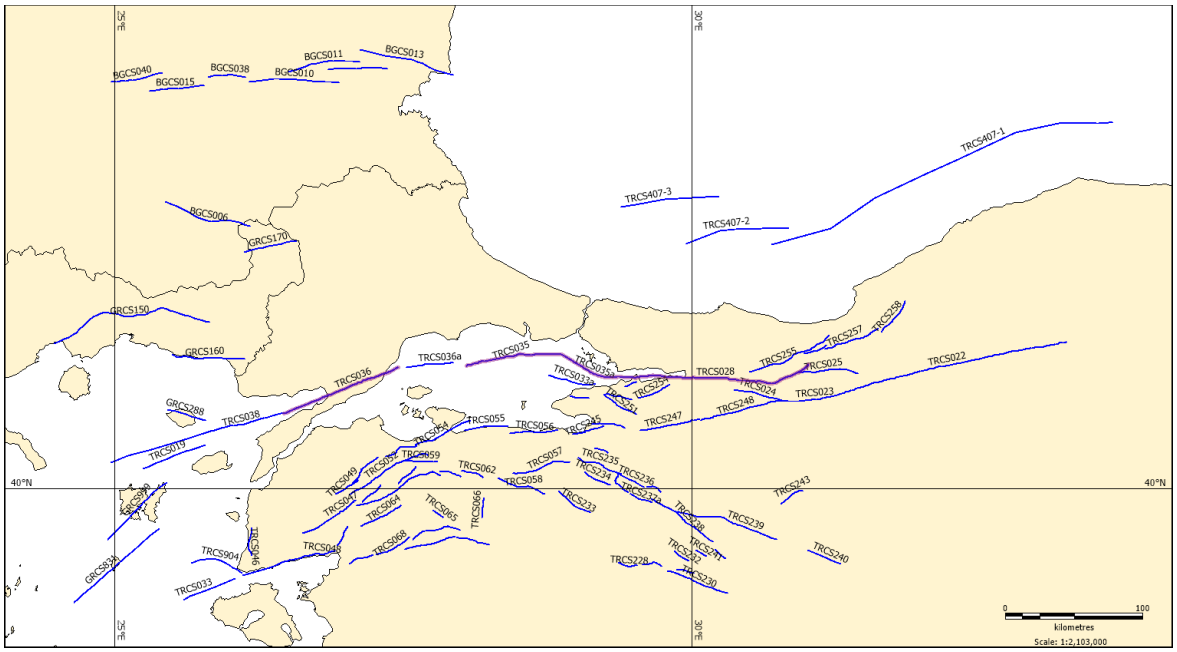

Figure 5.24. TRCS035, TRCS035, TRCS028 and TRCS036 fault sources

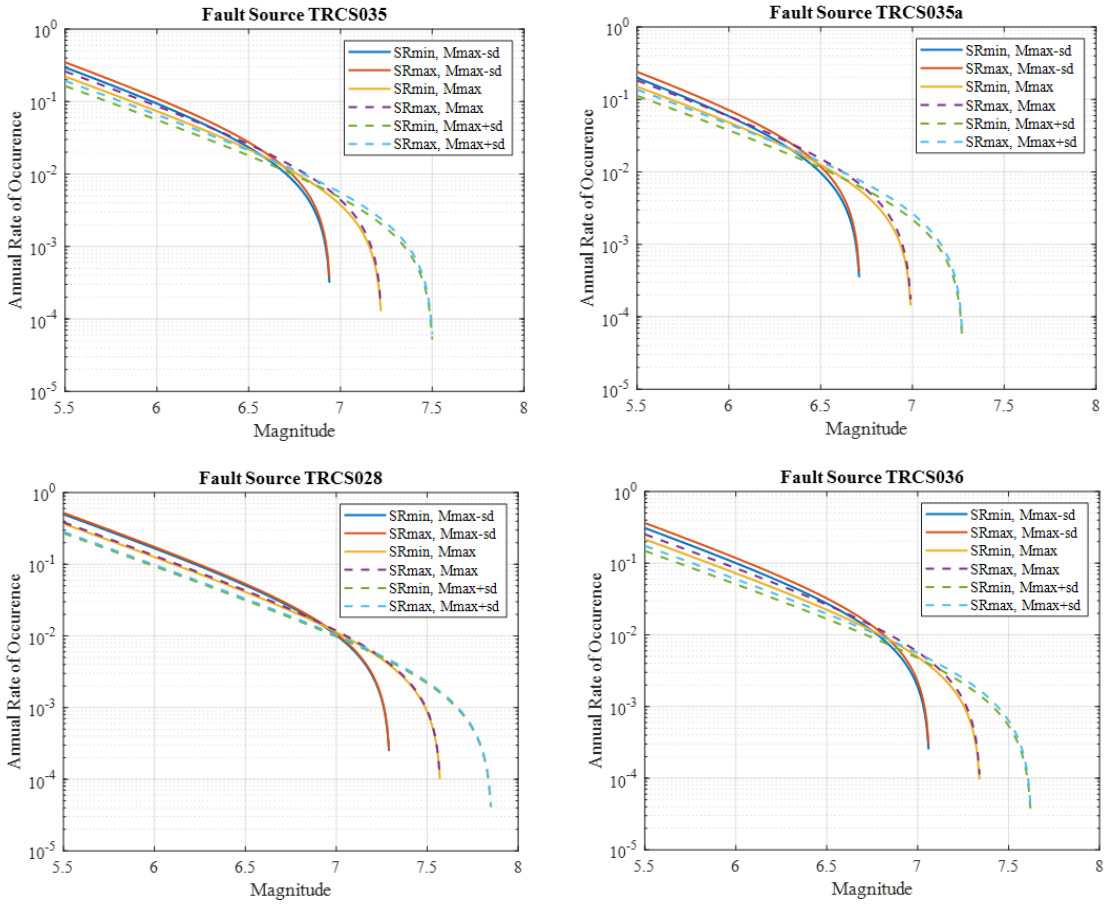

Figure 5.25. Recurrence rates of the fault sources TRCS035, TRCS035, TRCS028 and TRCS036

5.2.2.2. Smoothed Seismicity.

In the process of the delineation of seismic source boundaries, the researchers usually need to apply their subjective evaluations in addition to all field investigations and data examinations they conducted. For the fault source models, to represent the ambiguousness of the future locations of small magnitude earthquakes which can occur not directly on the faults, but within their broader deformation zones and to avoid any subjectivity in the delineation of the boundaries of these background sources, a grid-based background seismicity model can be developed (Frankel, 1995).

The reference study, Demircioğlu et al. (2018), took the threshold magnitude for the representation of the background seismicity as Mw 6.0, however in this study to capture the maximum magnitude ranges, which are presented in APPENDIX B: RECURRENCE PARAMETERS OF FAULT SOURCES, assigned to all fault sources, the upper-bound magnitude for the background seismicity within the buffer zones of the fault sources was set to Mw 5.5. The earthquakes with Mw < 5.5, which take place inside buffer zones of 15km around the surface projections of fault sources and all events outside the buffer zones are evaluated as background seismicity. To represent the background seismicity, a gridded source model is built, with occurrence rates computed through the smoothed seismicity approach of Frankel (1995).

The gridded point source model is constructed within the study region (24.9550^{o}-31.8980^{o}E, 39.3260^{o}-42.8160^{o}N) with 0.10^{o} x 0.10^{o} intervals. Representing the background smoothed seismicity, the point sources are modelled with the geometry properties like depth, dip, rake, strike and the tectonic region as are obtained from the area sources they fall in. The Guttenberg-Richter b value of each source is coming from the corresponding completeness region mean b value presented in APPENDIX B: RECURRENCE PARAMETERS OF FAULT SOURCES.

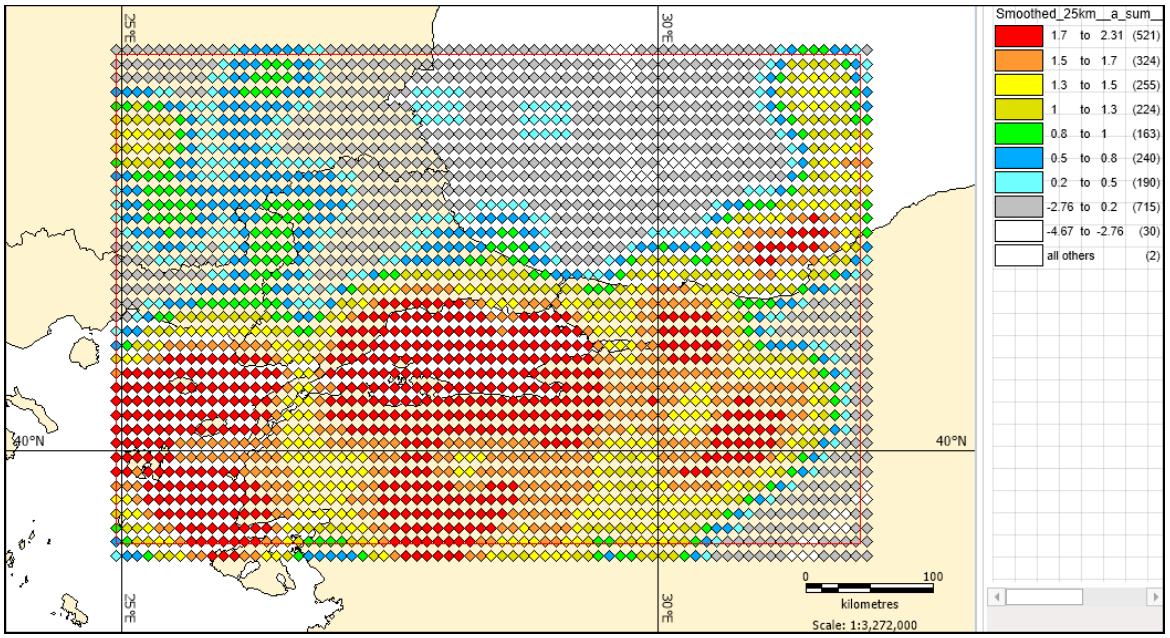

Figure 5.26. Smoothed seismicity "a" value distribution for the 25 km correlation distance

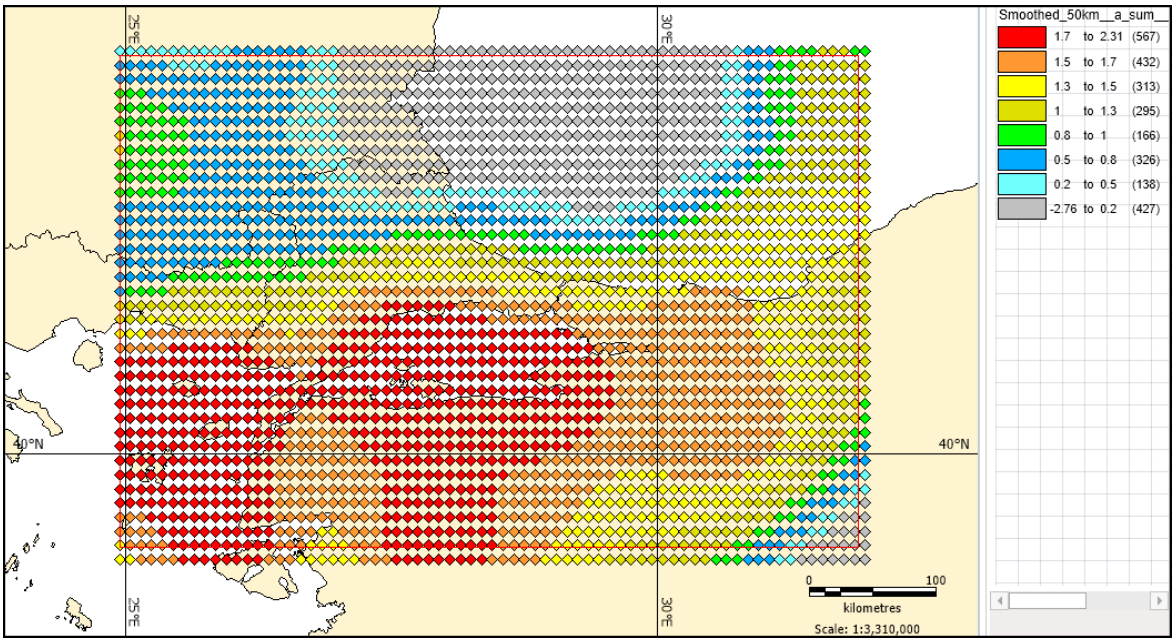

Figure 5.27. Smoothed seismicity "a" value distribution for the 50 km correlation distance

Demircioğlu et al. (2018), the reference study, examined the smoothed seismicity results they obtained with "the Gaussian correlation distances" of 15, 25 and 50 km. For the case of the "a" value distribution, they decided to continue their analysis only with the use of 50 km correlation distance. In this study, we preferred to use both 25km and 50km correlation distances of the smoothed seismicity analyses, which we think will be effective

in evaluating the effects of scattered earthquakes both together with the whole catalog and separately. The observed “a” value distributions of each gridded point source for 25 and 50 km correlation distances are presented in Figure 5.26 and Figure 5.27, respectively. The smoothing distance is included as a node in the final logic tree structure.

5.3. Ground Motion Prediction Equations

To estimate the ground motion level at a site resulting from the ruptures generated by the seismic source characterization model, attenuation relationships, also called ground motion prediction equations (GMPE) need to be used. The GMPEs are generated with the basis of statistical analysis of multiple ground motion records from different earthquakes and stations (Atik et al., 2010). Basically, producing a ground motion parameter, a GMPE model can simply be defined as in Eq. 4 (Atik et al., 2010).

$$Y = f(X_{es}, \theta) + \Delta \tag{4}$$

Here, “Y” means the observed ground motion, “$f(X_{es}, \theta)$” corresponds to the ground motion model, where “X_{es}” refers to the ground motion model parameters and “θ” to the coefficients described the GMPE in the model. Finally, “Δ” defines the total variability in the model.

To capture the epistemic uncertainties associated with ground motion modelling, a set of alternative models can be used, and the results be combined in a logic tree structure with weights. The GMPE logic tree used in the present study is the one used in the reference studies, Demircioğlu et al. (2018) and Şeşetyan et al. (2018) for the active shallow crustal regions. The uncertainty ranges introduced by the use of these models are presented, as well as the weighted mean results. The GMPEs used in the study are Akkar and Çağnan (2010), Akkar et al. (2014), Chiou and Youngs (2008)” and Zhao et al. (2006), with weights 0.3, 0.3, 0.3 and 0.1, respectively.

The model by Akkar and Çağnan (2010), derived with the use of a ground motion record set compiled from Turkey including earthquakes 3.5<Mw<7.6 and “Joyner-Boore

distance (R_{JB})" smaller than 200 km. The model is derived to estimate the active shallow seismicity and considers the fault type (strike-slip, normal and reverse), the soil behavior (V_{S30} is grouped in three categories as soft, stiff and rock) and magnitude reduction effects.

Akkar et al. (2014), which is developed using a data set originated from pan-Europe, derives equations with the regression coefficients for "epicentral", "hypocentral" and "Joyner-Boore" distances (R_{epi}, R_{hyp}, R_{JB} respectively) up to 200 km and earthquakes 4.0<Mw<8.0, for the active shallow crustal of Europe and Middle East regions with strike slip, normal and reverse faulting. The model covers the soil properties with 150m/s< V_{S30}<1200m/s.

Chiou and Youngs (2008) model is generated within the scope of the "Next Generation Attenuation model (NGA)" project by "Pacific Earthquake Engineering Research Center's (PEER)". They compiled a worldwide data set from the "PEER-NGA" database. The model considers the distances for "the closest distance to the rupture plane (R_{RUP})", "Joyner-Boore distance (R_{JB})", and "the surface projection of the distance to the updip edge of the rupture (R_X) with the limits of 3.5<Mw<7.6 for the reverse and normal, 3.5<Mw<7.6 for strike-slip faulting, up to the distance of 200 km and the soil classes for the range of 150m/s< V_{S30}<1500m/s.

The GMPE developed by Zhao et al. (2006) is derived both for the active shallow crust and subduction interface tectonic regions with the inclusion of the data set of subduction and shallow events mostly from Japanese territory with a contribution of a relatively small number of worldwide recordings. The method forms a list of site class terms including "rock", "hard soil", "medium soil", and "soft soil" for strike-slip, normal and reverse events.

5.4. The Logic Tree

As mentioned before, uncertainties constitute the main component of seismic hazard assessment. Therefore, knowledge of probability is necessary to know uncertainty. To capture the epistemic uncertainties associated with the seismic hazard, the logic tree method is a widely used tool in PSHA (Bommer et al., 2005).

The logic three generated for the PSHA conducted in this thesis consists of 192 individual branches in total. 144 branches for area source model and 48 branches for the fault source model with smoothed seismicity. The logic three schema is given in Figure 5.28.

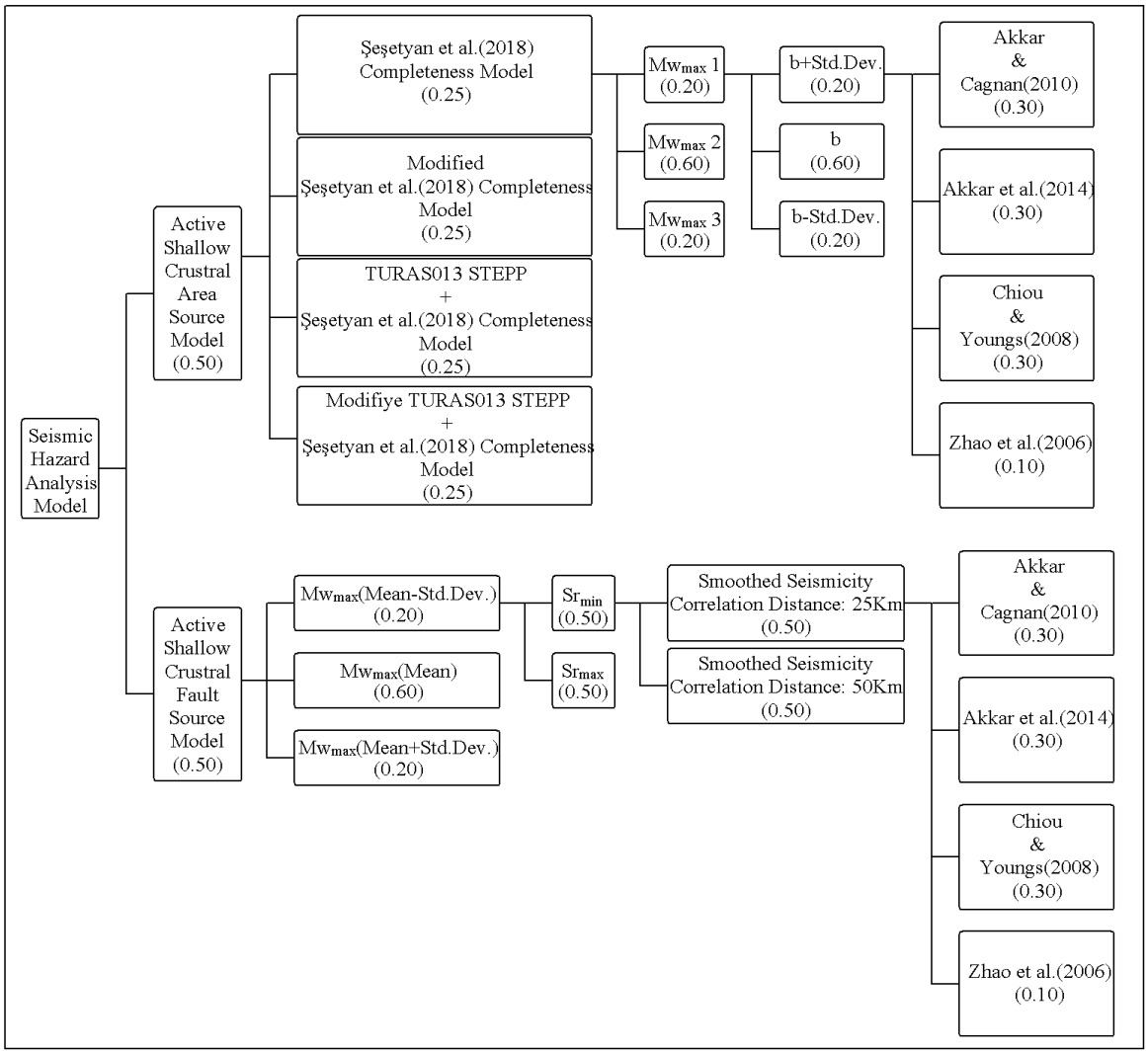

Figure 5.28. Logic tree structure of the present study

5.5. Seismic Hazard Calculations

The probabilistic earthquake hazard analyzes in this thesis were conducted with the "Openquake" (Pagani et al., 2014) program, which is a public-domain software and is also used in "the Turkey Earthquake Hazard Map (2018)" analysis. Analyzes were made for the average shear wave velocity of 760 m/s in the upper 30 m and at every 5 km point within the study region.

The results are obtained in alternative presentations, such as the weighted mean and different quantiles obtained from the logic tree structure, as well as the results obtained from the individual branches of the logic tree.

6. RESULTS AND DISCUSSION

Figure 6.1 presents a combined view of the area source (A) and fault source (FS) models and the main city centers of the Marmara Region. In the following sections, we first present the 475 and 2475 years return period mean ground motion distributions obtained from the analysis of AS, FS and combined models. City-based mean ground motion estimates are also presented for the same return periods. Following that, sensitivities of the hazard results to different modelling parameters treated in the logic tree structure are discussed through hazard curves of six cities. Uncertainty ranges of the hazard estimates are presented both as spatial distributions and through mean and quantile hazard curves at city centers. The chapter ends with a comparison of the weighted mean hazard outputs with the results of the "UDAP-Ç-13-06" project. The selected ground motion intensity measures are PGA and 5% damped pseudo spectral accelerations at T=0.2 s and 1.0 s (SA (T=0.2 s) and SA (T=1.0 s), respectively).

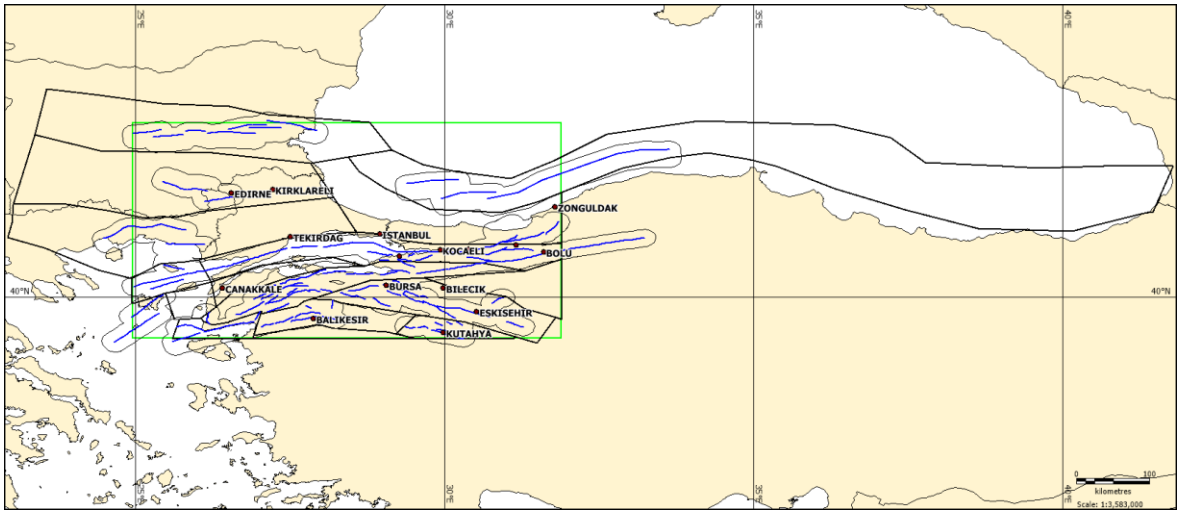

Figure 6.1. Area sources, fault sources with buffer zones and city centers

6.1. Full Model Analysis

6.1.1. Mean Ground Motion Distributions

The weighted mean 475 and 2475 years ground motion distributions obtained from the AS model are presented in Figure 6.2 to Figure 6.7 for PGA and 5% damped pseudo spectral accelerations at T=0.2 s and 1.0 s. Similarly, the weighted mean distributions obtained from the FS model are presented in Figure 6.8 to Figure 6.13. The results of the full logic tree, i.e., with 0.5 weight associated with both AS and FS models, are given in Figure 6.14 to Figure 6.19. A comparison of the mean results obtained in this project with the mean results of the base model (i.e., "UDAP-Ç-13-06" project) is provided in Section 6.4.

Comparing the AS and FS model results, we observe in the AS model the ground motion distributions are uniform within the individual area sources, while variability is observed from source to source. Here it should also be noted that some artificially low values are obtained at the study region borders (for instance, close to Bolu), but this is caused by the clipping of the sources at the border. For this reason, hazard values at the model borders should not be considered realistic.

The fault source model, on the other hand, yields very high ground motion values at sites located directly on the fault traces, while these values decay very rapidly with distance. The smoothed seismicity has a very localized contribution, which is mainly observed at regions without active fault traces, for instance, at some places of the Thrace peninsula.

In Figure 6.14 to Figure 6.19, we observe that a combination of the AS and FS models yields a more realistic representation of the seismic hazard, where the contribution of the fault sources is clearly observed, while these values decay more slowly with distance, as the contribution of the areas sources become higher going away from the fault traces.

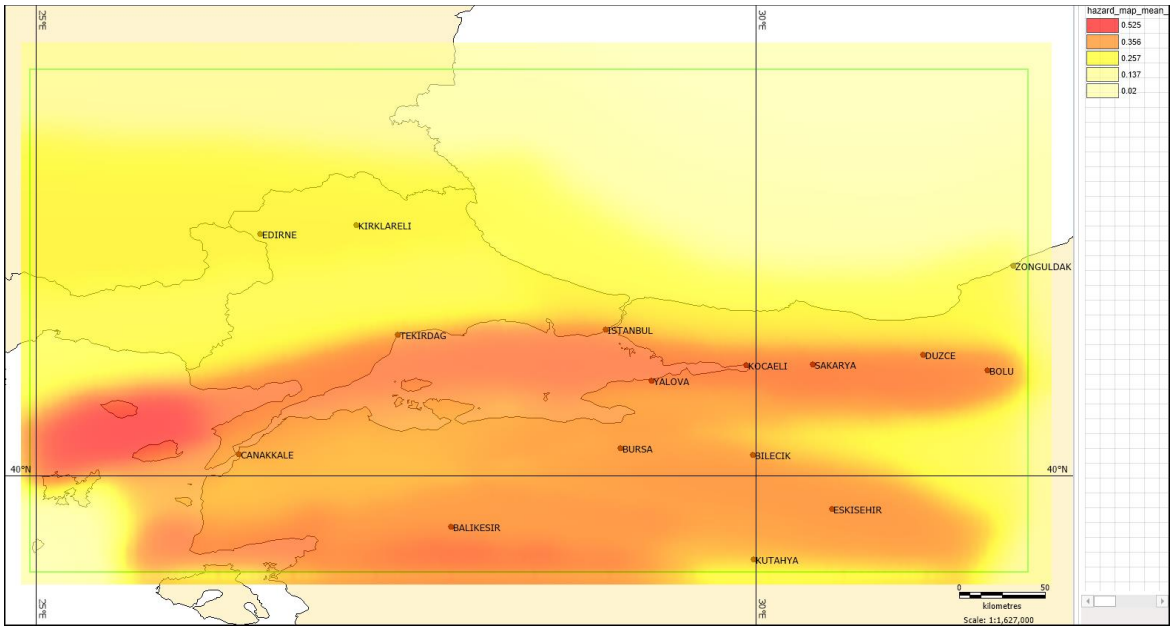

Figure 6.2. Area source model analysis, mean PGA, 475 years RP

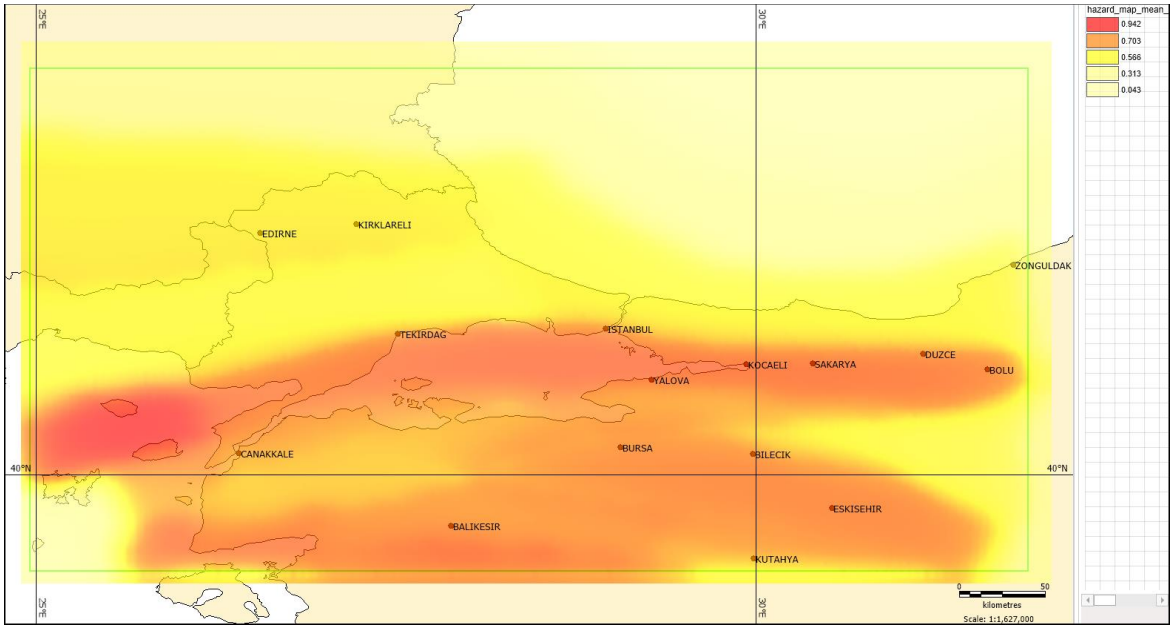

Figure 6.3. Area source model analysis, mean PGA, 2475 years RP

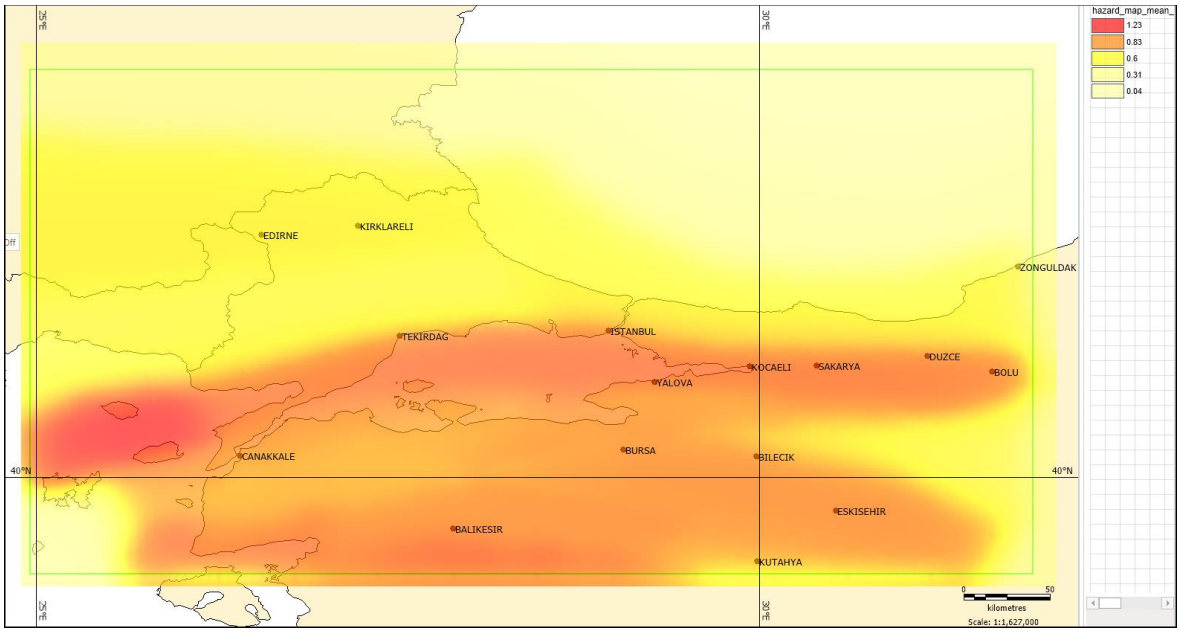

Figure 6.4. Area source model analysis, mean SA (T=0.2 s), 475 years RP

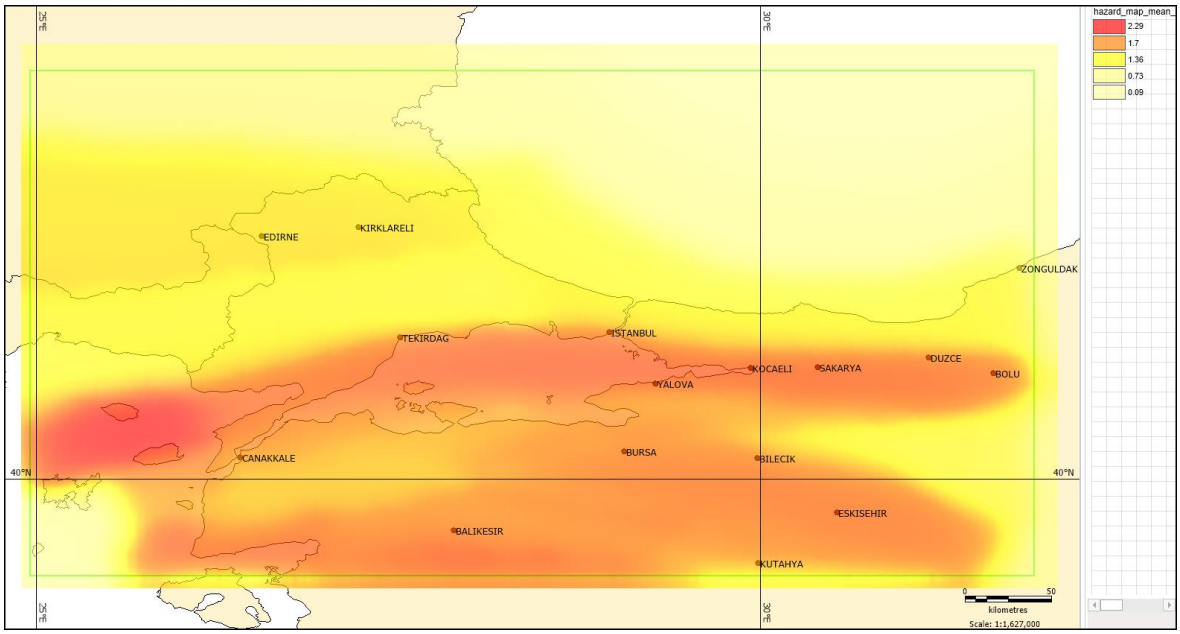

Figure 6.5. Area source model analysis, mean SA (T=0.2 s), 2475 years RP

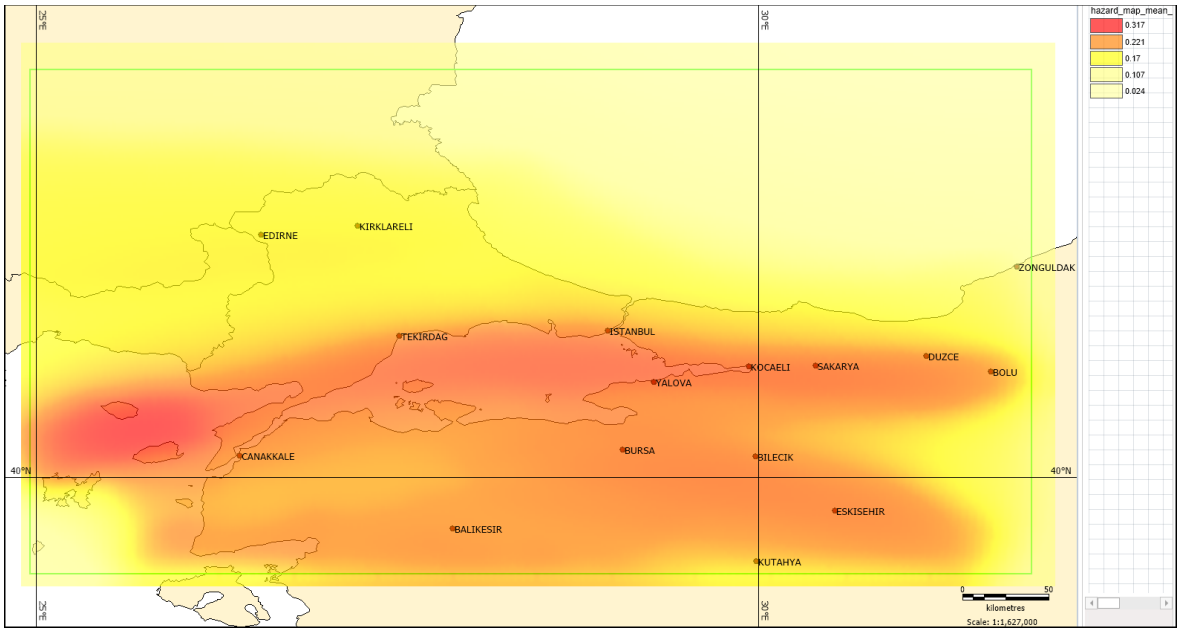

Figure 6.6. Area source model analysis, mean SA (T=1.0 s), 475 years RP

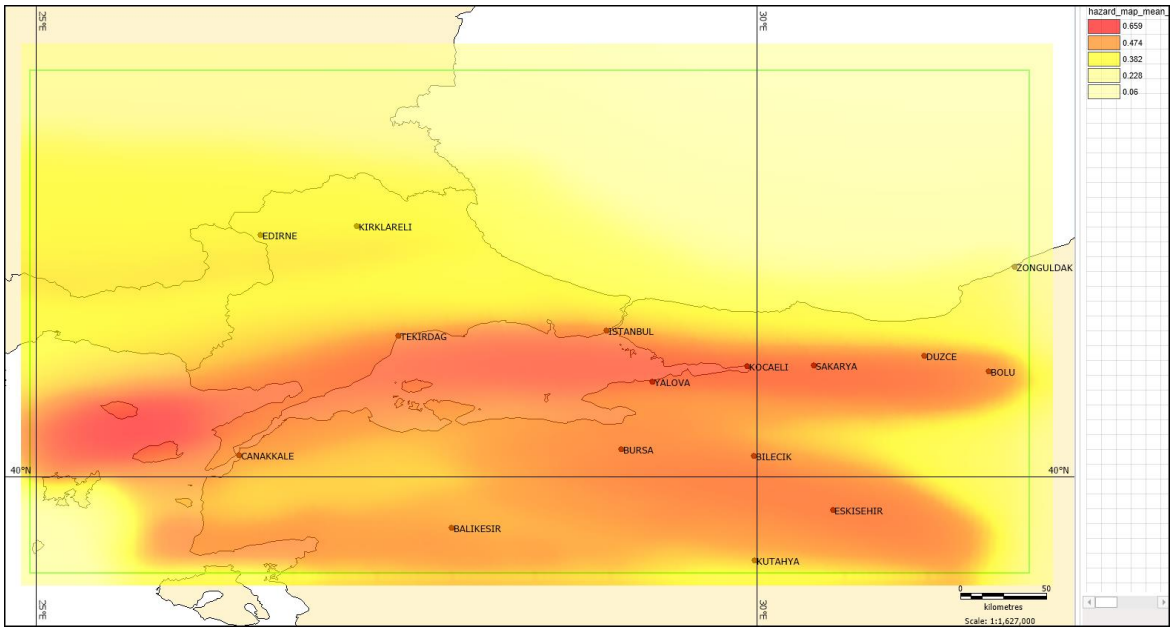

Figure 6.7. Area source model analysis, mean SA (T=1.0 s), 2475 years RP

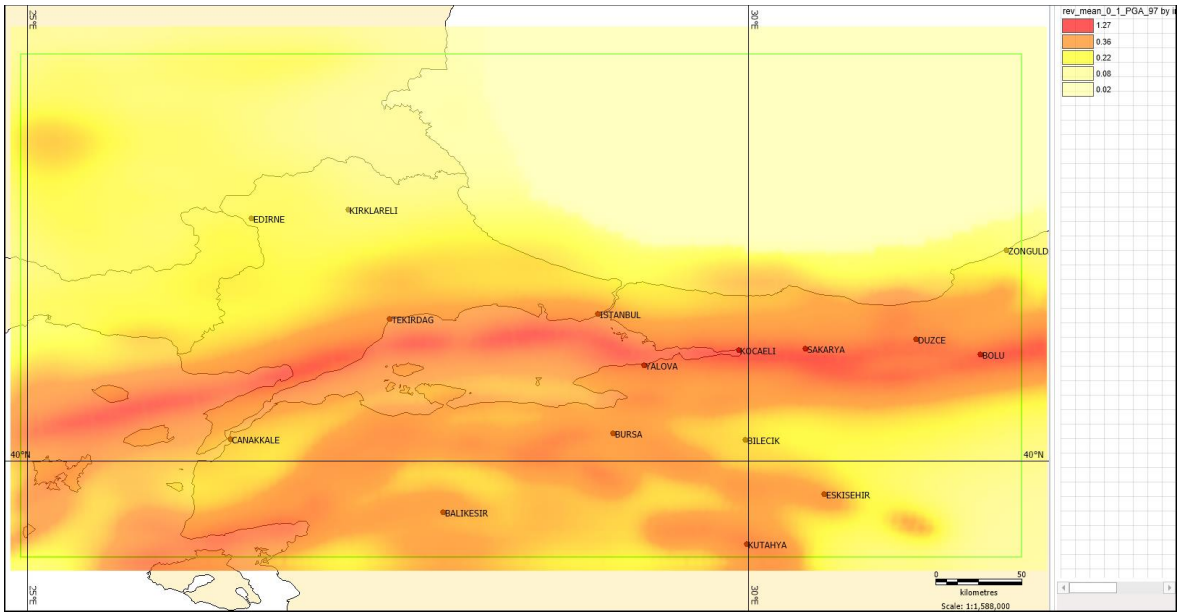

Figure 6.8. Fault source model analysis, mean PGA, 475 years RP

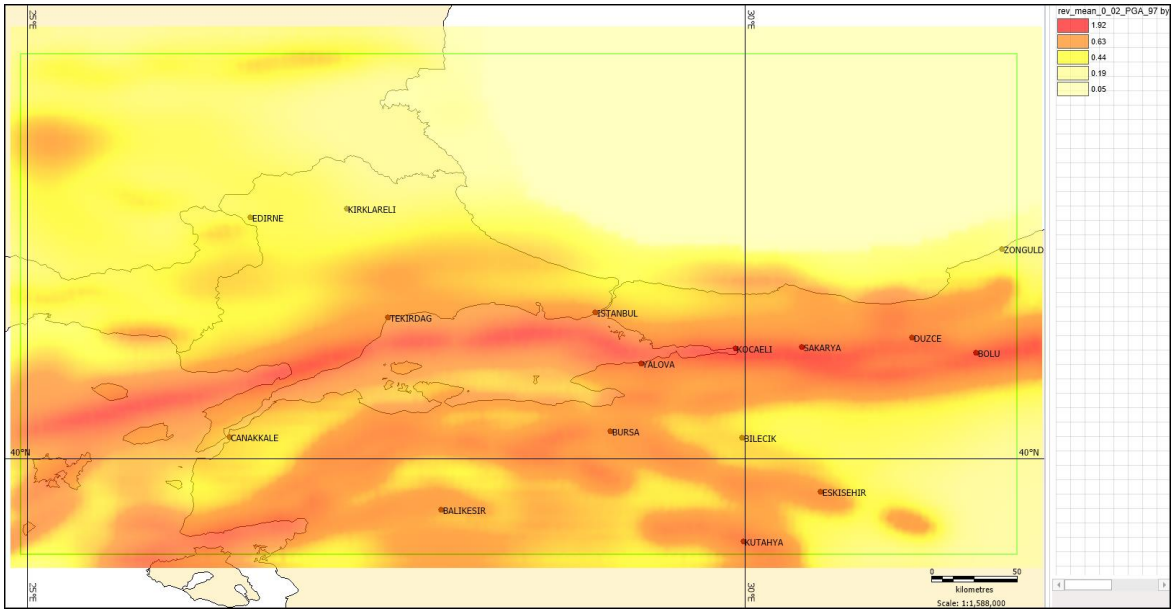

Figure 6.9. Fault source model analysis, mean PGA, 2475 years RP

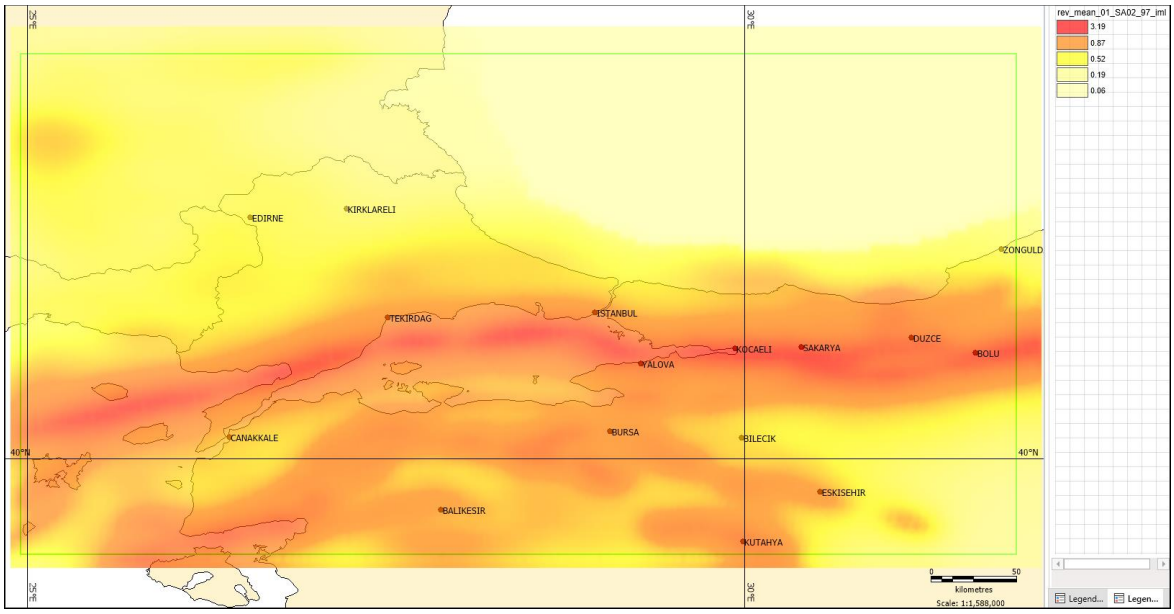

Figure 6.10. Fault source model analysis, mean SA (T=0.2 s), 475 years RP

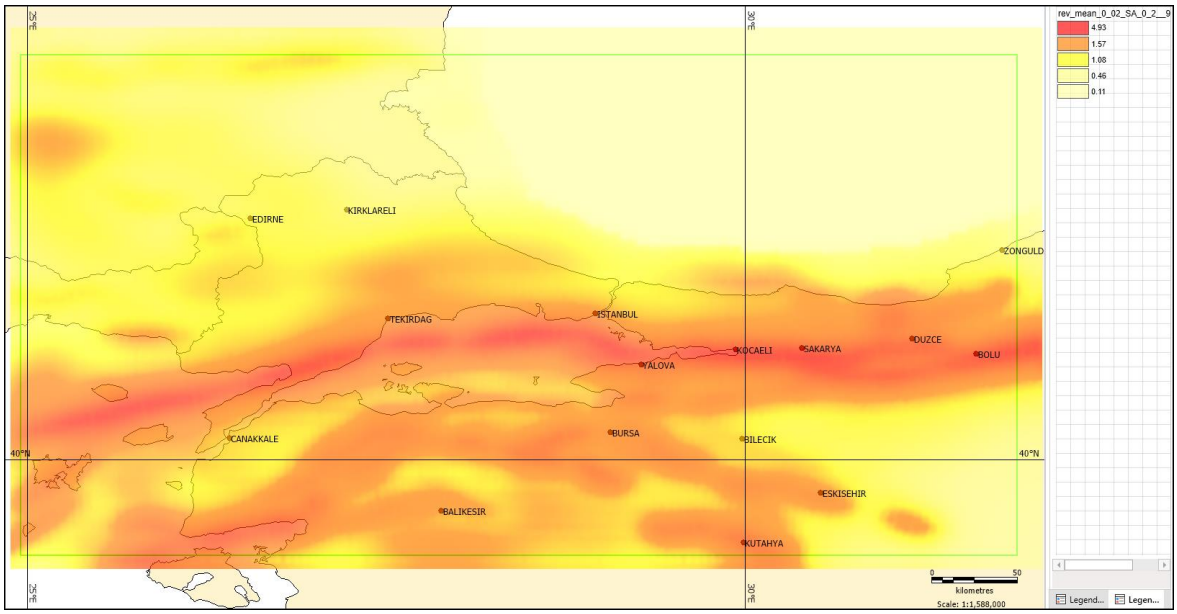

Figure 6.11. Fault source model analysis, mean SA (T=0.2 s), 2475 years RP

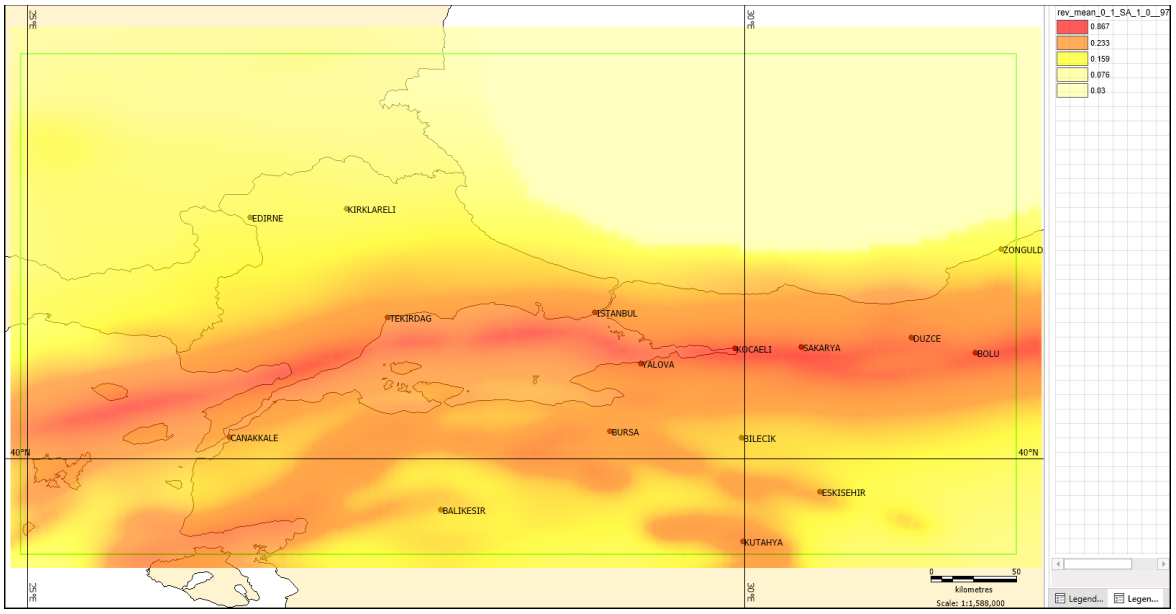

Figure 6.12. Fault source model analysis, mean SA (T=1.0 s), 475 years RP

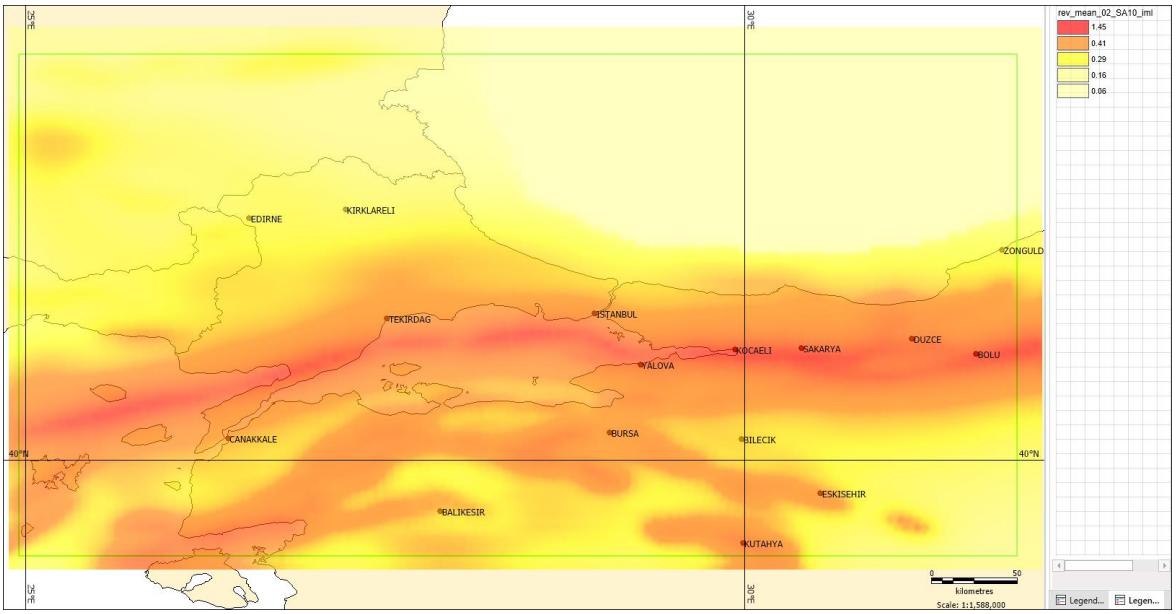

Figure 6.13. Fault source model analysis, mean SA (T=1.0 s), 2475 years RP

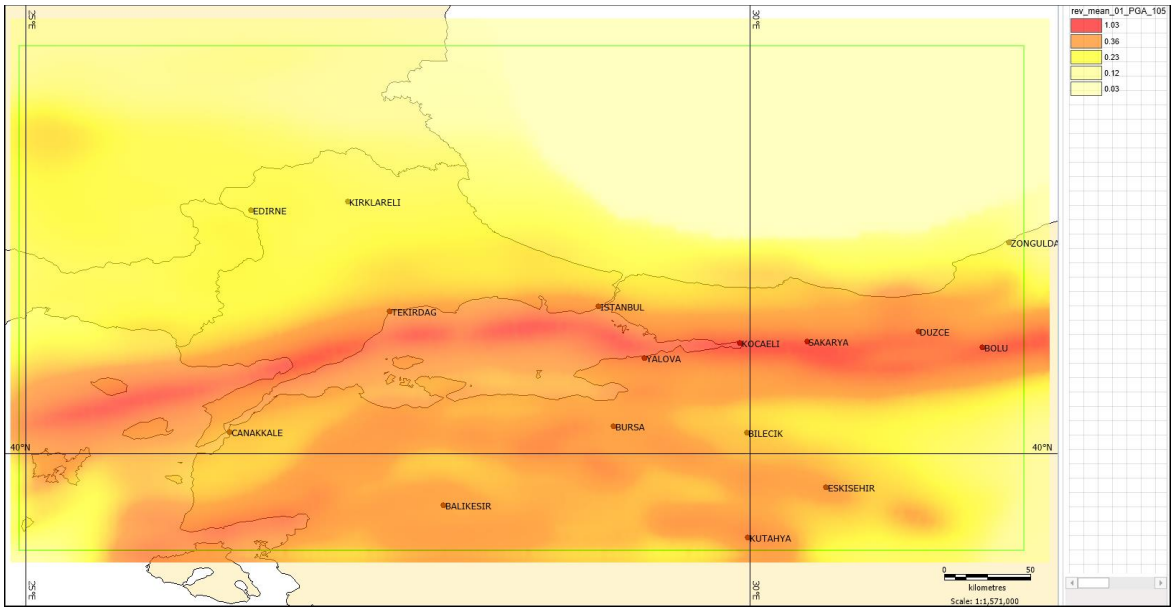

Figure 6.14. Full model analysis, mean PGA, 475 years RP

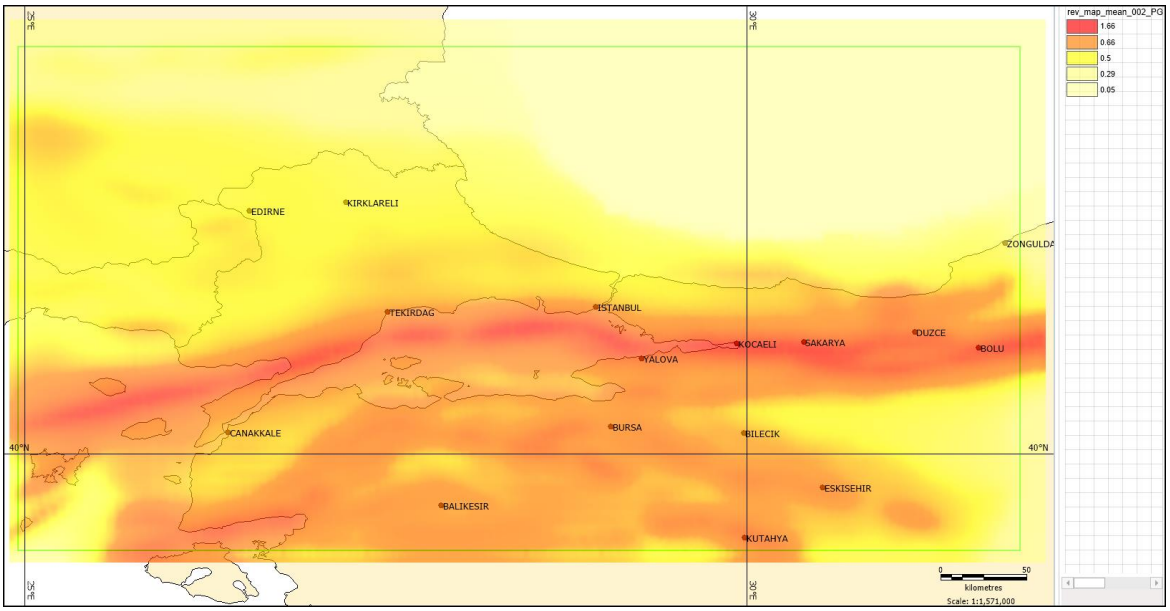

Figure 6.15. Full model analysis, mean PGA, 2475 years RP

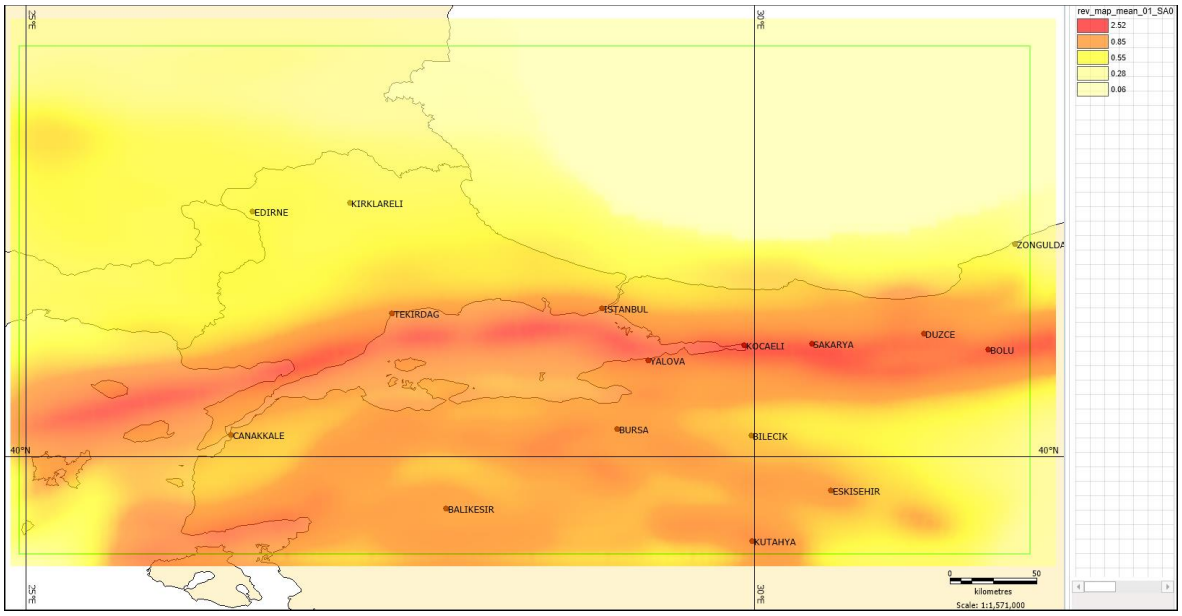

Figure 6.16. Full model analysis, mean SA (T=0.2 s), 475 years RP

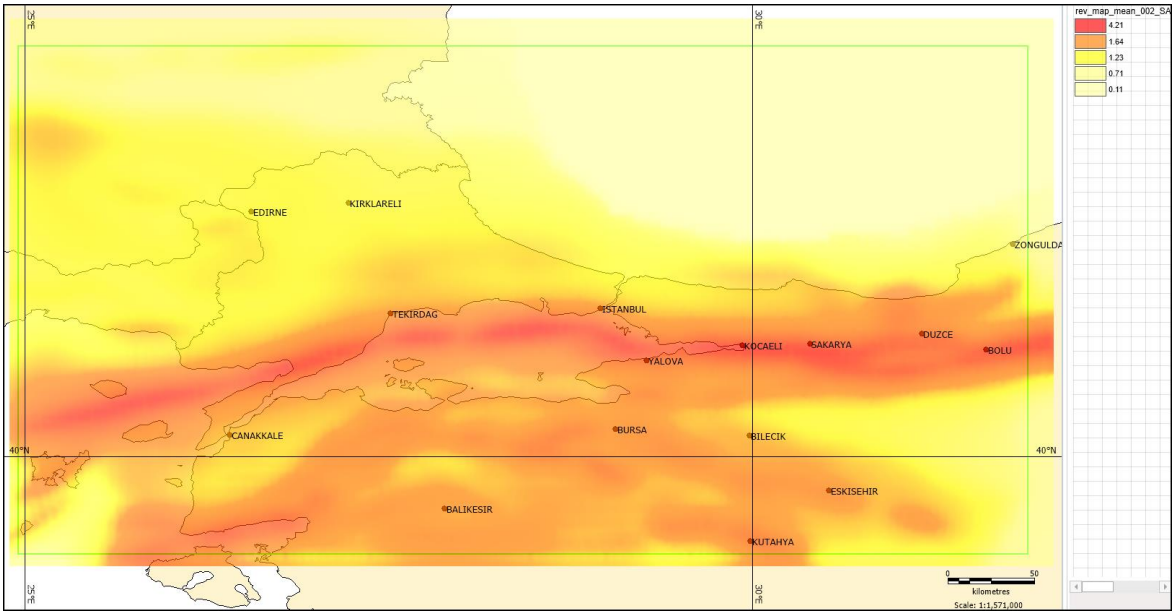

Figure 6.17. Full model analysis, mean SA (T=0.2 s), 2475 years RP

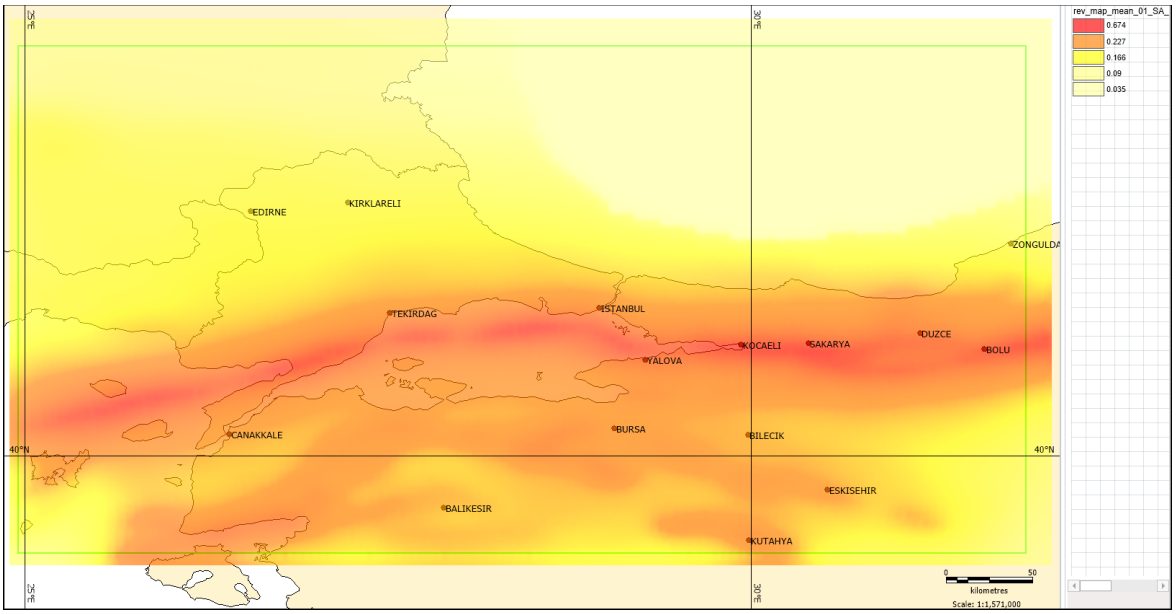

Figure 6.18. Full model analysis, mean SA (T=1.0 s), 475 years RP

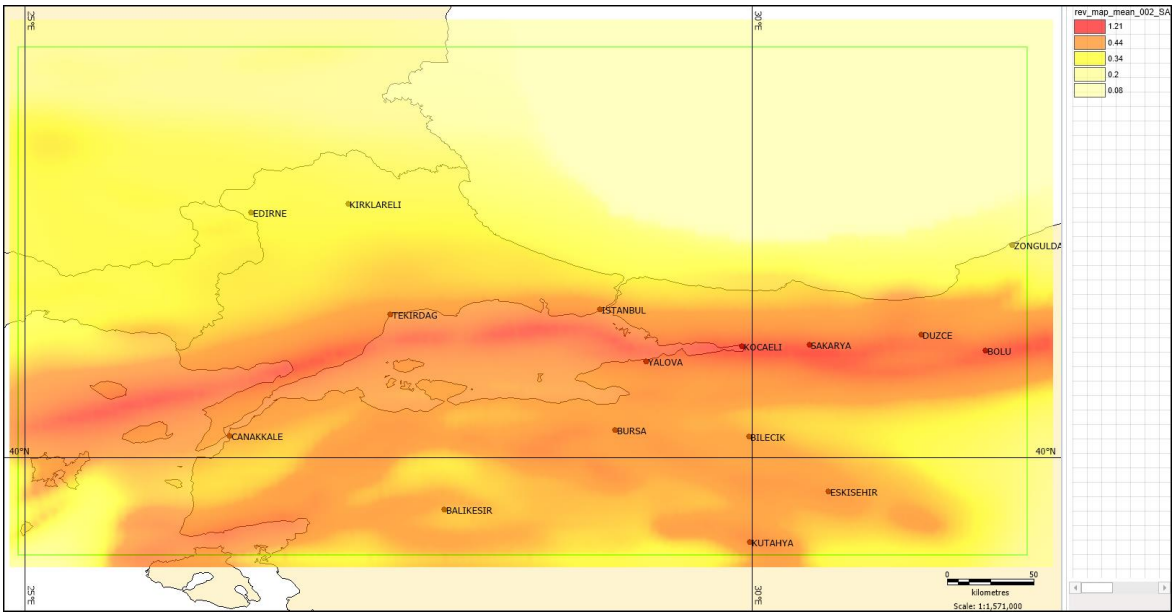

Figure 6.19. Full model analysis, mean SA (T=1.0 s), 2475 years RP

6.1.2. Point Based Hazard Results at City Centers

Mean hazard results at city centers within the study region are provided in terms of PGA (Table 6.1), 5% damped spectral accelerations of T=0.2 s (Table 6.2) and T=1.0 s (Table 6.3) for return periods of 475 and 2475 years.

One of the most striking observations is that the PGA values with 10% probability of exceedance in 50 years (475 years RP) from the full source model analysis are generally in the vicinity of 0.4 g or higher, the value defined as the upper limit for "the Turkey Earthquake Zonation Map" which was in force until the beginning of 2019. These results also demonstrate the necessity of the update of the national seismic hazard map of Turkey, which was realized with the "UDAP-Ç-13-06" Project.

Table 6.1. The mean PGA obtained for the city centers located in the study region, for the area source, the fault source with background seismicity and the full source models with the RP of 475 and 2475 years

City	475 years RP mean PGA (g)			2475 years RP mean PGA(g)		
	AS Model	FS Model	Full Model	AS Model	FS Model	Full Model
BALIKESIR	0.3877	0.3812	0.3892	0.7401	0.6857	0.7205
BILECIK	0.3538	0.2740	0.3156	0.7283	0.5359	0.6420
CANAKKALE	0.3473	0.3096	0.3300	0.6785	0.5537	0.6226
DUZCE	0.3747	0.7323	0.6188	0.7454	1.1130	1.0198
EDIRNE	0.2653	0.1756	0.2224	0.5864	0.3739	0.4960
ESKISEHIR	0.3804	0.4302	0.4105	0.7735	0.8542	0.8259
KIRKLARELI	0.2642	0.1350	0.2047	0.5842	0.3054	0.4752
KOCAELI	0.4216	1.1109	0.9231	0.8130	1.7064	1.4955
SAKARYA	0.4180	0.9551	0.8042	0.8085	1.4404	1.2651
TEKIRDAG	0.3293	0.4024	0.3817	0.6712	0.6271	0.6520
YALOVA	0.4183	0.8086	0.6884	0.8106	1.2335	1.1136
ISTANBUL	0.3628	0.4316	0.4135	0.7138	0.6653	0.6919
BURSA	0.3639	0.4323	0.4084	0.7356	0.8005	0.7795

Table 6.2. The mean 5% damped T=0.2 s spectral accelerations obtained for the city centers located in the study region, for the area source, the fault source with background seismicity and the full source model with the RP of 475 and 2475 years

City	475 years RP mean SA (T=0.2s) (g)			2475 years RP mean SA (T=0.2s) (g)		
	AS Model	FS Model	Full Model	AS Model	FS Model	Full Model
BALIKESIR	0.9068	0.8955	0.9007	1.7939	1.6648	1.7275
BILECIK	0.8271	0.6503	0.7352	1.7606	1.2898	1.5488
CANAKKALE	0.8137	0.7406	0.7740	1.6475	1.3479	1.5074
DUZCE	0.8658	1.8259	1.5147	1.7799	2.9186	2.5433
EDIRNE	0.6187	0.4135	0.5175	1.4308	0.9102	1.1882
ESKISEHIR	0.8916	1.0147	0.9527	1.8823	2.1118	2.0103
KIRKLARELI	0.6161	0.3159	0.4734	1.4255	0.7365	1.1368
KOCAELI	0.9792	2.7793	2.2123	1.9678	4.4156	3.7603
SAKARYA	0.9697	2.3853	1.9675	1.9536	3.7738	3.2586
TEKIRDAG	0.7676	1.0039	0.9169	1.6269	1.6140	1.6204
YALOVA	0.9703	2.0374	1.6748	1.9536	3.2433	2.8286
ISTANBUL	0.8394	1.0745	0.9947	1.7093	1.7154	1.7146
BURSA	0.8517	1.0491	0.9643	1.7818	1.9998	1.8985

Table 6.3. The mean 5% damped T=1.0 s spectral accelerations obtained for the city centers located in the study region, for the area source, the fault source with background seismicity and the full source model with the RP of 475 and 2475 years

City	475 years RP mean SA (T=1.0s) (g)			2475 years RP mean SA (T=1.0s) (g)		
	AS Model	FS Model	Full Model	AS Model	FS Model	Full Model
BALIKESIR	0.2258	0.1919	0.2073	0.4715	0.3649	0.4188
BILECIK	0.2389	0.1942	0.2130	0.5187	0.3395	0.4324
CANAKKALE	0.2303	0.2256	0.2270	0.4844	0.3974	0.4375
DUZCE	0.2233	0.4619	0.3807	0.5082	0.7519	0.6650
EDIRNE	0.1712	0.1256	0.1465	0.3882	0.2413	0.3185
ESKISEHIR	0.2475	0.2240	0.2341	0.5514	0.4777	0.5131
KIRKLARELI	0.1691	0.1221	0.1430	0.3842	0.2262	0.3099
KOCAELI	0.2623	0.7314	0.5651	0.5869	1.2131	1.0285
SAKARYA	0.2559	0.6291	0.5080	0.5767	1.0440	0.8966
TEKIRDAG	0.2205	0.2759	0.2536	0.4897	0.4632	0.4728
YALOVA	0.2681	0.5037	0.4189	0.5909	0.8246	0.7446
ISTANBUL	0.2282	0.3077	0.2759	0.4917	0.5071	0.4998
BURSA	0.2454	0.2543	0.2493	0.5260	0.4872	0.5043

6.2. Sensitivity to Different Parameters Considered in Hazard Modeling

Focusing on the mean hazard curve may blur the differentiation between aleatory and epistemic variabilities (Abrahamson & Bommer, 2005). Therefore, focusing on the branches of logic three may help us to examine the effects of the epistemic uncertainties considered. Being among the most crowded cities with different seismic properties, the city centers of Kocaeli, İstanbul, Çanakkale, Bursa, Tekirdağ and Kırklareli (Figure 6.1) are chosen for this analysis. Among these, Kocaeli city center is directly situated on the most active fault segment, Bursa is located on top of a less active fault source, Istanbul is 17 km and Tekirdağ is 20 km at a distance of to the Main Marmara Fault, Çanakkale city center is at 36 km to the Main Marmara Fault and is located in a background zone and Kırklareli is 106 km away from the Main Marmara Fault and the closest fault to the city is located at the distance of 55 km.

6.2.1. Sensitivity to Source Modeling

As the first branches of the logic tree of PSHA, in Figure 6.20, we present the sensitivity of the hazard results to the two main modelling approaches (i.e., the area source modeling and the fault source modelling). Figure 6.20 reveals that the sensitivity changes as a function of the location of the site with respect to the sources. For instance, at Kocaeli city center, the FS model yields much higher results as the trace of the NAF, located very close to the city, governs the hazard. The AS model tends to smooth the hazard over a wider region and consequently, the resulting hazard is lower. At Çanakkale, the AS model results are higher, which is in fact, a manifestation of the opposite case: the city is located far from the main source, but overall smoothing of the AS model results in higher ground motion estimations. In Bursa, which is located close to a less active fault source, both models yield comparable results. In Istanbul and Tekirdağ, the sensitivity to source modelling yields more interesting results, as up to about 2000 years return period the FS model governs the hazard, while for larger return periods, the AS model dominates, which is probably due to the fact that larger maximum magnitudes associated with AS model, the boundaries of which in fact come very close to the city center start to dominate the hazard. Kırklareli, which is located at the largest distance to the faults, has very low hazard results from the FS model, which is under the influence of background seismicity only, while the AS model results exhibit a

behavior similar to the results of Çanakkale, with the effect of earthquakes falling into the area source it is included in.

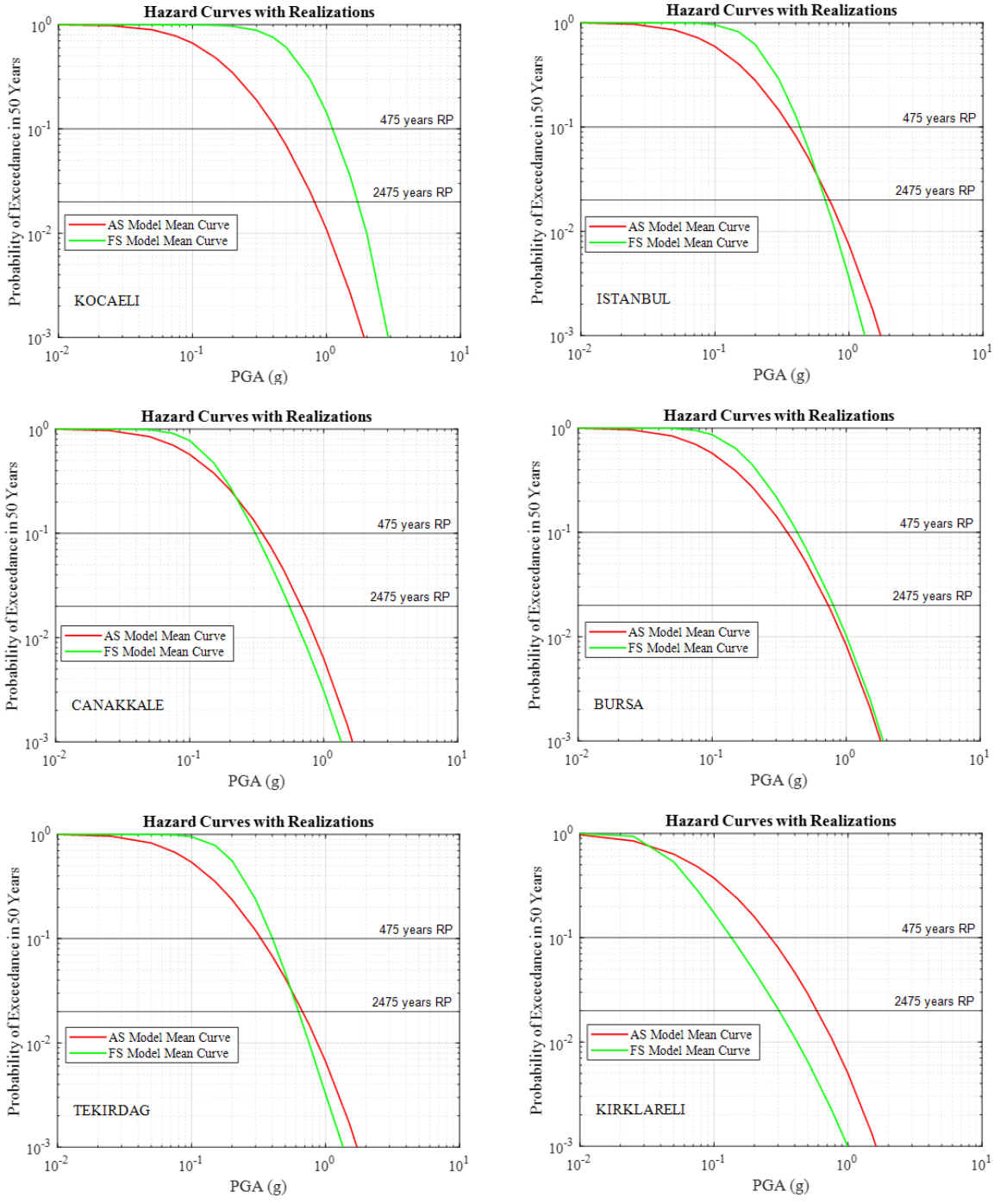

Figure 6.20. Sensitivity to source modelling for PGA hazard curves

6.2.2. Sensitivity to the Parametrization of the Area Source Model

The complete set of PGA hazard curves for Kocaeli, Istanbul, Çanakkale, Bursa, Tekirdağ and Kırklareli city centers obtained from the AS model is presented in Figure 6.21. The logic tree for the AS model has 144 branches and the sensitivity to three area source modelling parameters i.e., completeness of the earthquake catalog, maximum magnitude and b value are investigated. An observation that can be made from Figure 6.21 is that sites with relatively less seismicity (Çanakkale, Bursa and Kırklareli) are associated with larger uncertainties, which is mainly due to the large uncertainty of the computed b-value.

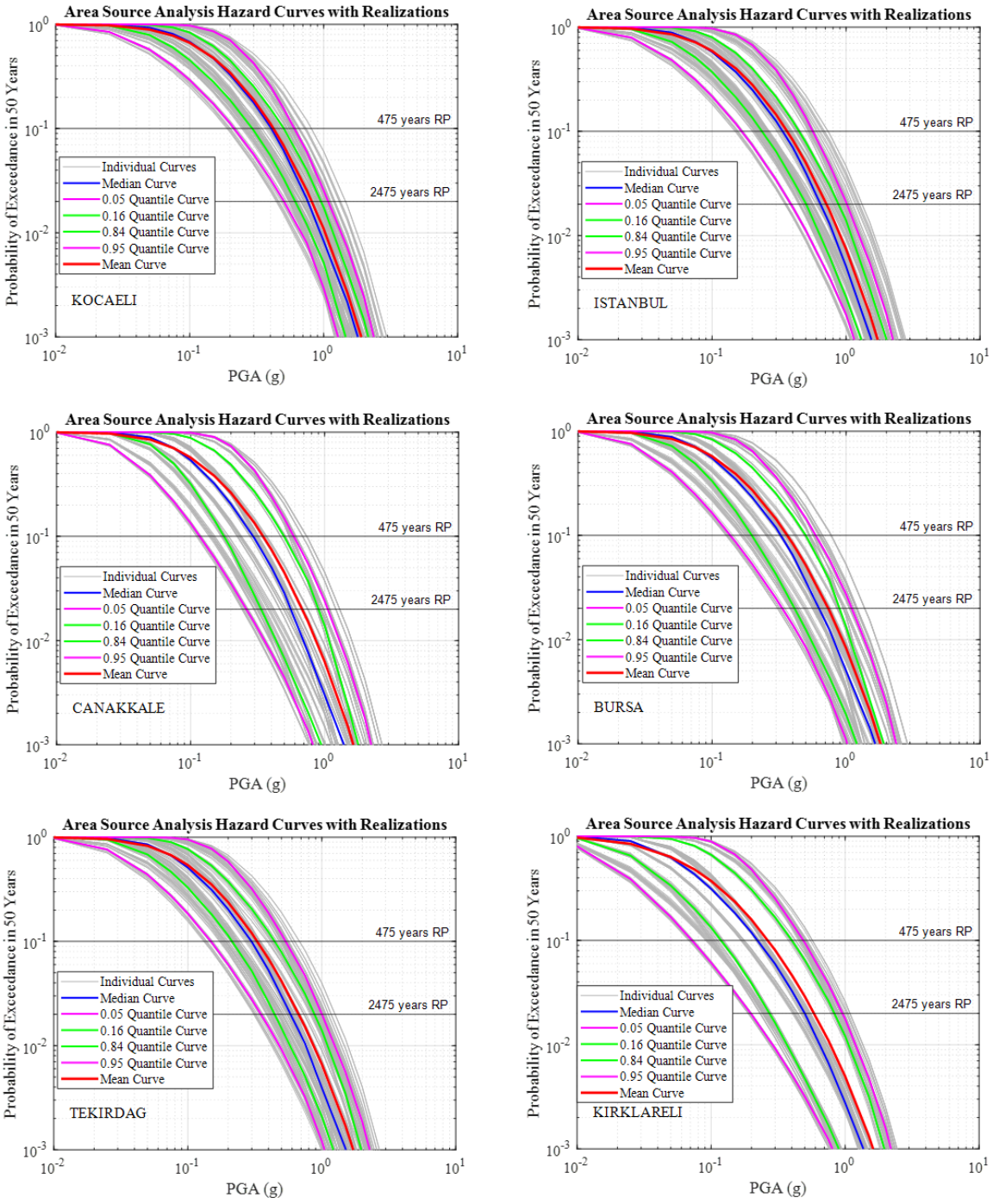

Figure 6.21. Complete set of PGA hazard curves for Kocaeli, Istanbul, Çanakkale, Bursa, Tekirdağ and Kırklareli city centers obtained from the AS model

Figure 6.22 and Figure 6.23 present the sensitivities to the maximum magnitude associated with the area sources and the b-value, respectively. Here it should be noted that the b-values are also computed with respect to the maximum magnitude levels assigned to the sources. We observe from the figures that the effect of the b-value uncertainty is much

larger than the effect of the maximum magnitude in the AS model. As expected, the effect of maximum magnitude becomes larger at longer return periods as this parameter is more effective when very large magnitude-small annual rate events are considered.

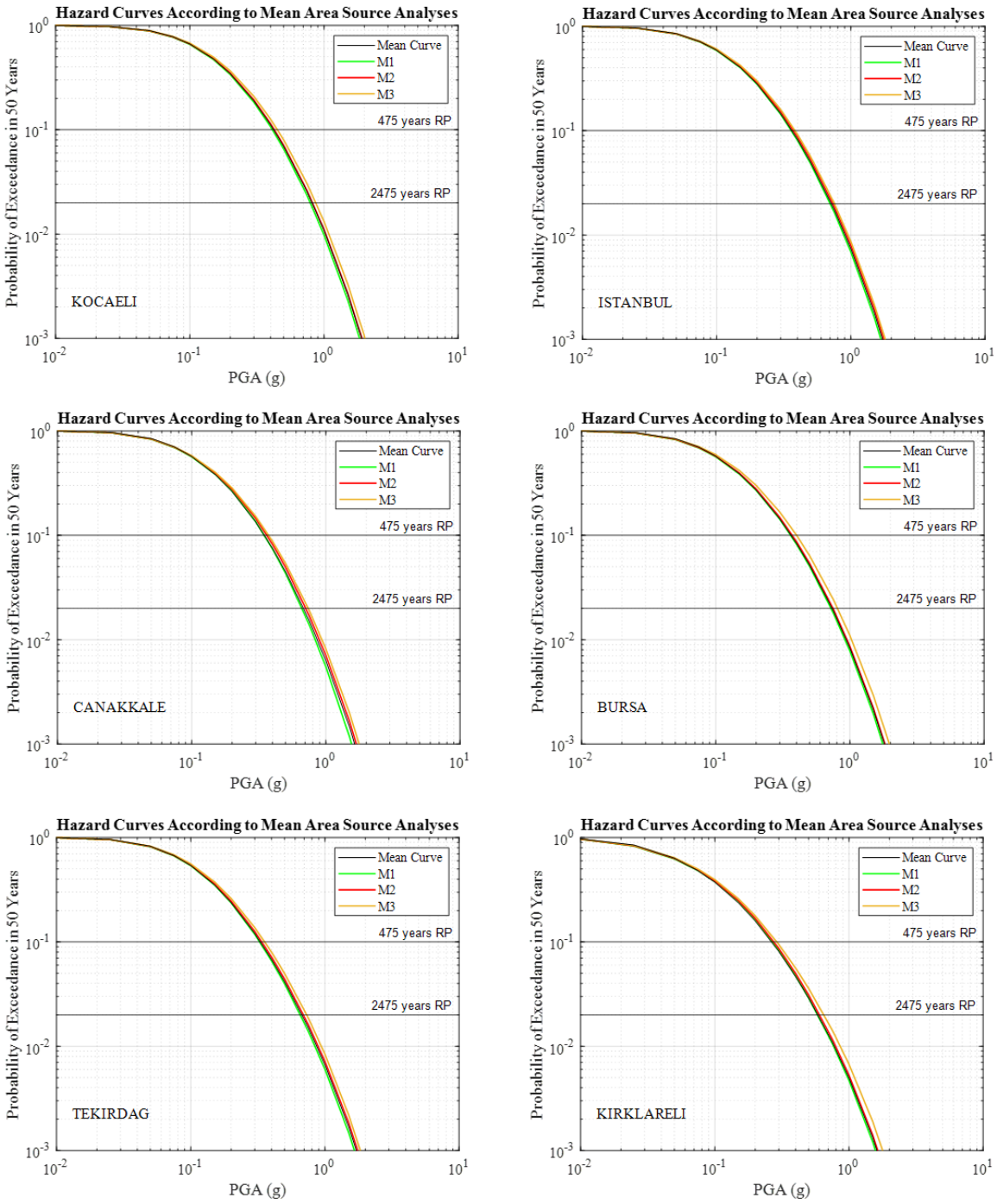

Figure 6.22. Sensitivity to maximum magnitude for PGA hazard curves

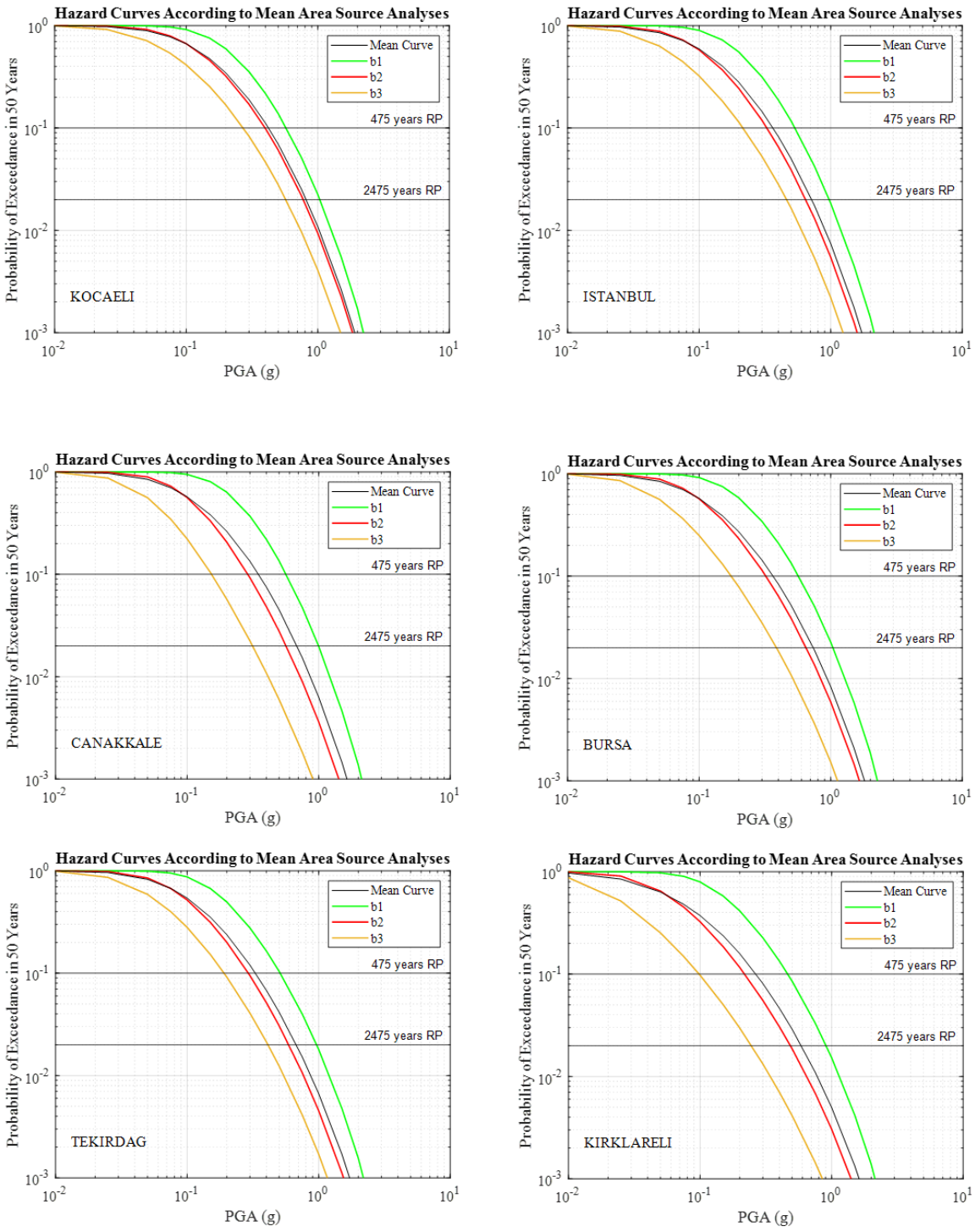

Figure 6.23. Sensitivity to the b-value for PGA hazard curves

6.2.3. Sensitivity to the Parametrization of the Fault Source Model

The PGA hazard curves for Kocaeli, Istanbul, Çanakkale, Bursa, Tekirdağ and Kırklareli city centers were obtained from the complete set of the FS model, which includes the fault line sources with the gridded smoothed seismicity model, is presented in Figure 6.24. The logic tree for the FS model has 48 branches, and the sensitivity to three modelling parameters i.e., slip rate, maximum magnitude and the kernel size of the background smoothed seismicity model, are investigated. Comparing Figure 6.21 and Figure 6.24, we observe that the AS model is associated with much larger uncertainties for all sites. One reason for the smaller uncertainty ranges in the FS model is that the fault source earthquake recurrence modelling is mainly governed by the slip rate and the slip rate ranges (minimum and maximum values) in the fault source database are relatively narrow, and consequently, the resulting uncertainties are small.

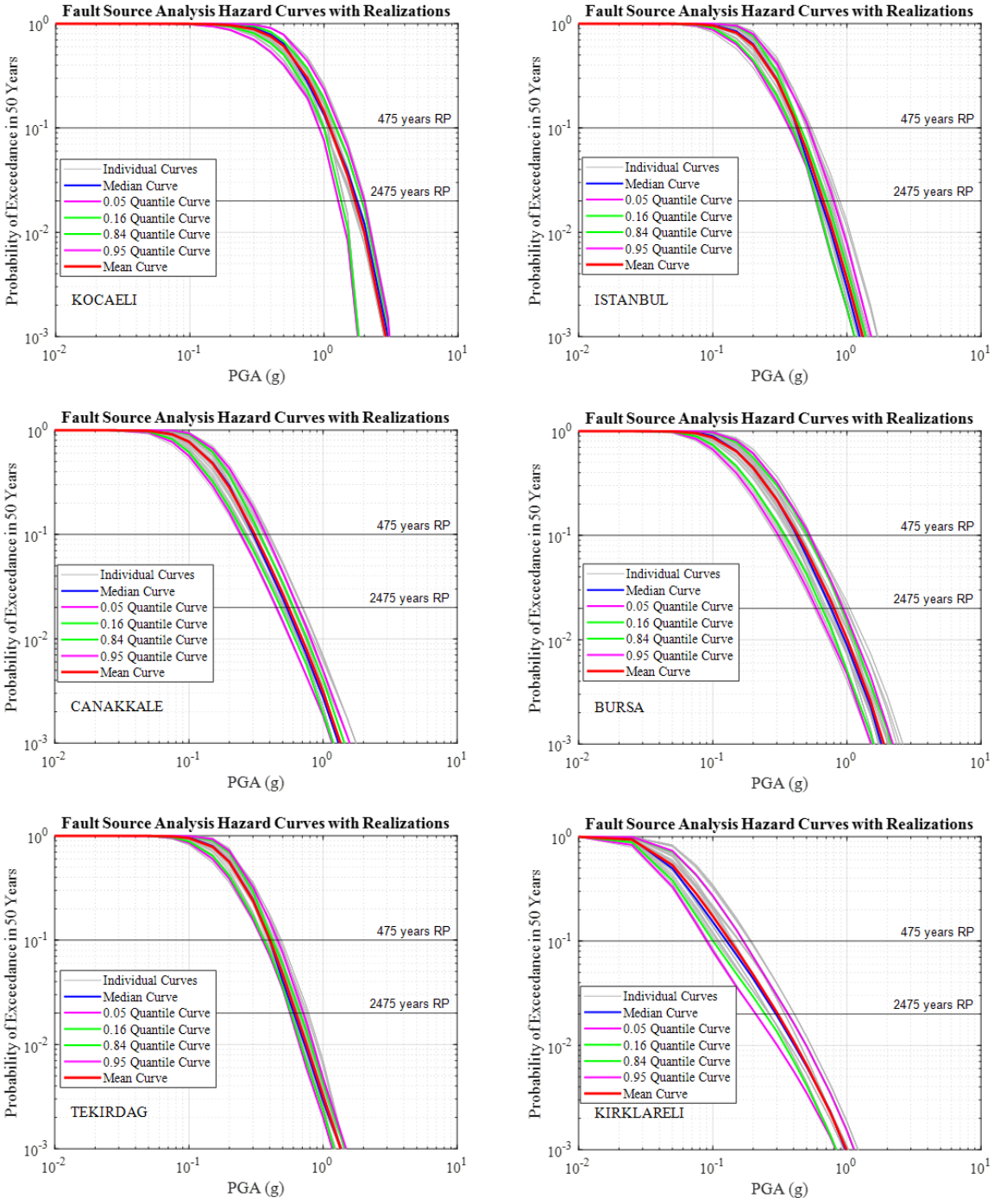

Figure 6.24. Complete set of PGA hazard curves for Kocaeli, Istanbul, Çanakkale, Bursa, Tekirdağ and Kırklareli city centers obtained from the FS model

Figure 6.25 presents the sensitivity of the FS model to the maximum magnitude. As the maximum magnitude assigned to the fault source directly affects the earthquake productivity due to the moment rate balancing concept (see Figure 5.25) a sensitivity to this parameter is observed at all sites.

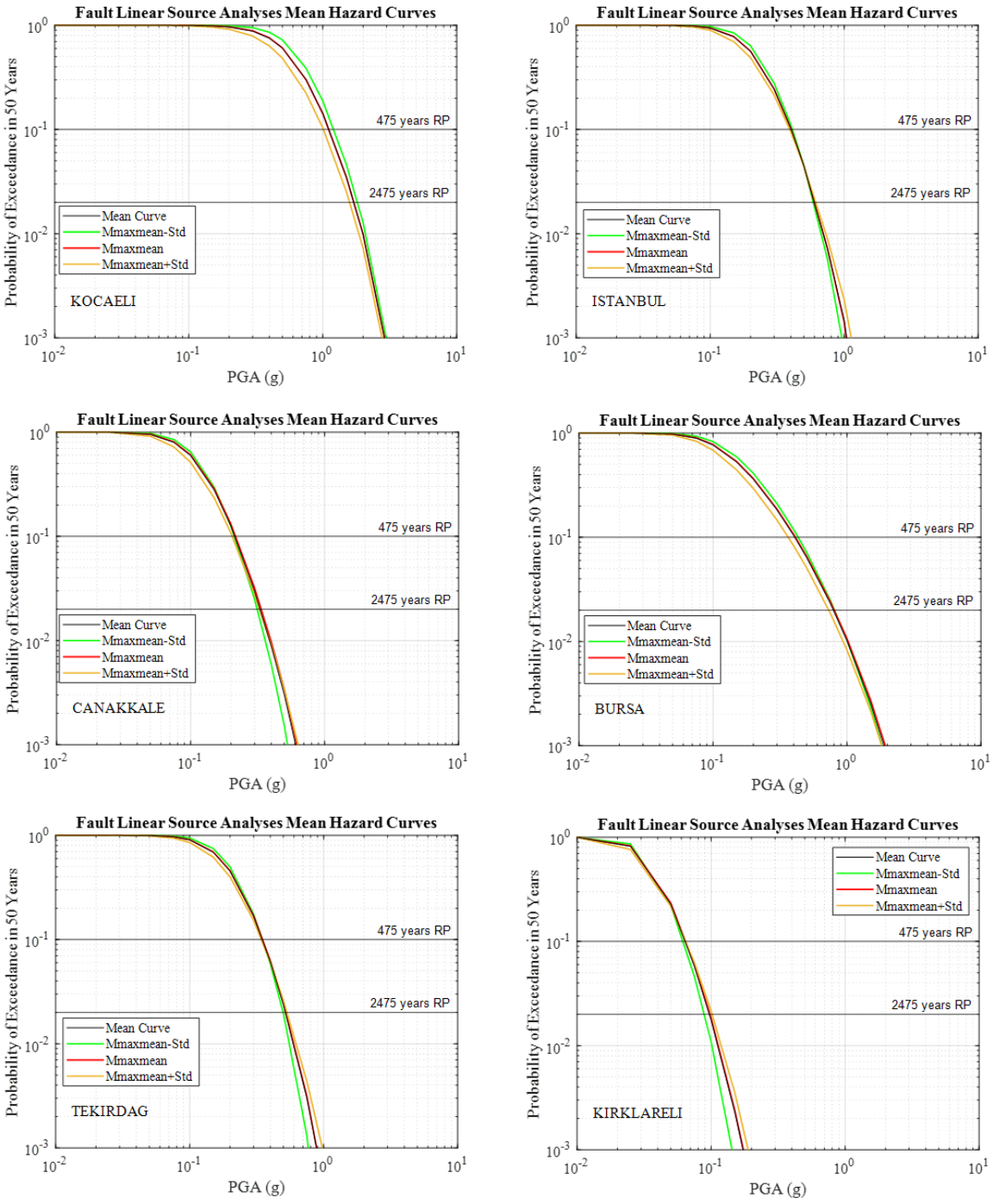

Figure 6.25. Sensitivity of the FS model to maximum magnitude for PGA hazard curves

Figure 6.26 presents the sensitivity to the slip rate range on the faults. This parameter is in fact the main parameter affecting the fault activity at all magnitude ranges. However, at Kocaeli for instance the effect is negligible due to the fact that the uncertainty associated with the slip rate of NAF is very small, as opposed to Bursa, where the uncertainty associated with the slip rate of the Bursa fault is much larger. Here it should be noted that the hazard

curves presented in Figure 6.26 are obtained only from the fault sources. The smoothed seismicity is not included in this sensitivity.

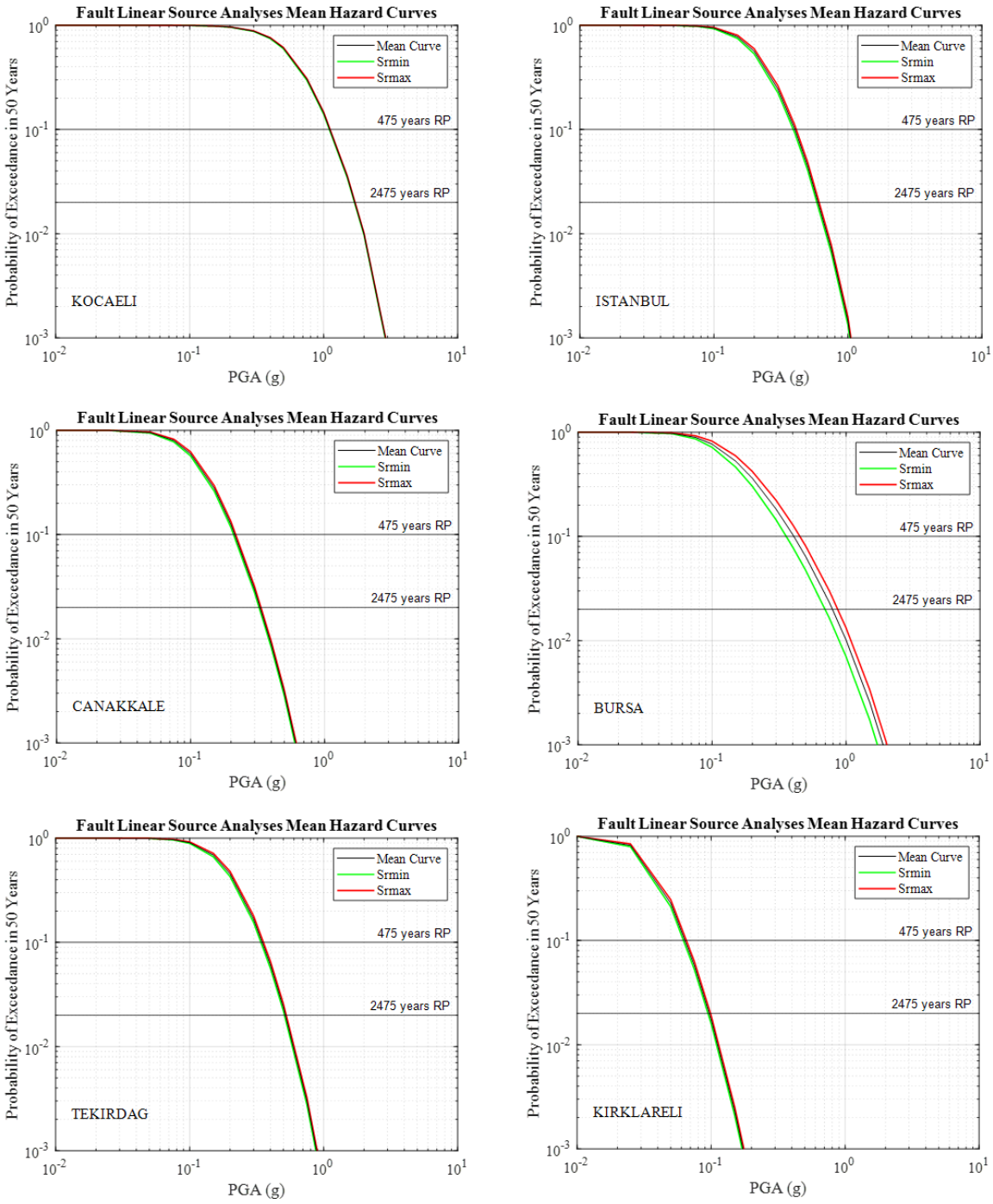

Figure 6.26. Sensitivity of the FS model to the slip rate for PGA hazard curves

Figure 6.27 presents the sensitivity to the size of the smoothing kernel in the smoothed seismicity model. This parameter is more effective at sites where the hazard is governed by

the smoothed seismicity (e.g., Kırklareli) and negligible at site where the hazard is governed by the faults (e.g., Kocaeli). The city of Kırklareli is located the largest distance from the fault sources among the presented cities, a smoothing governed hazard is obtained. Due to the distance, the increase in the hazard level as the correlation distance increase is pretty obvious. At Çanakkale and Kırklareli, the smoothing kernel of 50 m results in higher hazard, revealing that there is no seismicity concentration at close distance to the city center. However, the effect may be the opposite for sites near concentrated seismicity.

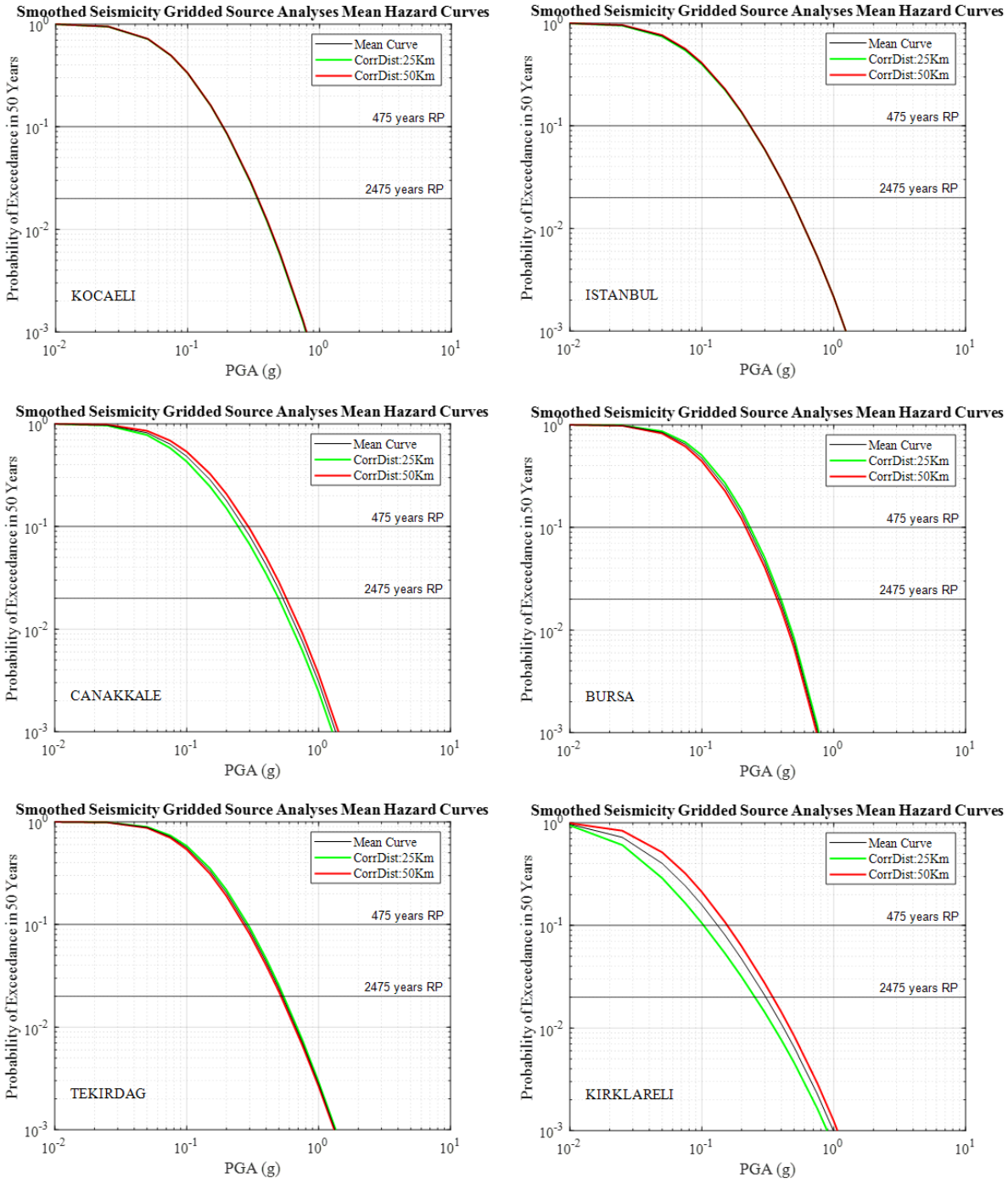

Figure 6.27. Sensitivity of the FS model to the size of the smoothing kernel for PGA hazard curves

6.2.1. Sensitivity to Ground Motion Models

Figure 6.28, Figure 6.29 and Figure 6.30 present the sensitivity of hazard results with respect to the GMPE models for the AS, FS and full models respectively. No particular differences are observed between the different source modeling approaches and the uncertainty ranges remain similar for all return periods.

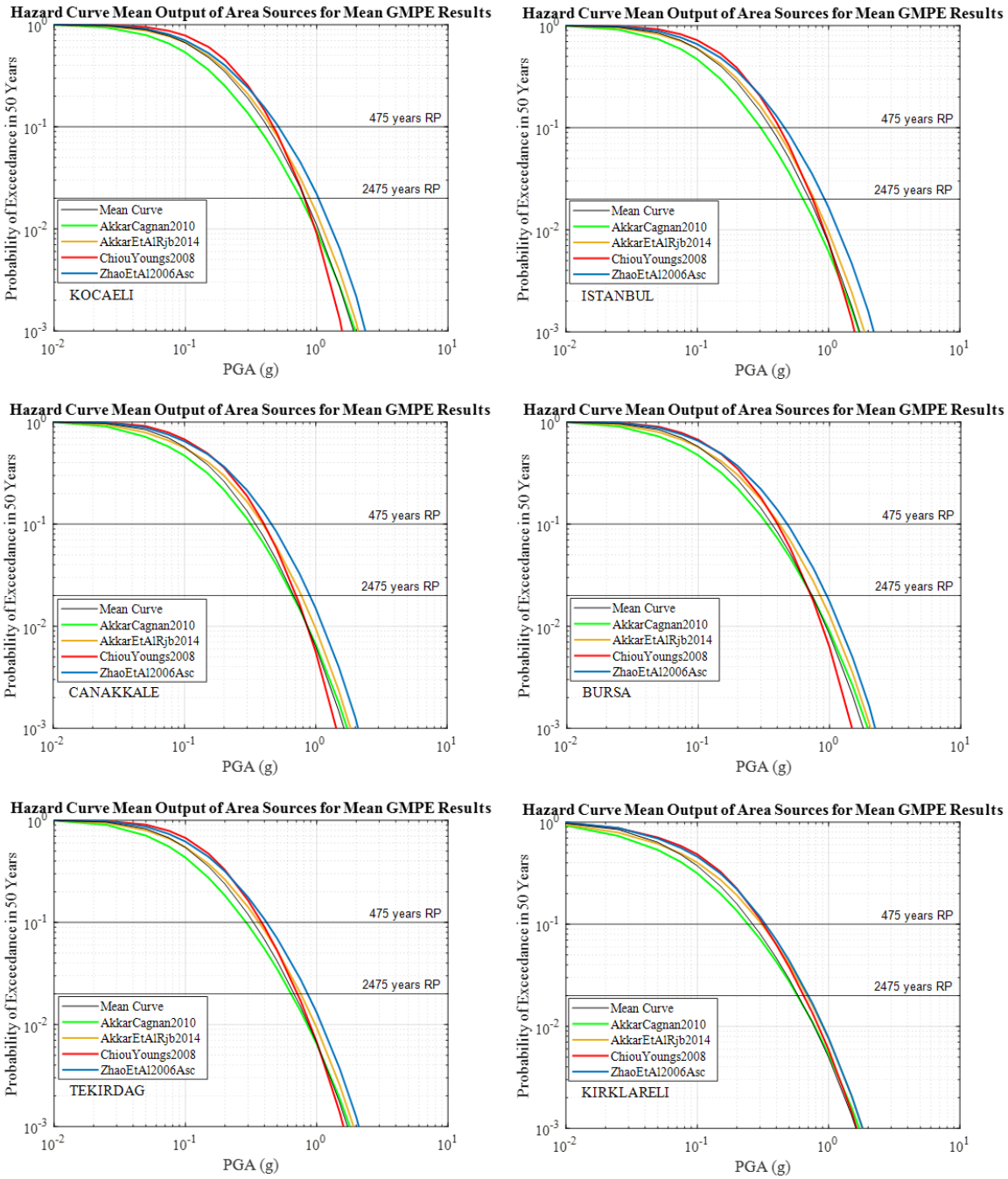

Figure 6.28. Sensitivity of the AS model to the GMPEs for PGA hazard curves

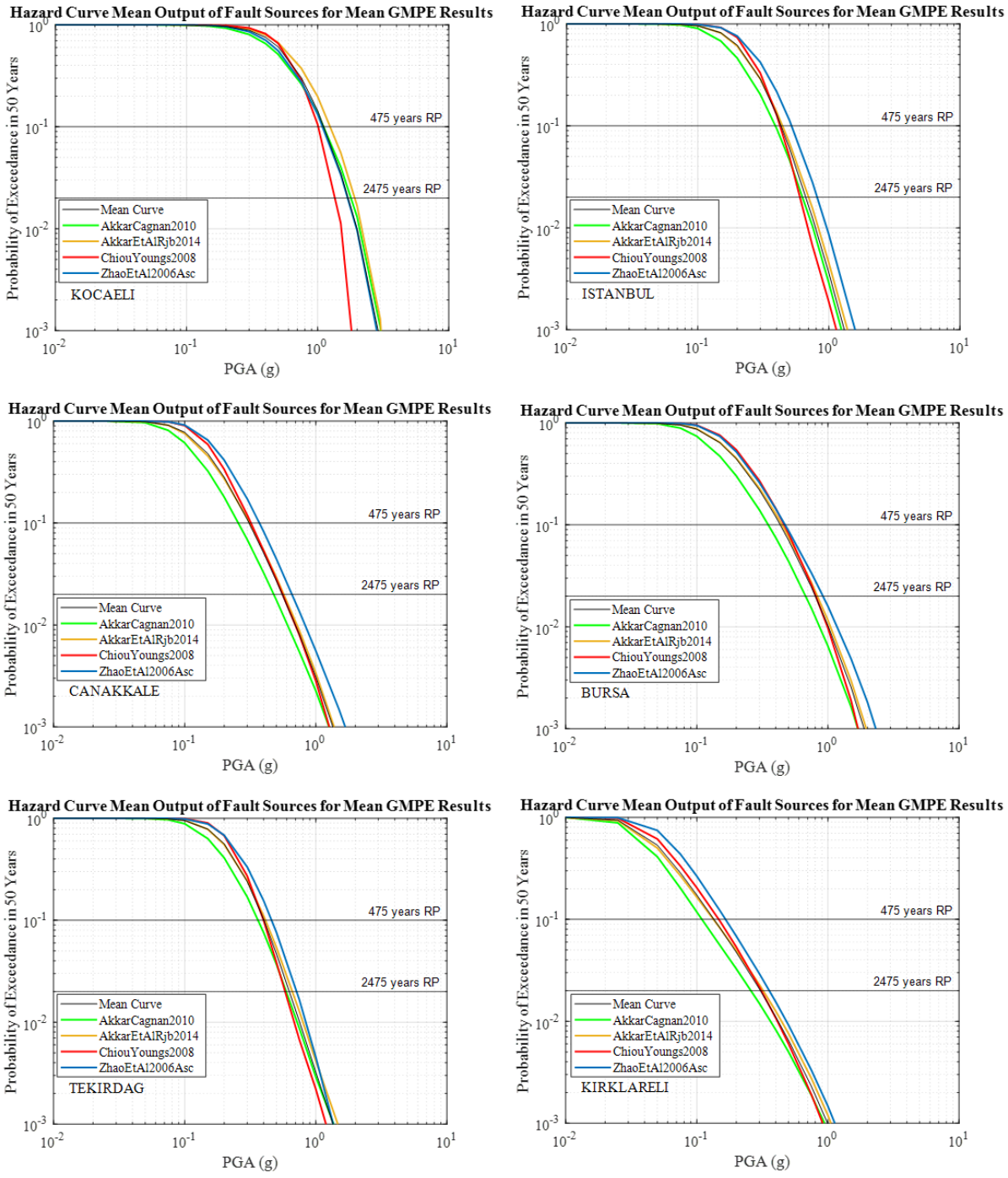

Figure 6.29. Sensitivity of the FS model to the GMPEs for PGA hazard curves

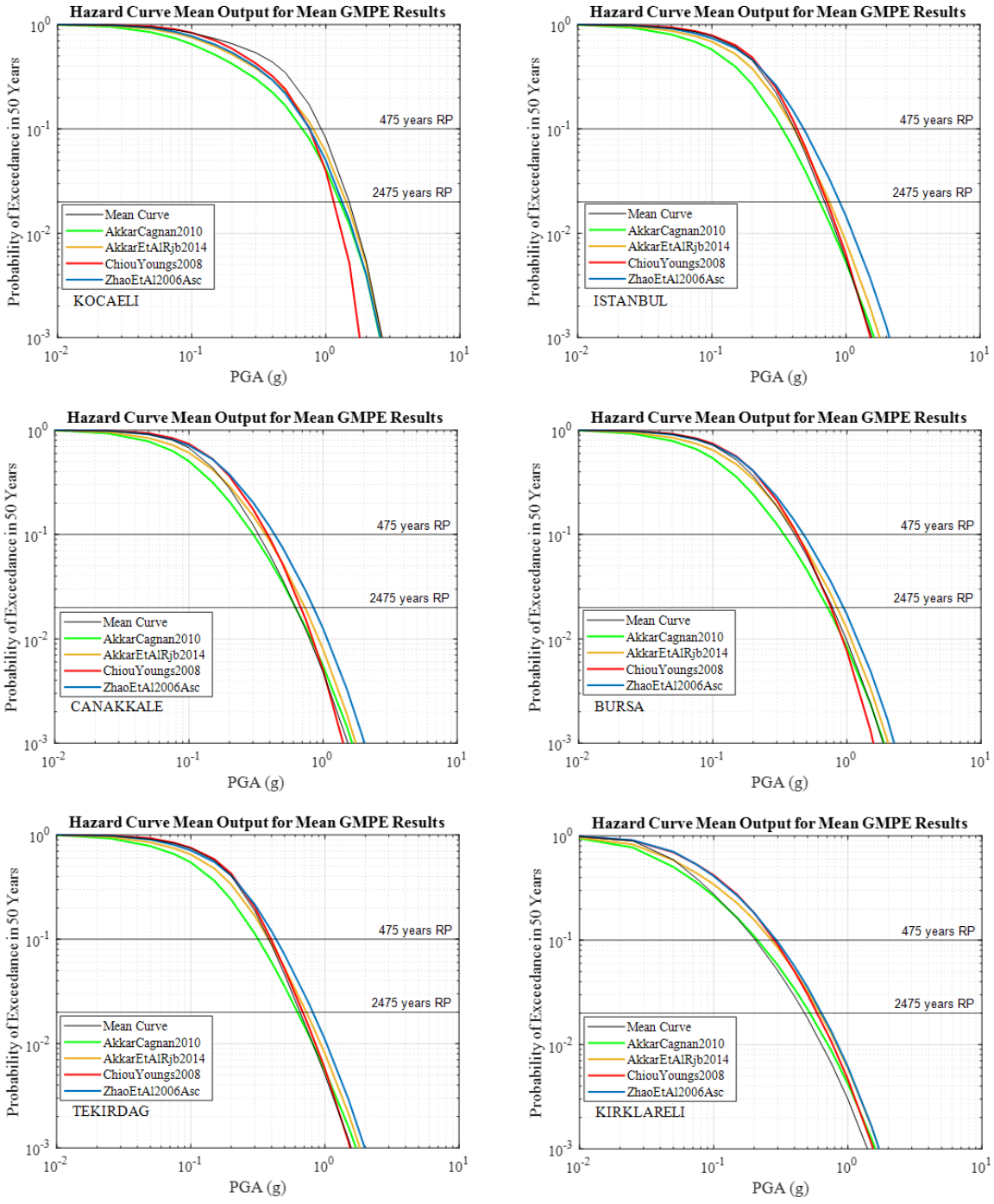

Figure 6.30. Sensitivity of the full model to the GMPEs for PGA hazard curves

6.3. Uncertainty Ranges

A logic tree structure with a large number of branches allows for a robust statistical treatment of the result values. The logic tree formed in the present study consists of 192 individual branches in total out of which the mean, median and quantile hazard values may be obtained.

6.3.1. Map Distribution of Uncertainty Ranges

The uncertainty ranges of the ground motion distributions (PGA and SA, T=1.0s) obtained for 475 and 2475 years return periods are presented in terms of the ratios of 84%/16% quantiles (corresponding to median ± 1 standard deviations of the resulting hazard values) in Figure 6.31 to Figure 6.34 for the full model, in Figure 6.35 to Figure 6.38 for the AS model and Figure 6.39 to Figure 6.42 for the FS model. The 84%/16% quantile ratios of the AS model (Figure 6.35 to Figure 6.38) indicate that the main parameter affecting the uncertainty is the number of earthquakes used in the statistics. The uncertainty range is much narrower in the active sources (higher number of earthquakes leading to more robust statistics) while they are much larger at less active/background sources (leading especially to higher b-value uncertainty). In the FS model the uncertainty is either caused by the slip rate range of the fault sources (if the range is large) or the smoothing kernel size at sites away from the fault sources.

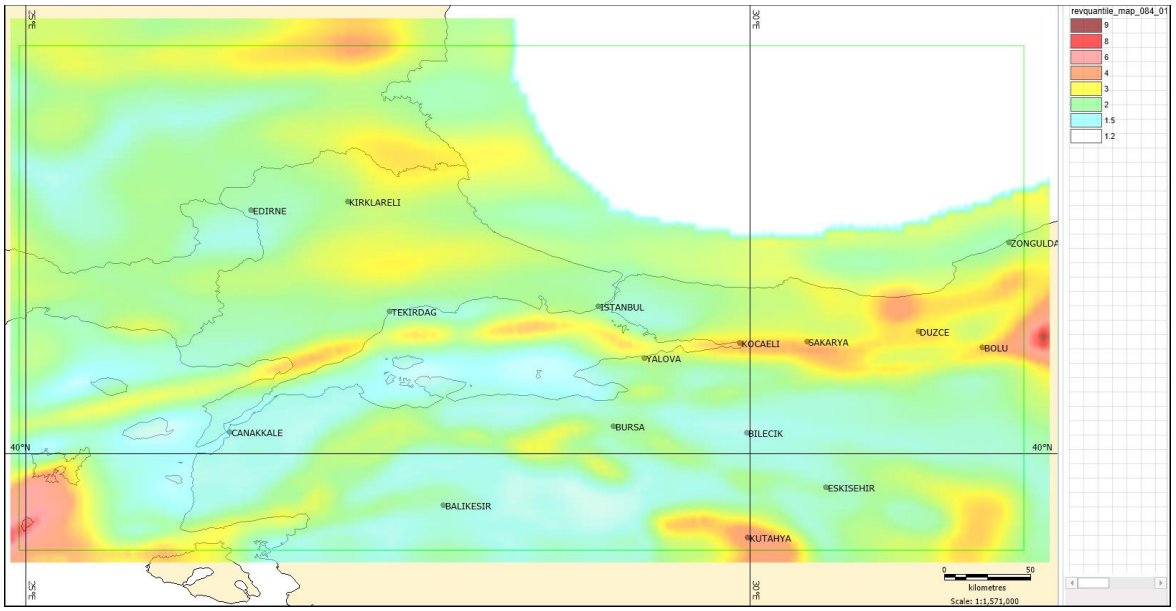

Figure 6.31. Full model %84/%16 (+Std/-Std) PGA ratio, 475 years RP

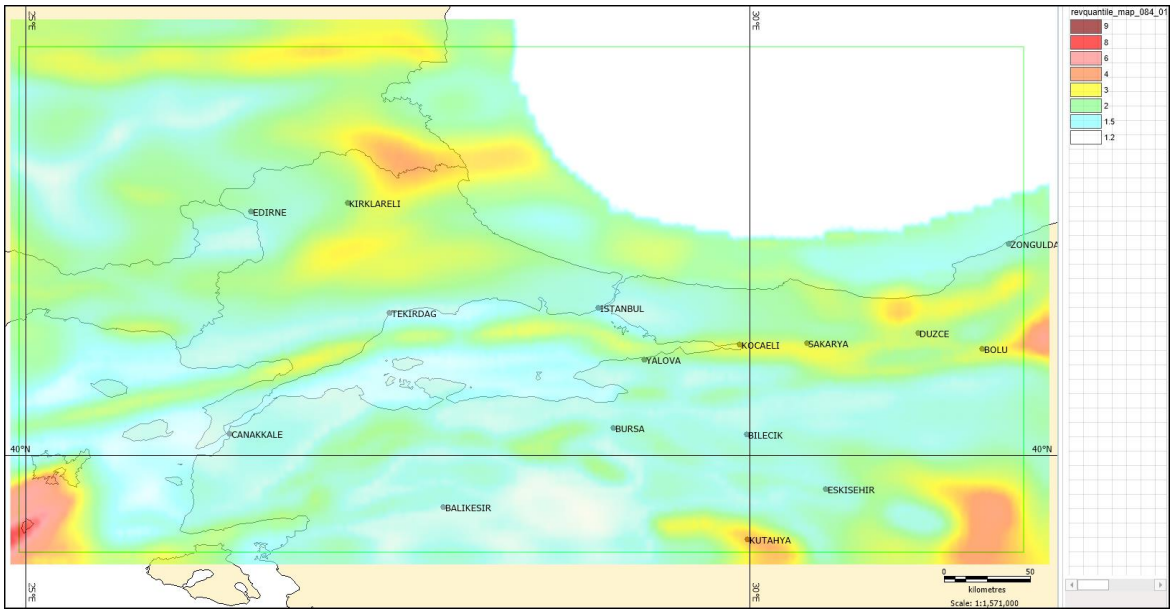

Figure 6.32. Full model %84/%16 (+Std/-Std) PGA ratio, 2475 years RP

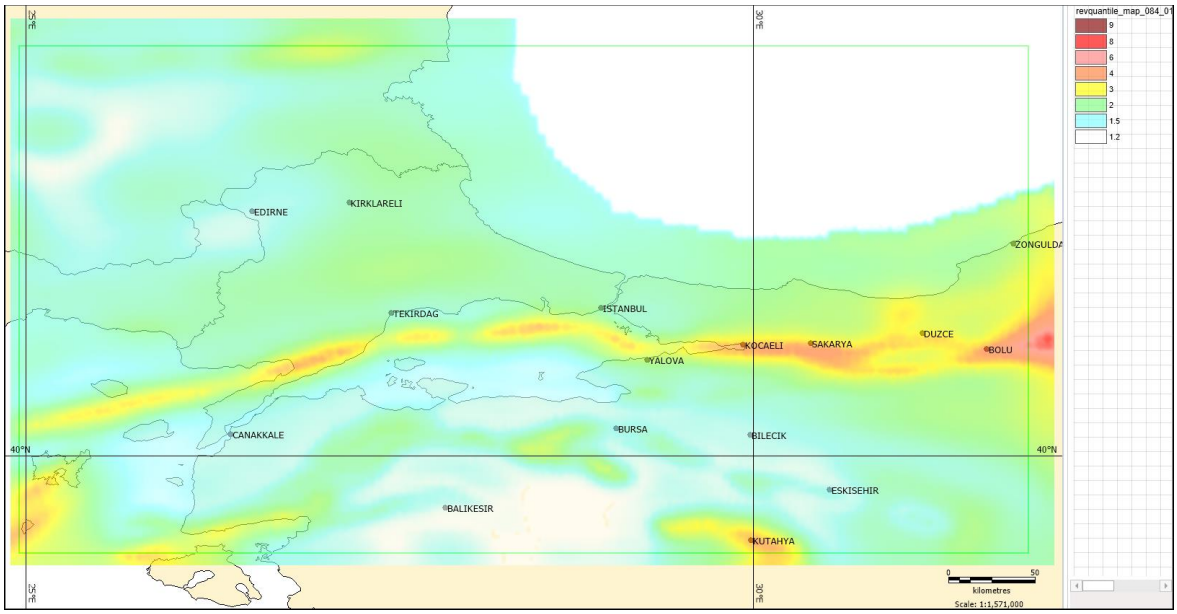

Figure 6.33. Full model %84/%16 (+Std/-Std) SA (T=1.0 s) ratio, 475 years RP

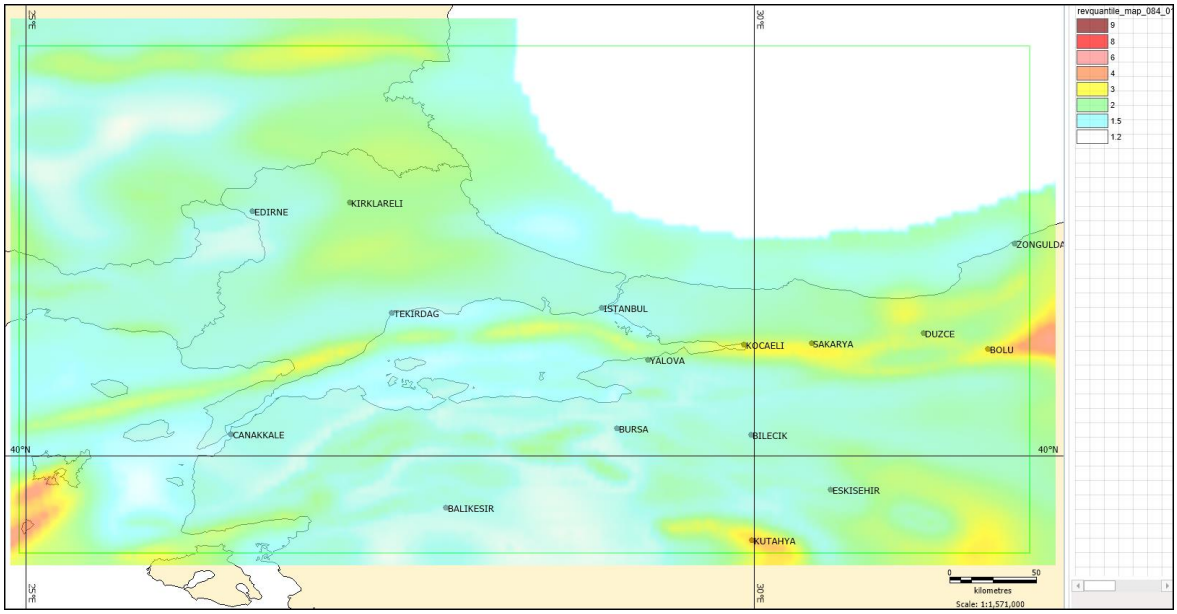

Figure 6.34. Full model %84/%16 (+Std/-Std) SA (T=1.0 s) ratio, 2475 years RP

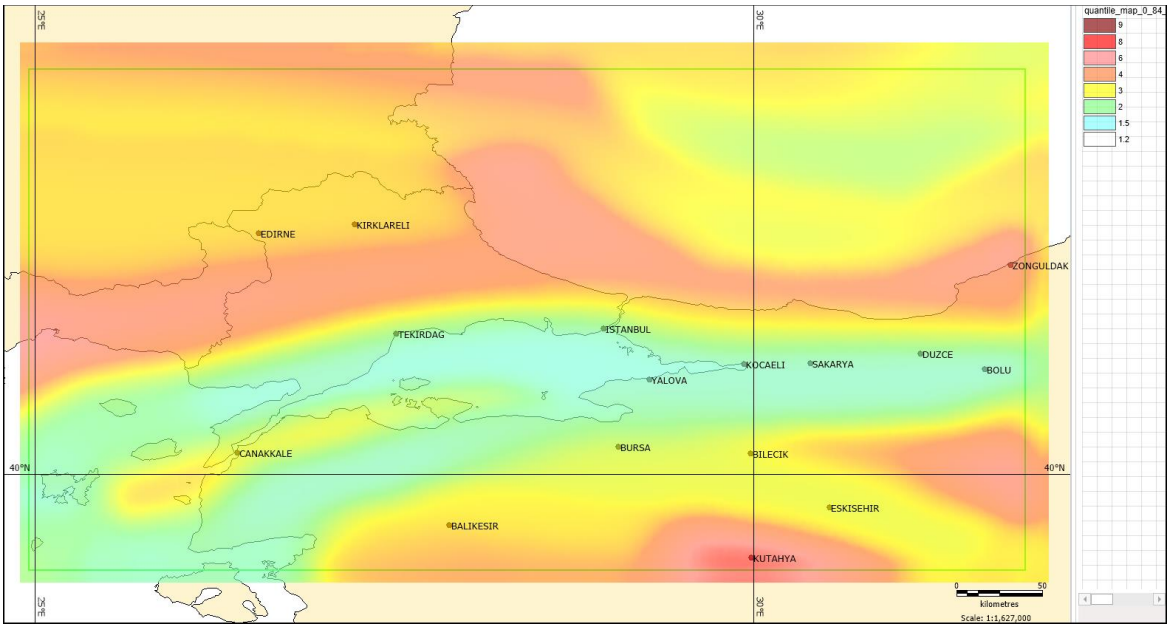

Figure 6.35. Area source model %84/%16 (+Std/-Std) PGA ratio, 475 years RP

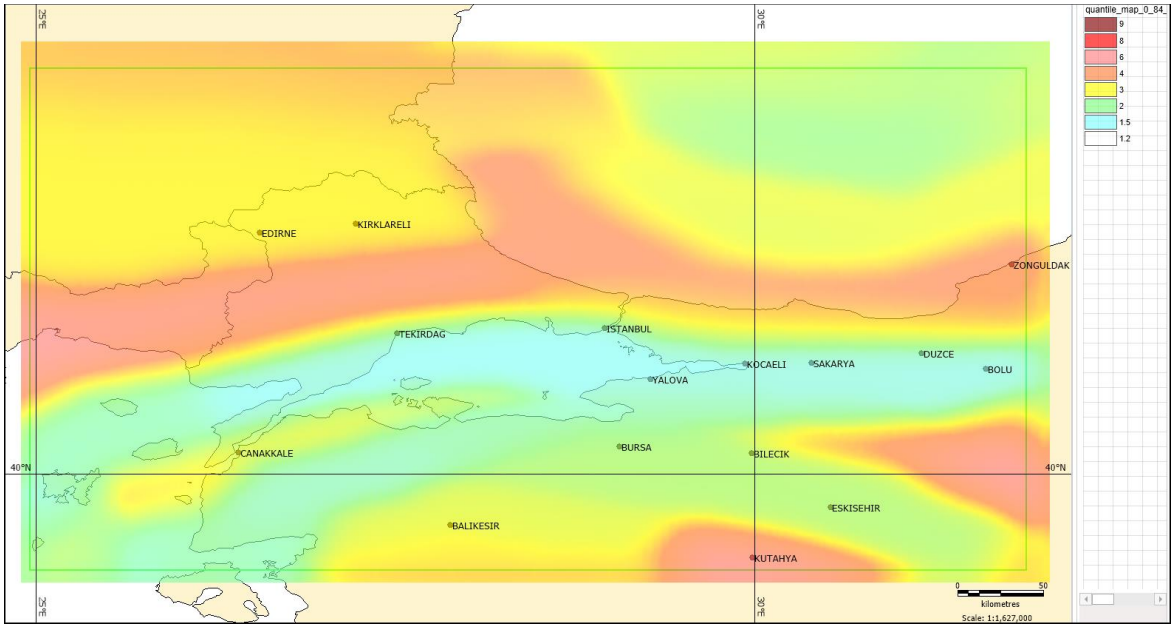

Figure 6.36. Area source model %84/%16 (+Std/-Std) PGA ratio, 2475 years RP

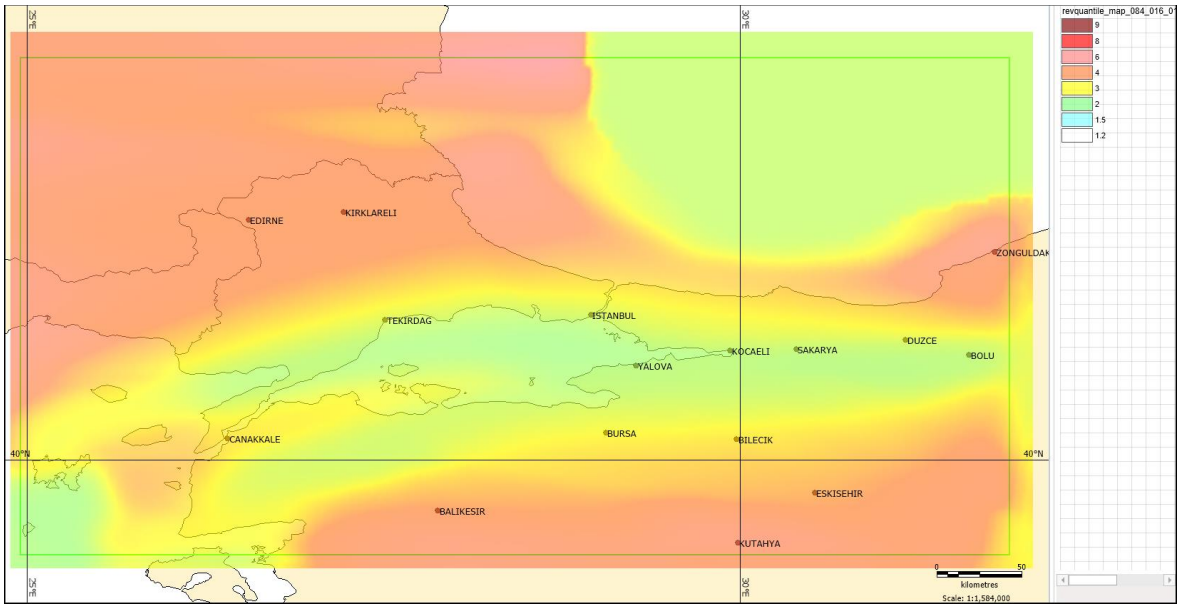

Figure 6.37. Area source model %84/%16 (+Std/-Std) SA (T=1.0 s) ratio, 475 RP

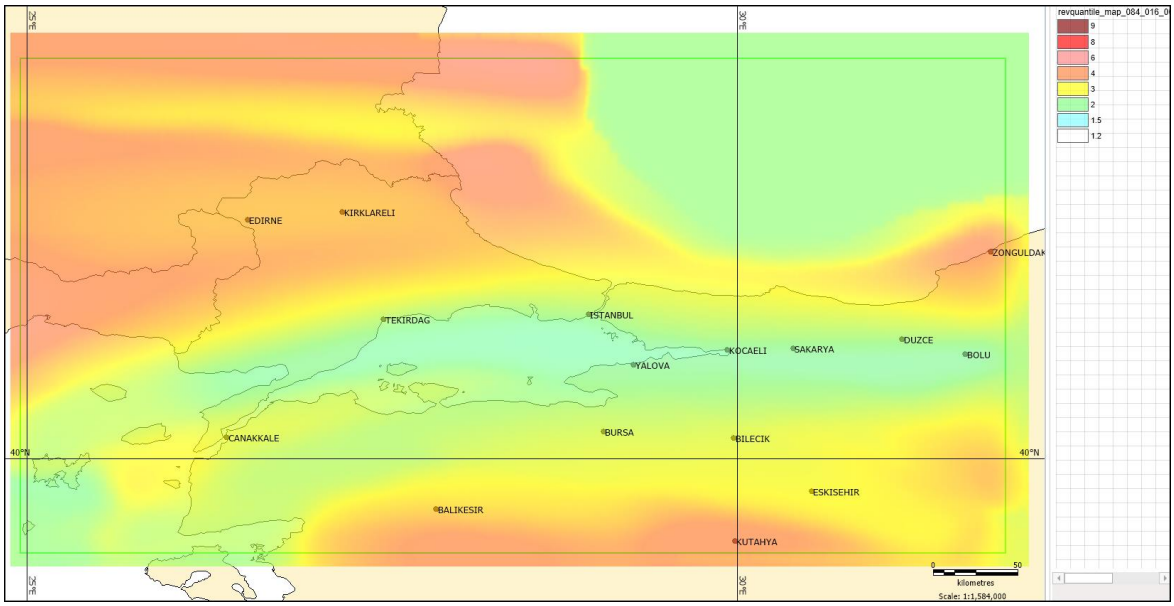

Figure 6.38. Area source model %84/%16 (+Std/-Std) SA (T=1.0 s) ratio, 2475 years RP

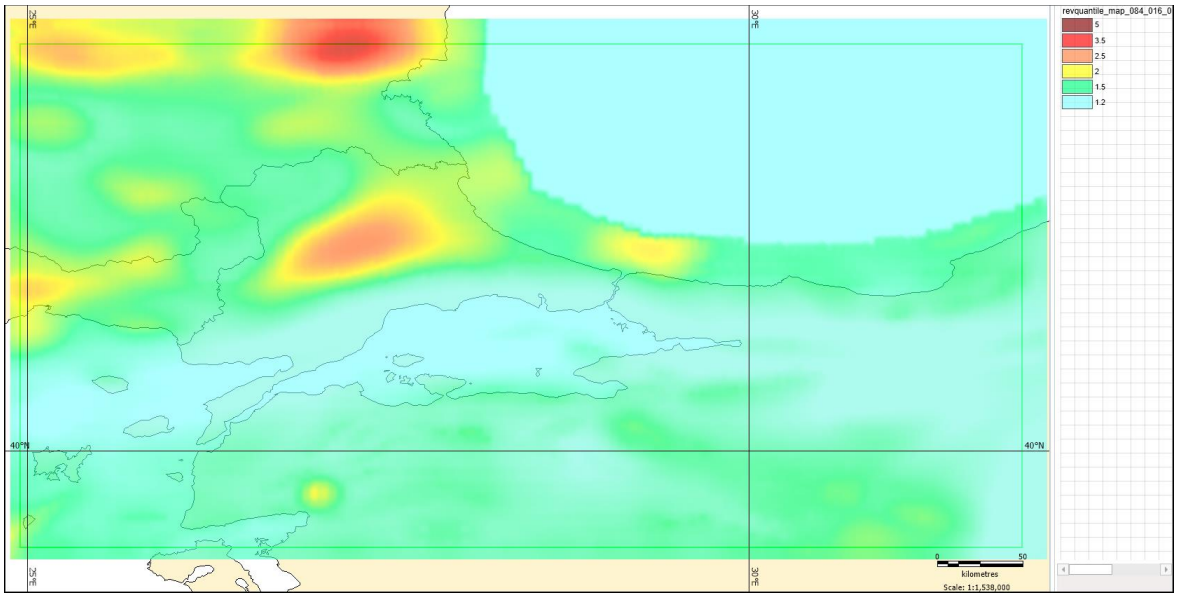

Figure 6.39. Fault source model %84/%16 (+Std/-Std) PGA ratio, 475 years RP

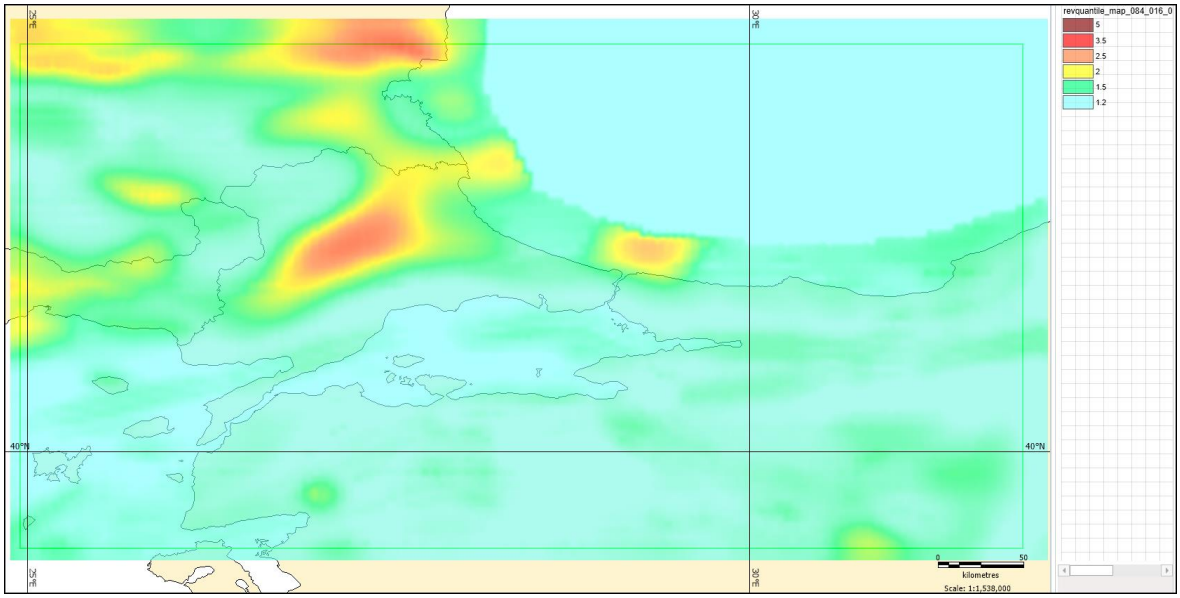

Figure 6.40. Fault source model %84/%16 (+Std/-Std) PGA ratio, 2475 years RP

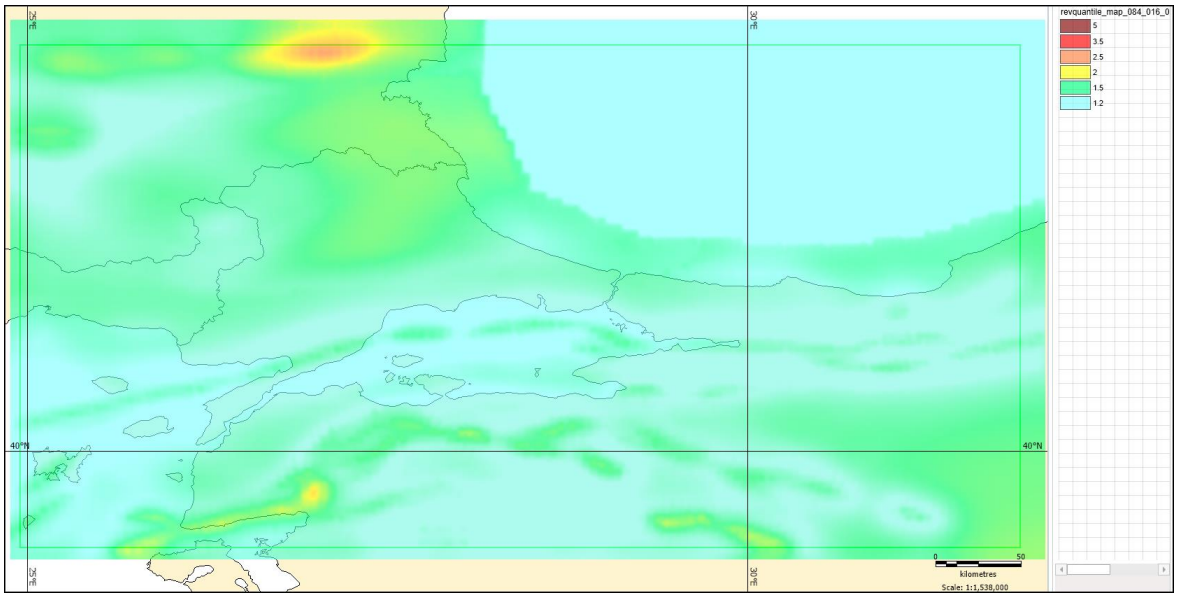

Figure 6.41. Fault source model %84/%16 (+Std/-Std) SA (T=1.0 s) ratio, 475 years RP

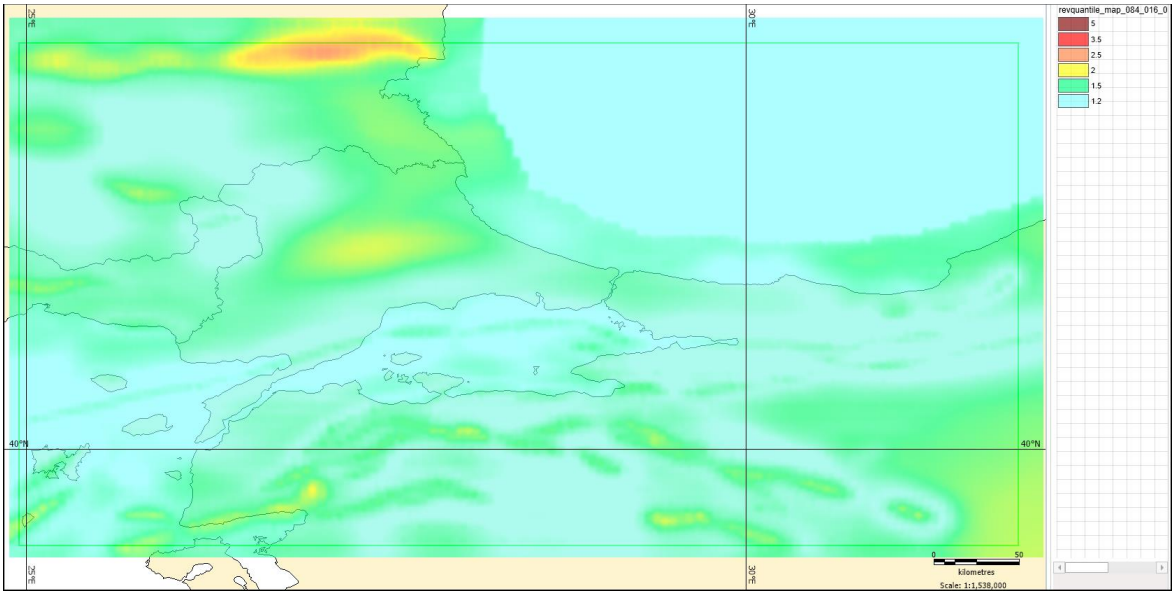

Figure 6.42. Fault source model %84/%16 (+Std/-Std) SA (T=1.0 s) ratio, 2475 years RP

6.3.2. Complete Uncertainty Distribution in the Point Based Results

The complete set of PGA hazard curves (192 branches) and the resulting mean and quantiles are presented in Figure 6.43 for the six city centers which were also used in the parameter sensitivity analysis. The variability obtained in the resulting hazard curves reveals

that a large uncertainty is associated with the estimations of the ground motion values, the uncertainties becoming relatively smaller for longer return periods.

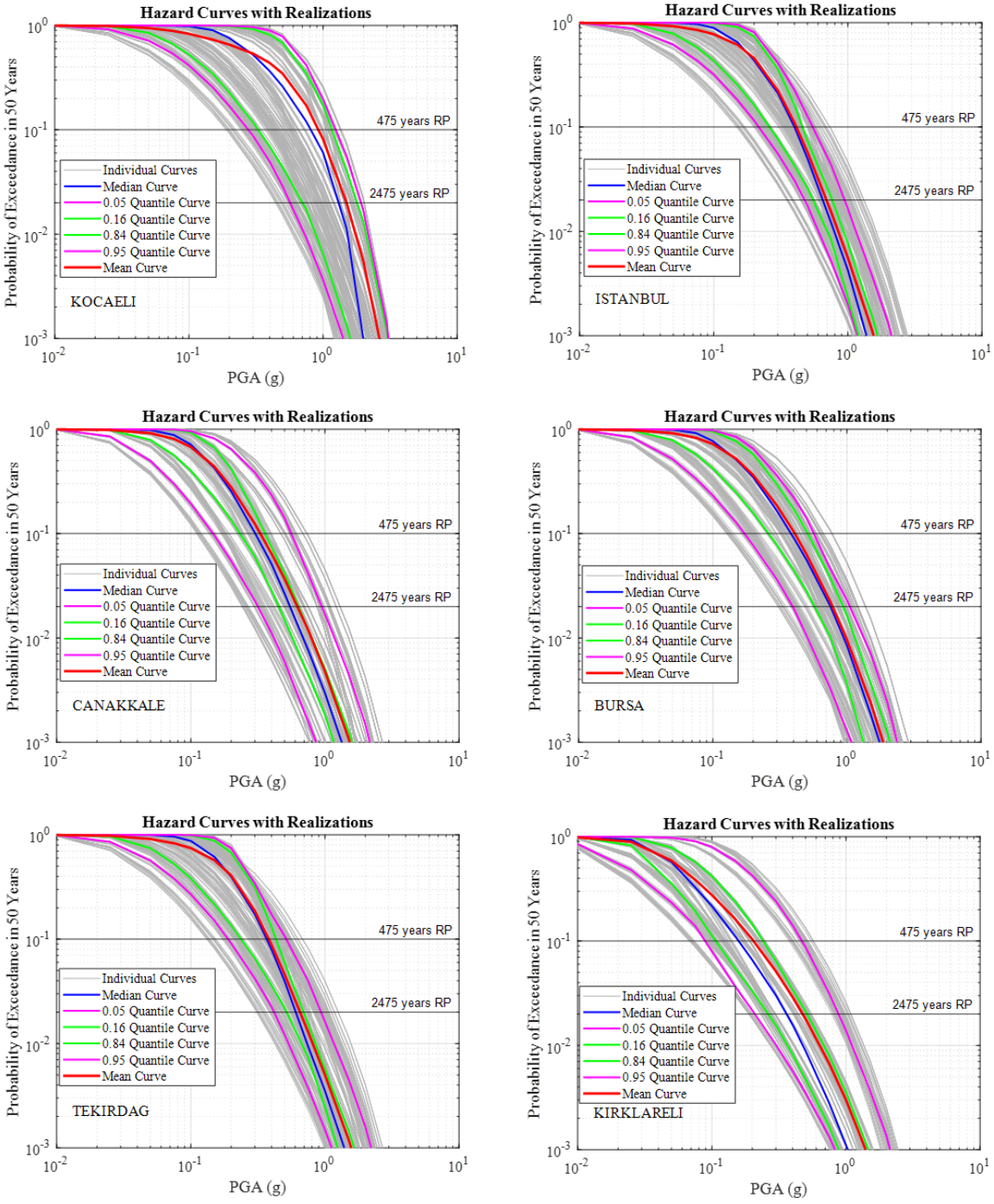

Figure 6.43. Complete set of PGA hazard curves for Kocaeli, Istanbul, Çanakkale, Bursa, Tekirdağ and Kırklareli city centers

The mean and the 0.16 and 0.84 quantile PGA and T=1.0s spectral acceleration results for 475 and 2475 years return period are listed in Table 6.4 and Table 6.5 for each city center located within the study region respectively. Here we observe that the uncertainty ranges obtained for PGA are generally larger than the uncertainty ranges obtained for SA (T=1.0), and 475 years uncertainties are larger than 2475 years uncertainties. The largest uncertainties are obtained for the cities of Kocaeli and Sakarya, resulting from the differences in source modeling (AS model vs FS model) as discussed in Section 6.2.1.

Table 6.4. The mean and the quantile peak ground accelerations obtained for the city centers located in the study region

City	PGA, 475 years RP (g)				PGA, 2475 years RP (g)			
	Mean	- 1 Std (16%)	+ 1 Std (84%)	84% / 16%	Mean	- 1 Std (16%)	+ 1 Std (84%)	84% / 16%
Balıkesir	0.389	0.249	0.451	1.82	0.721	0.524	0.772	1.47
Bilecik	0.316	0.223	0.328	1.47	0.642	0.455	0.665	1.46
Çanakkale	0.330	0.232	0.358	1.54	0.623	0.453	0.636	1.40
Düzce	0.619	0.274	0.768	2.81	1.020	0.593	1.179	1.99
Edirne	0.222	0.132	0.242	1.83	0.496	0.301	0.513	1.71
Eskisehir	0.411	0.267	0.528	1.98	0.826	0.598	0.960	1.60
Kırklareli	0.205	0.107	0.241	2.25	0.475	0.263	0.512	1.95
Kocaeli	0.923	0.328	1.165	3.55	1.496	0.702	1.796	2.56
Sakarya	0.804	0.324	0.986	3.04	1.265	0.695	1.512	2.18
Tekirdağ	0.382	0.237	0.432	1.82	0.652	0.518	0.693	1.34
Yalova	0.688	0.329	0.849	2.58	1.114	0.702	1.306	1.86
Istanbul	0.414	0.260	0.459	1.76	0.692	0.549	0.764	1.39
Bursa	0.408	0.261	0.511	1.96	0.780	0.574	0.935	1.63

Table 6.5. The mean and the quantile 5% damped T=1.0 s spectral accelerations obtained for the city centers located in the study region

City	SA (T=1.0), 475 years RP (g)				SA (T=1.0), 2475 years RP (g)			
	Mean	- 1 Std (16%)	+ 1 Std (84%)	84% / 16%	Mean	- 1 Std (16%)	+ 1 Std (84%)	84% / 16%
Balıkesir	0.207	0.162	0.214	1.32	0.419	0.309	0.430	1.39
Bilecik	0.213	0.154	0.222	1.44	0.432	0.295	0.461	1.56
Çanakkale	0.227	0.170	0.254	1.50	0.438	0.318	0.489	1.54
Düzce	0.381	0.177	0.454	2.57	0.665	0.391	0.737	1.88
Edirne	0.146	0.099	0.145	1.47	0.319	0.211	0.318	1.50
Eskisehir	0.234	0.186	0.264	1.42	0.513	0.357	0.588	1.65
Kırklareli	0.143	0.082	0.148	1.81	0.310	0.159	0.314	1.97
Kocaeli	0.565	0.212	0.738	3.48	1.029	0.467	1.226	2.62
Sakarya	0.508	0.207	0.625	3.02	0.897	0.455	1.038	2.28
Tekirdağ	0.254	0.170	0.297	1.75	0.473	0.356	0.539	1.51
Yalova	0.419	0.219	0.503	2.29	0.745	0.476	0.824	1.73
Istanbul	0.276	0.177	0.323	1.82	0.500	0.382	0.570	1.49
Bursa	0.249	0.186	0.289	1.55	0.504	0.383	0.592	1.55

6.4. Comparison with the Base Model (UDAP-Ç-13-06)

Comparisons of the mean hazard results obtained in this study and those from the base model (UDAP-Ç-13-06 Project) are presented in Figure 6.44 to Figure 6.49 for three ground motion parameters and two return periods. The use of a more comprehensive logic tree structure resulted in changes in the mean hazard in the range of 0.8 to 1.2. The mean hazard results became generally higher (20% at most) especially at sites that remain in the background sources. The main reason for this is the introduction of the b value uncertainty in the AS model, which is much larger in the sources with low seismicity (the so-called background sources). However, these results may also vary as a function of the weights associated with the different branches of the logic tree. Here it should be noted that although equal weights are assigned to the ± 1 σ branches of the b value (0.2), the net effect of the addition of this parameter in the logic tree structure is an increase of the mean hazard at sites located in low seismicity regions (i.e., larger b value uncertainty regions).

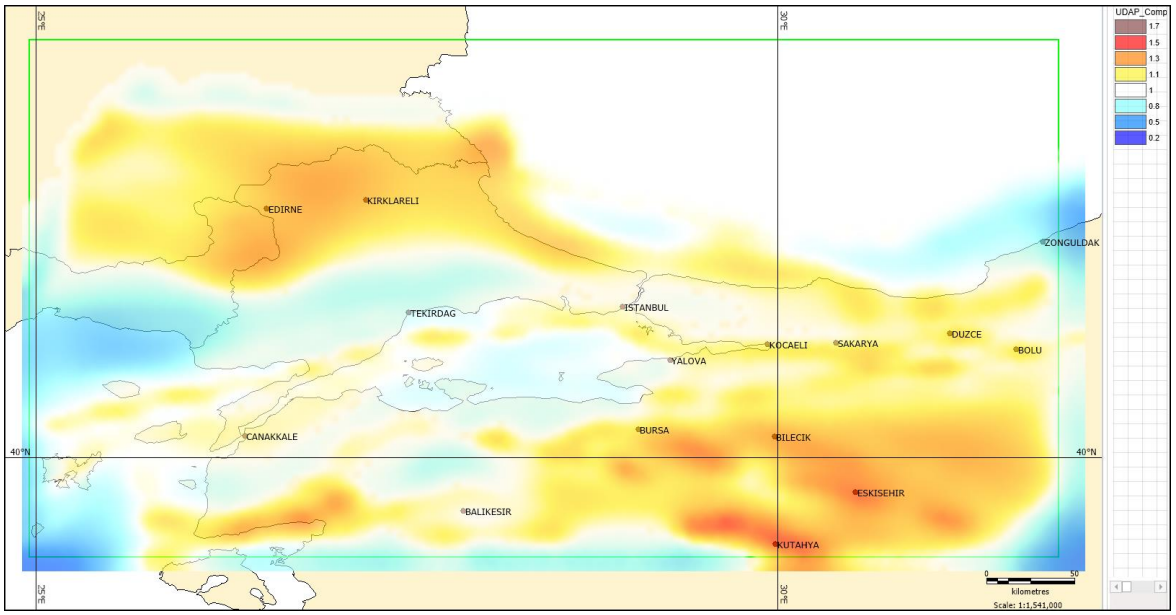

Figure 6.44. (PSHA)/(UDAP-Ç-13-06) ratio for mean PGA, 475 years RP

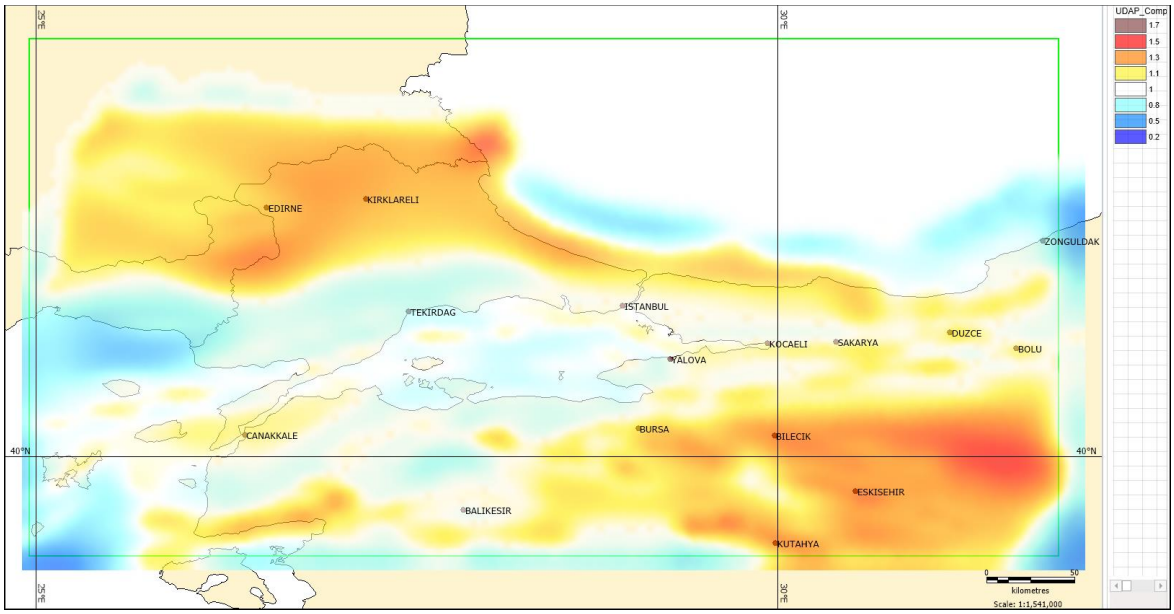

Figure 6.45. (PSHA)/(UDAP-Ç-13-06) ratio for mean PGA, 2475 years RP

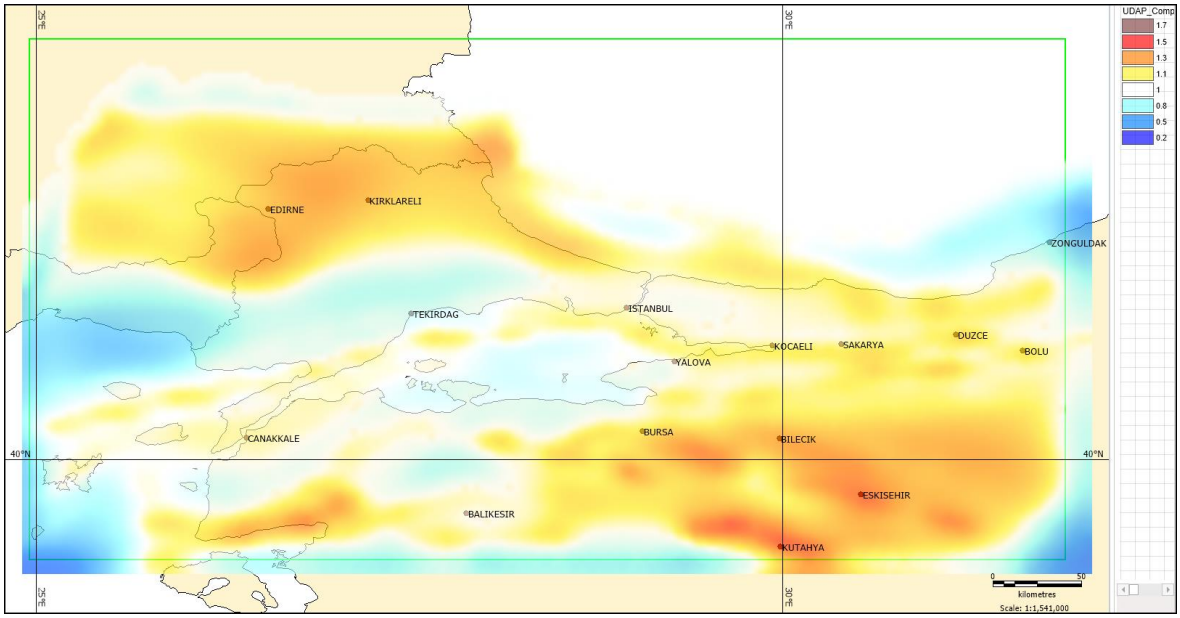

Figure 6.46. (PSHA)/(UDAP-Ç-13-06) ratio for mean SA (T=0.2 s), 475 years RP

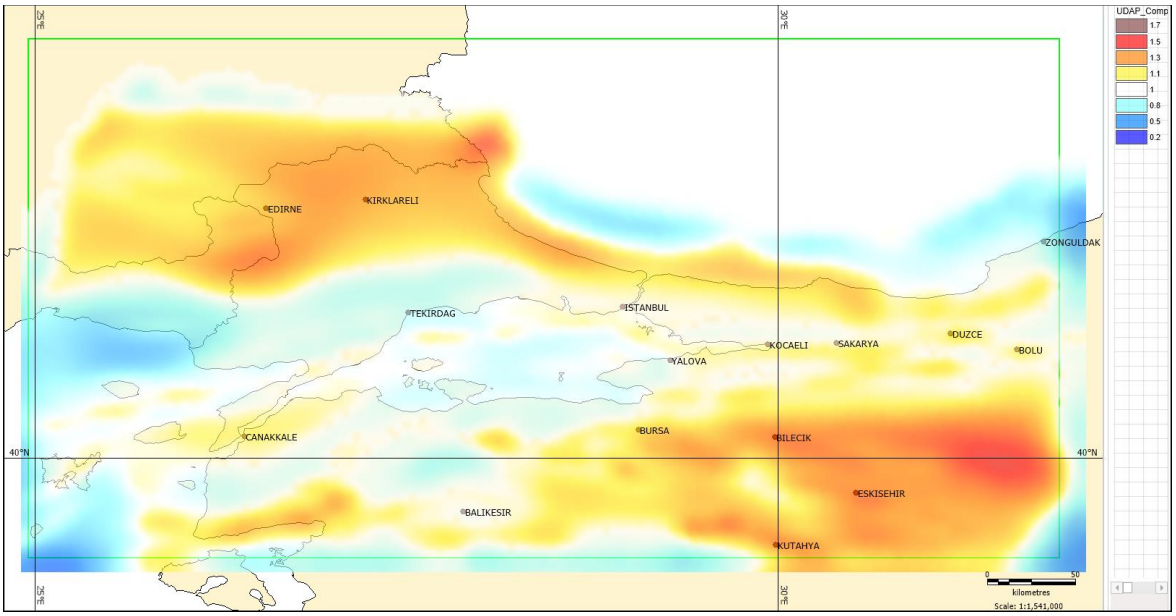

Figure 6.47. (PSHA)/(UDAP-Ç-13-06) ratio for mean SA (T=0.2 s), 2475 years RP

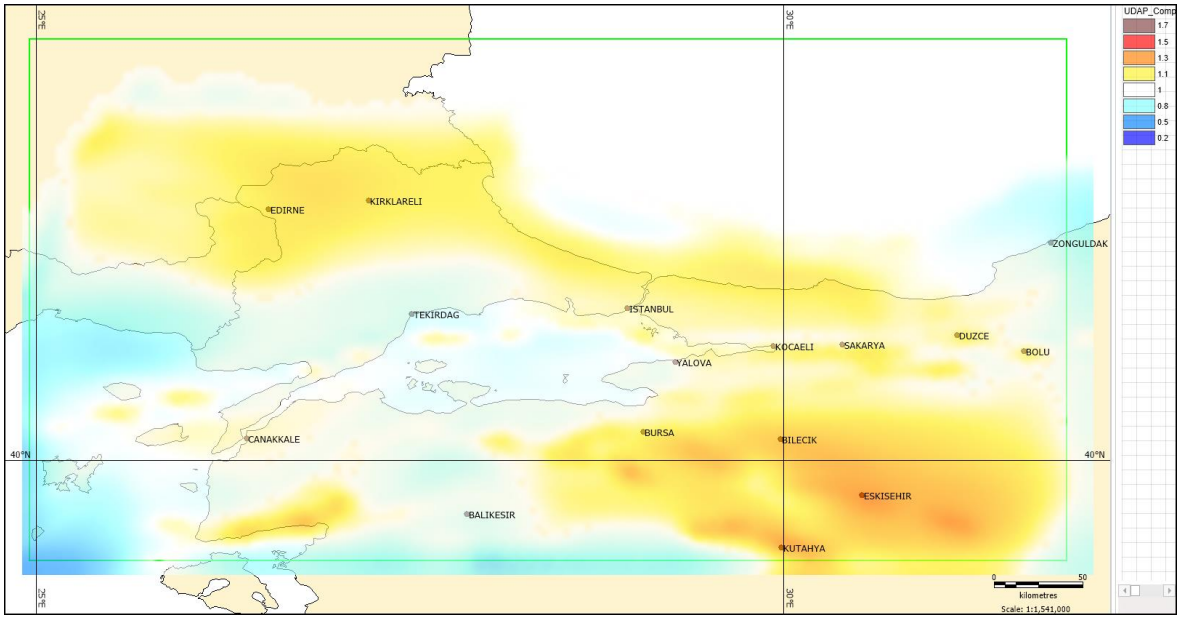

Figure 6.48. (PSHA)/(UDAP-Ç-13-06) ratio for mean SA (T= 1.0 s), 475 years RP

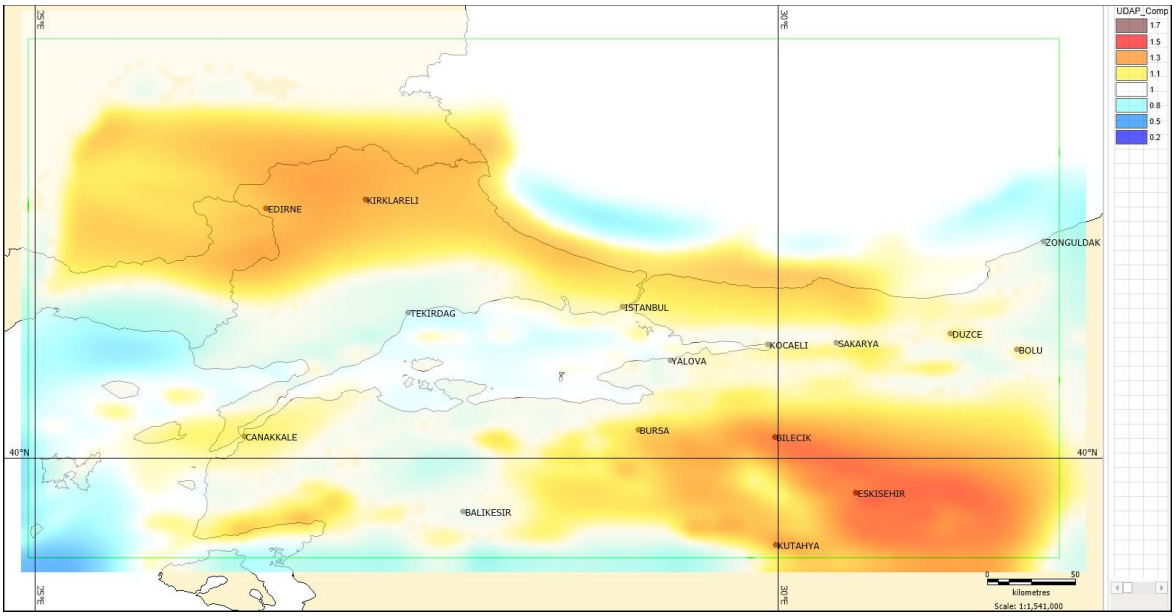

Figure 6.49. (PSHA)/(UDAP-Ç-13-06) ratio for mean SA (T= 1.0 s), 2475 years RP

7. CONCLUSIONS

Housing the western end of “the North Anatolian Fault (NAF)” which has the potential of producing large earthquakes (Tan et al., 2008) the Marmara region is one of the regions with the highest seismic activity in Turkey. Considering the building stock and human density the Marmara region contains; earthquake hazard assessment studies are of primary importance for the region. Accordingly, in this study, “the Turkish Seismic Hazard Map (2018)”, which is developed within the scope of the “UDAP-Ç-13-06” project and is in force in connection with the national seismic design code, has been evaluated for the Marmara region in terms of epistemic uncertainties that may be contained.

As a result of the seismic hazard assessment analysis conducted here, the PGA, 5% damped spectral accelerations of T= 0.2 s and T= 1.0 s corresponding to 475 and 2475 years are obtained. In addition to the hazard maps, comparative hazard curves for the selected city centers are discussed and evaluated in terms of epistemic uncertainties. Maps for quantile ratio distributions are developed and finally, the results obtained herein are compared with the mean ground motion distributions from the studies by Şeşetyan et al. (2018) and Demircioğlu et al. (2018) carried out within the scope of the “UDAP-Ç-13-06” project. In the light of these results, the following conclusions may be drawn:

- Although Marmara region is one of the best studied regions in terms of seismic activity and geological structure, the seismic hazard models built for the region can still be associated with large uncertainties.

- Consideration of epistemic uncertainties related with the model parameters can affect the mean hazard levels, even if equal or symmetric weights are assigned to alternative branches.

- The main modeling approach, i.e., AS model vs FS model is the largest source of uncertainty for sites located very close to or very far from the active fault sources.

- The uncertainty range of the area source model is generally wider than the fault source model.

- The b-value can be assumed as the most effective epistemic uncertainty factor for area sources.

- The slip rate and the maximum magnitudes share the same level of effect on fault sources.

- The smoothed seismicity correlation distance effect becomes more important when the distance from the fault sources increases.

As future work, we believe that the following attempts might be meaningful;

- Given to the fact that for the fault sources, with considerably wide range of SRmin-SRmax (such as the ones located in the vicinity of Bursa), more up-to-date fault source models may be utilized to further improve the accuracy of the obtained results.

- Future work on the topic may adopt the use of more recent GMPEs, such as "the Next Generation Attenuation (NGA) – West 2" models or GMPEs developed from local data that propose a better representation of regional tectonic properties.

- One of the most significant outcomes of the present study is the fact that insufficient earthquake catalog is among the main factors that increased the uncertainty of the computed earthquake hazard. Hence, catalogs with lower Mwmin values, which can only be obtained with denser and better instrumentation, may be helpful in future studies.

- The study presented herein may be further improved by utilizing characteristic modelling approaches for the fault sources, which can also allow for the development of the so-called Renewal models to investigate the expected earthquake hazard in areas located within the zones of silent faults (such as the seismic gap in the Marmara region). This approach is expected to yield interesting and valuable outcomes.

8. REFERENCES

Abrahamson, N. A. and J. J. Bommer, 2005, "Probability and uncertainty in seismic hazard analysis", *Earthquake spectra*, Vol. 21, No. 2, pp. 603-607.

Akkar, S. and Z. Çağnan, 2010, "A local ground-motion predictive model for Turkey, and its comparison with other regional and global ground-motion models", *Bulletin of the Seismological Society of America*, Vol. 100, No. 6, pp. 2978-2995.

Akkar, S., T. Azak, T. Çan, M. Demircioğlu Tümsa, T. Duman, M. Erdik, S. Ergintav, F. T. Kadirioğlu, D. Kalafat, Ö. Kale, R. F. Kartal, K. Kekovalı, T. Kılıç, S. Özalp, S. Altuncu Poyraz, K. Şeşetyan, S. Tekin, A. Yakut, M. T. Yılmaz, M. S. Yücemen, Ö. Zülfikar, 2018, "Evolution of seismic hazard maps in Turkey", *Bull Earthquake Engineering*, Vol. 16, No. 8, pp. 3197–3228.

Akkar, S., Ö. Kale, and U. Çeken, 2018, "Ground-motion characterization for the probabilistic seismic hazard assessment in Turkey", *Bulletin of Earthquake Engineering*, Vol. 16, No. 8, pp. 3439-3463.

Akkar, S., A. M. Sandıkkaya, and J. J. Bommer, 2014, "Empirical ground-motion models for point-and extended-source crustal earthquake scenarios in Europe and the Middle East", *Bulletin of earthquake engineering*, Vol. 12, No. 1, pp. 359-387.

Alsan, E., L. Tezuçan, and M. Båth, 1976, "An earthquake catalogue for Turkey for the interval 1913–1970", *Tectonophysics*, Vol. 31, No. 1-2, pp. T13-T19.

Ambraseys, N. N., and C. F. Finkel, 1987, "The Saros–Marmara earthquake of 9 August 1912", *Earthquake engineering and structural dynamics*, Vol. 15, No. 2, pp. 189-211.

Ambraseys, N. N., and J. A. Jackson, 2000, "Seismicity of the Sea of Marmara (Turkey) since 1500", *Geophysical Journal International*, Vol. 141, No. 3, pp. F1-F6.

Armijo, R., B. Meyer, S. Navarro, G. King, and A. Barka, 2002, "Asymmetric slip partitioning in the Sea of Marmara pull-apart: A clue to propagation processes of the North Anatolian fault?", *Terra nova*, Vol. 14, No. 2, pp. 80-86.

Atakan, K., A. Ojeda, M. Meghraoui, A. A. Barka, M. Erdik, and A. Bodare, 2002, "Seismic Hazard in Istanbul following the 17 August 1999 İzmit and 12 November 1999 Düzce Earthquakes", *Bulletin of the Seismological Society of America*, Vol. 92, No. 1, pp. 466–482.

Atik, L. A., N. Abrahamson, J. J. Bommer, F. Scherbaum, F. Cotton, and N. Kuehn, 2010, "The variability of ground-motion prediction models and its components", *Seismological Research Letters*, Vol. 81, No. 5, pp. 794-801.

Baker, J. W., 2008, "An introduction to probabilistic seismic hazard analysis (PSHA)", *White paper, version*, Vol 1, pp. 72.

Barka, A., H. S. Akyüz, E. Altunel, G., Sunal, Z. Çakır, A. Dikbaş, B. Yerli, R. Armijo, B. Meyer, J. B. de Chabalier, T. Rockwell, J. R. Dolan, R. Hartleb, T. Dawson, S. Christofferson, A. Tucker, T. Fumal, R. Langridge, H. Stenner, W. Lettis, J. Bachhube, W. Page, 2002, "The surface rupture and slip distribution of the 17 August 1999 Izmit earthquake (M 7.4), North Anatolian fault", *Bulletin of the Seismological Society of America*, Vol. 92, No. 1, pp. 43-60.

Bommer, J. J., 2002, "Deterministic vs. probabilistic seismic hazard assessment: an exaggerated and obstructive dichotomy", *Journal of Earthquake Engineering*, Vol. 6, No. 01, pp. 43-73.

Bommer, J. J., F. Scherbaum, H. Bungum, F. Cotton, F. Sabetta, F. Sabetta, and N. A. Abrahamson, 2005, "On the Use of Logic Trees for Ground-Motion Prediction Equations in Seismic-Hazard Analysis" *Bulletin of the Seismological Society of America*, Vol. 95, No. 2, pp. 377–389.

Boore, D. M., and W. B. Joyner, 1982., "The Empirical Prediction of Ground Motion", *Bulletin of the Seismological Society of America*, Vol. 72, No. 6B, pp. 43-S60.

Bozkurt, E., 2001, "Neotectonics of Turkey–a synthesis", *Geodinamica acta*, Vol. 14, No. 1-3, pp. 3-30.

Bungum, H., 2007, "Numerical modelling of fault activities", *Computers and geosciences*, Vol. 33, No. 6, pp. 808-820.

Chiou, B. J., and R. R. Youngs, 2008, "An NGA model for the average horizontal component of peak ground motion and response spectra", *Earthquake spectra*, Vol. 24, No. 1, pp. 173-215.

Cornell, C., 1968 “Engineering Seismic Risk Analysis”, *Bulletin of the seismological society of America*, Vol. 58, No. 5.

Demircioğlu, M., K. Şeşetyan, T. Duman, T. Çan, S. Tekin, and S. Ergintav, 2018, “A probabilistic seismic hazard assessment for the Turkish territory: part II—fault source and background seismicity model”, *Bulletin of Earthquake Engineering*, Vol. 16, No. 8, pp. 3399-3438.

Duman, T. Y., T. Çan, Ö. Emre, T. F. Kadirioğlu, N. Başarır Baştürk, T. Kılıç, S. Arslan, S. Özalp, R. F. Kartal, D. Kalafat F. Karakaya, T. Eroğlu Azak, N. M. Özel, S. Ergintav, S. Akkar, Y. Altınok, S. Tekin, A. Cingöz, A. Kurt, 2016, “Seismotectonic database of Turkey”, *Bull Earthquake Eng*, Vol. 16, No. 8, pp. 3277-3316.

Duman, T. Y., Ö. Emre, A. Dogan, and S. Özalp, 2005, “Step-over and bend structures along the 1999 Duzce earthquake surface rupture, North Anatolian fault, Turkey”, *Bulletin of the Seismological Society of America*, Vol. 95, No. 4, pp. 1250-1262.

Emre, Ö., T. Y. Duman, S. Özalp, H. Elmacı, Ş. Olgun, and Ş. Şaroğlu, 2013, "Active fault map of Turkey with explanatory text. Special Publication Series” Ankara: *General Directorate of Mineral Research and Exploration.*

Emre, Ö., T. Y. Duman, S. Özalp, F. Şaroğlu, Ş. Olgun, H. Elmacı, and T. Çan, 2016, “Active fault database of Turkey”, *Bulletin of Earthquake Engineering*, Vol. 16, pp. 3229–3275.

Erdik, M., M. B. Demircioğlu, K. Şeşetyan, E. Durukal, and B. Siyahi, 2004, “Earthquake hazard in Marmara Region, Turkey”, *Soil Dynamics and Earthquake Engineering*, Vol. 24, No. 8, pp. 605–631.

Erdik, M., V. Doyuran, N. Akkaş, and P. Gülkan, 1985, “A probabilistic assessment of the seismic hazard in Turkey.”, *Tectonophysics*, Vol. 117, No. 3-4, pp. 295–344.

Eroğlu Azak, T., D. Kalafat, K. Şeşetyan, and M. Demircioğlu, 2018, “Effects of seismic declustering on seismic hazard assessment: a sensitivity study using the Turkish earthquake catalogue”, *Bulletin of Earthquake Engineering*, Vol. 16, No. 8, pp. 3339-3366.

Frankel, A., 1995, “Mapping seismic hazard in the central and eastern United States”, *Seismological Research Letters*, Vol. 66, No. 4, pp. 8-21.

Gardner, J., and L. Knopoff, 1974, "Is the sequence of earthquakes in Southern California, with aftershocks removed, Poissonian?", *Bulletin of the seismological society of America*, Vol. 64, No. 5, pp. 1363-1367.

Gülerce, Z., and S. Ocak, 2013, "Probabilistic seismic hazard assessment of Eastern Marmara Region", *Bulletin of Earthquake Engineering*, Vol. 11, No. 5, pp. 1259-1277.

Gülkan, P., A. Koçyiğit, M. Yücemen, V. Doyuran, and N. Başöz, 1993, "En son verilere göre hazırlanan Türkiye deprem bölgeleri haritası", Vol. 93-01, ODTÜ Deprem Mühendisliği Araştırma Merkezi.

Hanks, T. C., and A. C. Cornell, 2001, "Probabilistic Seismic Hazard Analysis: a Beginner's Guide", *Earthquake Spectra*.

Hanks, T., and H. Kanamori, 1979, "A moment magnitude scale", *Journal of Geophysical Research: Solid Earth*, Vol. 84, pp. 2348-2350.

Hubert-Ferrari, A., A. Barka, E. Jacques, Nalbant, S. S., Meyer, B., Armijo, R., . . . King, G. C., 2000, "Seismic hazard in the Marmara Sea region following the 17 August 1999 Izmit earthquake", *Nature*, Vol. 404, No. 6775, pp. 269-273.

Kadirioğlu, F., R. F. Kartal, T. Kılıç, D. Kalafat, T. Y. Duman, T. Eroğlu Azak, S. Özalp, Ö. Emre, 2018, "An improved earthquake catalogue ($M \geq 4.0$) for Turkey and its near vicinity (1900–2012)", *Bull Earthquake Eng*, Vol. 16, No. 8, pp. 3317-3338.

Kalafat, D., 2011, "Marmara Bölgesi'nin Depremselliği ve Deprem Ağının Önemi", *1. Türkiye Deprem Mühendisliği ve Sismoloji Konferansı*, pp. 11-14.

Kalkan, E., and P. Gülkan, 2004, "Site-dependent spectra derived from ground motion records in Turkey", *Earthquake Spectra*, Vol. 20, No. 4, pp. 1111-1138.

Kalkan, E., P. Gülkan, N. Yilmaz, and M. Çelebi, 2009, "Reassessment of Probabilistic Seismic Hazard in the Marmara Region", *Bulletin of the Seismological Society of America*, Vol. 99, No. 4, pp. 2127–2146.

Karabulut, H., S. Güvercin, F. Eskiköy, A. Ö. Konca, and S. Ergintav, 2021, "The moderate size 2019 September M w 5.8 Silivri earthquake unveils the complexity of the Main Marmara Fault shear zone", *Geophysical Journal International*, Vol. 224, No. 1, pp. 377-388.

Kramer, S. L. (1996). *Geotechnical Earthquake Engineering*. Upper Saddle River, N.J.: Prentice Hall.

Kürçer, A., A. Chatzipetros, S. Z. Tutkun, S. Pavlides, Ö. Ateş, and S. Valkaniotis, 2008, "The Yenice–Gönen active fault (NW Turkey): Active tectonics and palaeoseismology", *Tectonophysics*, Vol. 453, No. 1-4, pp. 263-275.

Le Pichon, X., Şengör, E. Demirbağ, C. Rangin, C. İmren, R. Armijo, N. Görür, N. Çağatay, B. Mercier de Lepinay, B. Meyer, R. Saatçılar, B. Tok, 2001, "The active Main Marmara Fault", *Earth and Planetary Science Letters*, Vol. 192, No. 4, pp. 595-616.

McGuire, R., 2008, "Probabilistic seismic hazard analysis: Early history", *Earthquake Engineering and Structural Dynamics*, Vol. 37, pp. 329–338.

McGuire, R. K. (1993). "Computations of Seismic Hazard", *Annals of Geophysics*, Vol. 36, No. 3-4.

McGuire, R. K., 2004, *Seismic Hazard and Risk Analysis*, Colorado: Earthquake Engineering Research Institute.

McGuire, R. K., and W. J. Arabasz, 1990, "An Introduction to Probabilistic Seismic Hazard Analysis", In S. o. Geophysicists, In Geotechnical an Environmental Geophysics: Vol.1: Review and Tutorial pp. 333-354.

Meade, B., B. Hager, S. McClusky, R. E. Reilinger, S. Ergintav, O. Lenk, A. Barka, H. Özener, 2002, "Estimates of seismic potential in the Marmara Sea region from block models of secular deformation constrained by global positioning system measurements", *Bulletin of the Seismological Society of America*, Vol. 92, No. 1, pp. 208-215.

Okay, A., E. Demirbağ, H. Kurt, N. Okay, and İ. Kuşçu, 1999 "An active, deep marine strike-slip basin along the North Anatolian fault in Turkey", *Tectonics*, Vol. 18, No. 1, pp. 129-147.

Özmen, B., 2012 "Türkiye Deprem Bölgeleri Haritalarının Tarihsel Gelişimi." *Türkiye Jeoloji Bülteni*, Vol. 55, No. 1.

Pagani, M., D. Monelli, G. Weatherill, L. Danciu, H. Crowley, V. Silva, P. Henshaw, P. Henshaw, L. Butler, M. Nastasi, D. Vigano, 2014, L. Panzeri, M. Simionato, D. Vigano, "OpenQuake

engine: An open hazard (and risk) software for the global earthquake model", *Seismological Research Letters*, Vol. 85(3), pp. 692-702.

Parsons, T., S. Toda, R. S. Stein, A. Barka, and J. H. Dieterich, 2000, "Heightened odds of large earthquakes near Istanbul: An interaction-based probability calculation", *Science*, Vol. 288, pp. 661–665.

Pınar, N., and E. Lahn, 1952, "Türkiye depremleri izahlı kataloğu. Bayındırlık Bakanlığı", *Yapı ve İmar İşleri Reisliği*, 6.

Working Group on California Earthquake, 1990, *Earthquake probabilities in the San Francisco Bay Region*, California, Department of the Interior, US Geological Survey, Vol. 1053,

Reasenberg, P., 1985, "Second-order moment of central California seismicity, 1969–1982", *Journal of Geophysical Research: Solid Earth*, Vol. 90, No. B7, pp. 5479-5495.

Reilinger, R., S. McClusky, P. Vernant, S. Lawrence, S. Ergintav, R. Cakmak, H. Ozener, F. Kadirov, I. Guliev, R. Stepanyan, M. Nadariya, G. Hahubia, S. Mahmoud, K. Sakr, A. ArRajehi, D. Paradissis, A. Al-Aydrus, M. Prilepin, T. Guseva, E. Evren, A. Dmitrotsa, S. V. Filikov, F. Gomez, R. Al-Ghazzi, G. Karam, 2006, "GPS constraints on continental deformation in the Africa-Arabia-Eurasia continental collision zone and implications for the dynamics of plate interactions", *Journal of Geophysical Research: Solid Earth*, Vol. 111, No. B5.

Reiter, L., 1990, *Earthquake hazard analysis: issues and insights*., New York: Columbia University Press.

Selim, H. H., O. Tüysüz, A. Karakaş, and K. Ö. Taş, 2013, "Morphotectonic evidence from the southern branch of the North Anatolian Fault (NAF) and basins of the south Marmara sub-region, NW Turkey", *Quaternary international*, Vol. 292, pp. 176-192.

Sieberg, A., 1932, *Erdbebengeographie*. Berlin.

Soyluk, A., and Z. Y. Harmankaya, 2012, "Examination of earthquake resistant design in the education of architecture", *Procedia-Social and Behavioral Sciences*, Vol. 51, pp. 1080-1086.

Spagnuolo, E., A. Akıncı, A. Herrero, and S. Pucci, 2016, "Implementing the Effect of the Rupture Directivity on PSHA for the City of Istanbul, Turkey", *Bulletin of the Seismological Society of America*, Vol. 106, No. 6, pp. 2599-2613.

Stepp, J. C., 1972, "Analysis of completeness of the earthquake sample in the Puget Sound area and its effect on statistical estimates of earthquake hazard.", *In: Proceedings of the International Conference on Microzonation*, Seattle. pp. 897–910.

Şengör, A. M. C., N. Görür, and F. Şaroğlu, 1985, "Strike-slip faulting and related basin formation in zones of tectonic escape: Turkey as a case study".

Şengör, A. M. C., O. Tüysüz, C. Imren, M. Sakınç, H. Eyidoğan, N. Görür, X. Le Pichon, C. Rangin, 2005, "The North Anatolian fault: A new look", *Annual Review of Earth and Planetary Sciences*, Vol. 33, pp. 37-112.

Şengör, C. A., C. Grall, C. İmren, X. L. Pichon, N. Görür, P. Henry, H. Karabulut, M. Siyako, 2014, "The geometry of the North Anatolian transform fault in the Sea of Marmara and its temporal evolution: implications for the development of intracontinental transform faults", *Canadian Journal of Earth Sciences* Vol. 51, No. 3, pp. 222-242.

Şeşetyan, K., M. Demircioğlu Tümsa, and A. Akinci, 2019, "Evaluation of the seismic hazard in the Marmara region (Turkey) based on updated databases", *Geosciences*, Vol. 9, No. 12, pp. 489.

Şeşetyan, K., M. Demircioğlu, T. Duman, T. Çan, S. Tekin, T. Eroğlu Azak, and Ö. Zülfikar Fercan, 2018, "A probabilistic seismic hazard assessment for the Turkish territory—part I: the area source model", *Bulletin of Earthquake Engineering*, Vol. 16, No. 8, pp. 3367-3397.

Tan, O., Tapırdamaz, M. C., and Yörük, A., 2008, "The earthquake catalogues for Turkey", *Turkish Journal of Earth Sciences*, Vol. 17(2), pp. 405-418.

Utsu, T., 1969, "Aftershocks and earthquake statistics (1): Some parameters which characterize an aftershock sequence and their interrelations", *Journal of the Faculty of Science, Hokkaido University*, (Series 7), Vol. 3, No. 3, pp. 129-195.

Weichert, D. H., 1980, "Estimation of the earthquake recurrence parameters for unequal observation periods for different magnitudes", *Bulletin of the Seismological Society of America*, Vol. 70, No. 4, pp. 1337-1346.

Wells, D. L., and K. J. Coppersmith, 1994, "New empirical relationships among magnitude, rupture length, rupture width, rupture area, and surface displacement", *Bulletin of the seismological Society of America*, Vol. 84, No. 4, pp. 974-1002.

Working Group on California Earthquake Probabilities., 2003, "Earthquake probabilities in the San Francisco Bay Region", 2002–2031. U.S. Geological Society Open File, Report 03–214.

Youngs, R. R., and K. J. Coppersmith, 1985, "Implications of fault slip rates and earthquake recurrence models to probabilistic seismic hazard estimates", *Bulletin of the Seismological society of America*, Vol. 75, No. 4, pp. 939-964.

Zaliapin, I., A. Gabrielov, V. Keilis-Borok, and H. Wong, 2008, "Clustering analysis of seismicity and aftershock identification", *Physical review letters*, Vol. 101, No. 1, pp. 018501.

Zhao, J. X., J. Zhang, A. Asano, Y. Ohno, T., Oouchi, T. Takahashi, . . ., Y., Y. Fukushima, 2006, "Attenuation relations of strong ground motion in Japan using site classification based on predominant period", *Bulletin of the Seismological Society of America*, 96, No. 3, pp. 898-913.

APPENDIX A: RECURRENCE PARAMETERS OF AREA SOURCES

Area sources that are not clipped but overflow the study region							
Source ID	Completeness Zone	Mwmax	a	b	bStdev	b+bStdev	b-bStdev
BGRAS043	Balkan	7.3	3.4341	0.8146	0.1139	0.9285	0.7007
	Balkan	7.6	3.4962	0.8280	0.1115	0.9395	0.7165
	Balkan	7.9	3.5324	0.8358	0.1099	0.9457	0.7259
	Balkan_BGRAS043	7.3	3.5749	0.8420	0.1113	0.9533	0.7307
	Balkan_BGRAS043	7.6	3.6290	0.8538	0.1092	0.9630	0.7446
	Balkan_BGRAS043	7.9	3.6603	0.8605	0.1078	0.9683	0.7527
BGRAS048	Balkan	7.6	3.4423	0.8955	0.1761	1.0716	0.7194
	Balkan	7.9	3.4627	0.9000	0.1723	1.0723	0.7277
	Balkan	8.2	3.4743	0.9026	0.1696	1.0722	0.7330
BGRAS078	Balkan	7.3	2.9900	0.8660	0.1233	0.9893	0.7427
	Balkan	7.6	3.0287	0.8747	0.1214	0.9961	0.7533
	Balkan	7.9	3.0508	0.8796	0.1201	0.9997	0.7595
GEOAS019	Black Sea	7.3	3.3258	0.8660	0.1233	0.9893	0.7427
	Black Sea	7.6	3.3645	0.8747	0.1214	0.9961	0.7533
	Black Sea	7.9	3.3866	0.8796	0.1201	0.9997	0.7595

Area sources that are clipped by the study region							
Source ID	Completeness Zone	Mwmax	a	b	bStdev	b+bStdev	b-bStdev
BGRAS032	Naf Zone	7.0	3.3499	0.8729	0.1667	1.0396	0.7062
	Naf Zone	7.3	3.4195	0.8884	0.1627	1.0511	0.7257
	Naf Zone	7.6	3.5025	0.9068	0.1573	1.0641	0.7495
	Naf Zone_BGRAS032	7.0	2.7238	0.7355	0.1380	0.8735	0.5975
	Naf Zone_BGRAS032	7.3	2.8131	0.7556	0.1339	0.8895	0.6217
	Naf Zone_BGRAS032	7.6	2.9237	0.7807	0.1284	0.9091	0.6523
GRCAS064	Aegean	7.5	3.4694	0.9054	0.0742	0.9796	0.8312
	Aegean	7.8	3.5016	0.9127	0.0732	0.9859	0.8395
	Aegean	8.1	3.5197	0.9168	0.0725	0.9893	0.8443
TURAS034	Central Anatolia	7.1	3.0447	0.9488	0.2232	1.1720	0.7256
	Central Anatolia	7.4	3.0854	0.9581	0.2198	1.1779	0.7383
	Central Anatolia	7.7	3.1076	0.9631	0.2176	1.1807	0.7455
TURAS050	Aegean	7.1	3.1239	0.9488	0.2232	1.1720	0.7256
	Aegean	7.4	3.1646	0.9581	0.2198	1.1779	0.7383
	Aegean	7.7	3.1868	0.9631	0.2176	1.1807	0.7455
NEWTURAS	Aegean	7.1	3.9620	1.0016	0.1575	1.1591	0.8441
	Aegean	7.4	3.9960	1.0094	0.1555	1.1649	0.8539
	Aegean	7.7	4.0141	1.0135	0.1542	1.1677	0.8593

Area sources that are within the study region							
Source ID	Completeness Zone	Mwmax	a	b	bStdev	b+bStdev	b-bStdev
GRCAS080	Marmara	7.5	3.5962	0.8593	0.0876	0.9469	0.7717
	Marmara	7.8	3.6343	0.8680	0.0862	0.9542	0.7818
	Marmara	8.1	3.6562	0.8729	0.0853	0.9582	0.7876
TURAS004	Aegean	7.3	2.3891	0.6247	0.1015	0.7262	0.5232
	Aegean	7.6	2.4746	0.6438	0.0984	0.7422	0.5454
	Aegean	7.9	2.5288	0.6559	0.0962	0.7521	0.5597
	Aegean_TURAS004	7.3	2.4144	0.6255	0.0988	0.7243	0.5267
	Aegean_TURAS004	7.6	2.4996	0.6446	0.0958	0.7404	0.5488
	Aegean_TURAS004	7.9	2.5535	0.6567	0.0937	0.7504	0.5630
TURAS013	Marmara	7.8	3.4654	0.7664	0.0556	0.8220	0.7108
	Marmara	8.1	3.4986	0.7738	0.0548	0.8286	0.7190
	Marmara	8.4	3.5188	0.7783	0.0542	0.8325	0.7241
	TURAS013-STEPP	7.8	4.0092	0.8694	0.0610	0.9304	0.8084
	TURAS013-STEPP	8.1	4.0371	0.8754	0.0602	0.9356	0.8152
	TURAS013-STEPP	8.4	4.0533	0.8789	0.0597	0.9386	0.8192
	TURAS013-STEPP_M	7.8	3.5025	0.7887	0.0539	0.8426	0.7348
	TURAS013-STEPP_M	8.1	3.5254	0.7947	0.0532	0.8479	0.7415
	TURAS013-STEPP_M	8.4	3.5462	0.7983	0.0528	0.8511	0.7455
TURAS049	Marmara	7.5	3.8295	0.9054	0.0742	0.9796	0.8312
	Marmara	7.8	3.8617	0.9127	0.0732	0.9859	0.8395
	Marmara	8.1	3.8798	0.9168	0.0725	0.9893	0.8443
TURAS071	Marmara	7.0	2.4044	0.7876	0.1439	0.9315	0.6437
	Marmara	7.3	2.5175	0.8134	0.1390	0.9524	0.6744
	Marmara	7.6	2.5804	0.8277	0.1359	0.9636	0.6918
TURAS073	Aegean	6.9	3.3083	0.8441	0.1357	0.9798	0.7084
	Aegean	7.2	3.3889	0.8625	0.1322	0.9947	0.7303
	Aegean	7.5	3.4342	0.8728	0.1299	1.0027	0.7429
	Aegean_TURAS073	6.9	3.3123	0.8409	0.1325	0.9734	0.7084
	Aegean_TURAS073	7.2	3.3936	0.8594	0.1290	0.9884	0.7304
	Aegean_TURAS073	7.5	3.4394	0.8698	0.1267	0.9965	0.7431
TURAS077	Marmara	7.0	2.6732	0.7876	0.1439	0.9315	0.6437
	Marmara	7.3	2.7863	0.8134	0.1390	0.9524	0.6744
	Marmara	7.6	2.8492	0.8277	0.1359	0.9636	0.6918

APPENDIX B: RECURRENCE PARAMETERS OF FAULT SOURCES

Source ID	a_1	a_2	a_3	a_4	a_5	a_6	b	WC_Mmax1	WC_Mmax2	WC_Mmax3	SRmin	SRmax
BGCS006	1.6276	2.2297	1.3964	1.9985	1.1641	1.7661	0.8132	6.91	7.25	7.59	0.1	0.4
GRCS150	1.9433	2.3413	1.7109	2.1089	1.4780	1.8760	0.8132	7.28	7.62	7.96	0.2	0.5
GRCS160	2.7366	2.9797	2.5383	2.7814	2.3391	2.5822	0.9116	6.81	7.15	7.49	0.4	0.7
GRCS170	2.0353	2.0353	1.8058	1.8058	1.5744	1.5744	0.8132	6.61	6.95	7.29	0.2	0.3
GRCS288	2.0748	3.0748	1.8785	2.8785	1.6803	2.6803	0.9116	6.45	6.79	7.13	0.1	1
GRCS831	3.0375	3.3385	2.8737	3.1747	2.7095	3.0105	0.9116	7.03	7.31	7.59	0.8	1.6
GRCS999	3.4855	3.5313	3.3221	3.3679	3.1581	3.2039	0.9116	6.87	7.15	7.43	1.8	2
TRCS019	3.2092	3.5102	3.0461	3.3471	2.8822	3.1833	0.9116	6.77	7.05	7.33	1	2
TRCS904	3.3513	3.3970	3.1537	3.1994	2.9548	3.0006	0.9116	6.65	6.99	7.33	1.8	2
BGCS010	1.6404	2.1175	1.4092	1.8863	1.1768	1.6540	0.8132	6.91	7.25	7.59	0.1	0.3
BGCS011	1.5203	1.9974	1.2896	1.7667	1.0576	1.5347	0.8132	6.79	7.13	7.47	0.1	0.3
BGCS012	1.5865	2.1886	1.3566	1.9586	1.1249	1.7270	0.8132	6.67	7.01	7.35	0.1	0.4
BGCS013	1.5319	2.0090	1.3005	1.7776	1.0681	1.5452	0.8132	6.95	7.29	7.63	0.1	0.3
BGCS015	1.6217	2.0988	1.3921	1.8692	1.1606	1.6377	0.8132	6.63	6.97	7.31	0.1	0.3
BGCS038	1.6001	2.0772	1.3724	1.8496	1.1420	1.6191	0.8132	6.41	6.75	7.09	0.1	0.3
BGCS040	1.6133	2.0905	1.3840	1.8611	1.1526	1.6298	0.8132	6.59	6.93	7.27	0.1	0.3
TRCS407-3	2.4770	2.7781	2.2865	2.5875	2.0952	2.3962	0.8132	6.97	7.25	7.53	0.5	1
TRCS407-2	3.4719	3.7729	3.3280	3.6290	3.1837	3.4848	0.9835	7.01	7.29	7.57	0.5	1
TRCS407-1	4.1502	4.2752	4.0058	4.1307	3.8612	3.9862	0.9835	7.67	7.95	8.23	1.5	2
TRCS033	3.5537	3.6787	3.3457	3.4706	3.1362	3.2611	0.8799	6.66	7	7.34	3	4
TRCS022	3.9803	3.9988	3.7820	3.8005	3.5833	3.6017	0.7883	7.38	7.66	7.94	23	24
TRCS023	3.5219	3.5597	3.3261	3.3639	3.1288	3.1666	0.7883	6.67	6.95	7.23	11	12
TRCS024	4.1901	4.2278	4.0276	4.0654	3.8641	3.9019	0.9116	6.62	6.9	7.18	11	12
TRCS025	3.4427	3.4884	3.2466	3.2923	3.0492	3.0950	0.7883	6.71	6.99	7.27	9	10
TRCS028	4.6790	4.6992	4.5148	4.5350	4.3503	4.3706	0.9116	7.3	7.58	7.86	21	22
TRCS033a	3.3586	3.6596	3.1615	3.4625	2.9629	3.2639	0.9116	6.56	6.9	7.24	2	4
TRCS035	4.4928	4.5634	4.3292	4.3998	4.1651	4.2356	0.9116	6.95	7.23	7.51	17	20
TRCS036	4.5187	4.5893	4.3548	4.4254	4.1906	4.2612	0.9116	7.07	7.35	7.63	17	20
TRCS038	4.5223	4.5767	4.3582	4.4125	4.1938	4.2481	0.9116	7.25	7.53	7.81	15	17
TRCS046	1.7242	2.0253	1.5297	1.8307	1.3323	1.6333	0.9116	6.27	6.61	6.95	0.05	0.1
TRCS047	3.2211	3.3460	3.0581	3.1830	2.8943	3.0193	0.9116	6.74	7.02	7.3	1.5	2
TRCS048	3.6562	3.8323	3.4497	3.6257	3.2410	3.4171	0.8799	6.44	6.78	7.12	4	6
TRCS049	2.8146	2.9116	2.6541	2.7510	2.4917	2.5886	0.9116	6.33	6.61	6.89	0.8	1
TRCS050	2.7622	2.8591	2.6035	2.7004	2.4421	2.5390	0.9116	6.16	6.44	6.72	0.8	1
TRCS051	2.7726	2.8696	2.6135	2.7104	2.4518	2.5487	0.9116	6.2	6.48	6.76	0.8	1
TRCS052	3.4123	3.5372	3.2487	3.3737	3.0847	3.2096	0.9116	6.92	7.2	7.48	1.5	2
TRCS054	3.0229	3.1778	2.8599	3.0148	2.6962	2.8511	0.9116	6.73	7.01	7.29	0.7	1
TRCS055	2.8315	2.9864	2.6693	2.8242	2.5059	2.6608	0.9116	6.57	6.85	7.13	0.7	1
TRCS056	2.8522	3.0071	2.6897	2.8446	2.5262	2.6811	0.9116	6.62	6.9	7.18	0.7	1
TRCS057	3.4745	3.5995	3.3030	3.4279	3.1306	3.2555	0.8799	6.72	7	7.28	3	4
TRCS058	3.4588	3.5837	3.2877	3.4126	3.1154	3.2404	0.8799	6.64	6.92	7.2	3	4
TRCS059	2.9335	3.2345	2.7723	3.0733	2.6095	2.9105	0.9116	6.41	6.69	6.97	1	2
TRCS060	1.7335	2.0345	1.5651	1.8661	1.3944	1.6954	0.8799	6.28	6.56	6.84	0.1	0.2
TRCS061	3.0967	3.2217	2.9244	3.0493	2.7515	2.8765	0.8799	6.95	7.23	7.51	1.5	2
TRCS062	3.2689	3.3481	3.0666	3.1458	2.8600	2.9392	0.8799	6.11	6.45	6.79	3	3.6
TRCS063	1.7396	2.0406	1.5709	1.8719	1.4000	1.7010	0.8799	6.31	6.59	6.87	0.1	0.2
TRCS064	2.7297	2.8266	2.5589	2.6558	2.3868	2.4837	0.8799	6.59	6.87	7.15	0.8	1
TRCS065	1.8300	2.1310	1.6359	1.9370	1.4333	1.7343	0.8799	5.79	6.13	6.47	0.1	0.2
TRCS066	1.8077	2.1087	1.6067	1.9078	1.4008	1.7018	0.8799	6.04	6.38	6.72	0.1	0.2
TRCS067	2.8807	3.0567	2.7119	2.8880	2.5411	2.7172	0.8799	6.31	6.59	6.87	1	1.5
TRCS068	2.9410	3.1171	2.7707	2.9468	2.5989	2.7750	0.8799	6.5	6.78	7.06	1	1.5
TRCS070	2.5979	2.7441	2.4286	2.5748	2.2575	2.4036	0.8799	6.37	6.65	6.93	0.5	0.7
TRCS071	2.6796	2.8258	2.5084	2.6545	2.3361	2.4822	0.8799	6.66	6.94	7.22	0.5	0.7
TRCS072	2.6263	2.7724	2.4563	2.6025	2.2848	2.4309	0.8799	6.45	6.73	7.01	0.5	0.7
TRCS228	3.3311	3.4103	3.1298	3.2090	2.9236	3.0028	0.8799	6.06	6.4	6.74	2.5	3

Source ID	a_1	a_2	a_3	a_4	a_5	a_6	b	WC_Mmax1	WC_Mmax2	WC_Mmax3	SRmin	SRmax
TRCS229	3.3398	3.4190	3.1381	3.2173	2.9318	3.0109	0.8799	6.08	6.42	6.76	2.5	3
TRCS230	3.4635	3.5426	3.2549	3.3341	3.0453	3.1245	0.8799	6.74	7.08	7.42	2.5	3
TRCS231	2.6476	2.6476	2.4468	2.4468	2.2410	2.2410	0.8799	6.03	6.37	6.71	0.4	0.5
TRCS232	2.5260	2.5260	2.3595	2.3595	2.1898	2.1898	0.8799	6.13	6.41	6.69	0.4	0.5
TRCS233	3.5460	3.5460	3.3755	3.3755	3.2037	3.2037	0.8799	6.53	6.81	7.09	3	4
TRCS234	2.8142	2.9691	2.6093	2.7642	2.4014	2.5563	0.8799	6.29	6.63	6.97	0.7	1
TRCS235	2.7509	3.0520	2.5435	2.8445	2.3343	2.6353	0.8799	6.56	6.9	7.24	0.5	1
TRCS236	2.7174	3.0184	2.5129	2.8140	2.3053	2.6063	0.8799	6.25	6.59	6.93	0.5	1
TRCS237	2.8141	2.9690	2.6099	2.7648	2.4024	2.5573	0.8799	6.23	6.57	6.91	0.7	1
TRCS238	2.8818	3.0367	2.7099	2.8648	2.5372	2.6921	0.8799	6.83	7.11	7.39	0.7	1
TRCS239	3.0167	3.1306	2.8086	2.9225	2.5991	2.7130	0.8799	6.66	7	7.34	1	1.3
TRCS240	2.9317	3.0456	2.7617	2.8756	2.5901	2.7040	0.8799	6.46	6.74	7.02	1	1.3
TRCS241	2.4692	2.7122	2.2755	2.5185	2.0730	2.3161	0.8799	5.78	6.12	6.46	0.4	0.7
TRCS242	2.4848	2.7278	2.2887	2.5317	2.0851	2.3281	0.8799	5.85	6.19	6.53	0.4	0.7
TRCS243	2.4582	2.7592	2.3188	2.6199	2.1779	2.4790	0.9908	6.33	6.61	6.89	0.1	0.2
TRCS244	2.3938	2.6157	2.1977	2.4196	1.9941	2.2160	0.8799	5.85	6.19	6.53	0.3	0.5
TRCS245	2.7794	3.0804	2.6182	2.9192	2.4554	2.7564	0.9116	6.41	6.69	6.97	0.5	1
TRCS246	3.4895	3.6357	3.3280	3.4742	3.1651	3.3112	0.9116	6.45	6.73	7.01	2.5	3.5
TRCS247	3.1799	3.4809	3.0170	3.3180	2.8533	3.1543	0.9116	6.72	7	7.28	1	2
TRCS248	3.2281	3.5291	3.0646	3.3657	2.9006	3.2016	0.9116	6.89	7.17	7.45	1	2
TRCS250	2.7968	2.9517	2.6060	2.7609	2.4104	2.5653	0.9116	6.03	6.37	6.71	0.7	1
TRCS251	2.8156	2.9705	2.6537	2.8086	2.4906	2.6455	0.9116	6.51	6.79	7.07	0.7	1
TRCS252	2.8413	2.9962	2.6474	2.8023	2.4503	2.6052	0.9116	6.22	6.56	6.9	0.7	1
TRCS253	2.3631	2.5849	2.2088	2.4306	2.0497	2.2715	0.9116	5.91	6.19	6.47	0.3	0.5
TRCS254	2.7956	2.9505	2.6342	2.7891	2.4713	2.6262	0.9116	6.44	6.72	7	0.7	1
TRCS255	2.3719	2.4688	2.1764	2.2733	1.9793	2.0762	0.7883	6.62	6.9	7.18	0.8	1
TRCS256	2.5833	2.6802	2.3886	2.4855	2.1921	2.2890	0.7883	6.51	6.79	7.07	0.8	1
TRCS257	2.5057	2.6026	2.3096	2.4065	2.1123	2.2092	0.7883	6.7	6.98	7.26	0.8	1
TRCS258	2.3887	2.4856	2.1941	2.2910	1.9975	2.0944	0.7883	6.51	6.79	7.07	0.8	1
TRCS256s1	2.5407	2.6377	2.3494	2.4463	2.1548	2.2517	0.7883	6.22	6.5	6.78	0.8	1
TRCS048a	3.6924	3.8685	3.4842	3.6603	3.2747	3.4508	0.8799	6.67	7.01	7.35	4	6
TRCS048b	3.0054	3.7044	2.8031	3.5021	2.5965	3.2955	0.8799	6.11	6.45	6.79	1	5
TRCS062a	2.7169	3.0179	2.5490	2.8501	2.3787	2.6797	0.8799	6.23	6.51	6.79	1	2
TRCS236a	2.6635	2.9645	2.4649	2.7659	2.2600	2.5610	0.8799	5.94	6.28	6.62	0.5	1
TRCS237a	2.8049	2.9598	2.6019	2.7568	2.3950	2.5499	0.8799	6.15	6.49	6.83	0.7	1
TRCS239a	3.0003	3.1143	2.7928	2.9068	2.5837	2.6976	0.8799	6.56	6.9	7.24	1	1.3
TRCS035a	4.3536	4.4379	4.1907	4.2750	4.0270	4.1113	0.9116	6.72	7	7.28	14	17
TRCS069	2.5599	2.7060	2.3921	2.5382	2.2217	2.3678	0.8799	6.23	6.51	6.79	0.5	0.7
TRCS053	3.0629	3.1598	2.9013	2.9983	2.7384	2.8353	0.9116	6.46	6.74	7.02	0.8	1
TRCS036a	4.3727	4.4432	4.2102	4.2808	4.0468	4.1173	0.9116	6.61	6.89	7.17	17	20

FS1=a_1, bmean, Mmean-Std, Srmin

FS2=a_2, bmean, Mmean-Std, Srmax

FS3=a_3, bmean, Mmean, Srmin

FS4=a_4, bmean, Mmean, Srmax

FS5=a_5, bmean, Mmean+Std, Srmin

FS6=a_6, bmean, Mmean+Std, Srmax